Categorization and classification of different ABCA3 variants causing interstitial lung disease

Dissertation

der Mathematisch-Naturwissenschaftlichen Fakultät

der Eberhard Karls Universität Tübingen

zur Erlangung des Doktorgrades

Doktor der Naturwissenschaften

(Dr. rer. nat.)

vorgelegt von

Thomas Wittmann

aus Neumarkt in der Oberpfalz, Deutschland

Tübingen

2016

Gedruckt mit Genehmigung der Mathematisch-Naturwissenschaftlichen Fakultät der Eberhard Karls Universität Tübingen.

Tag der mündlichen Qualifikation:	15.07.2016
Dekan:	Prof. Dr. Wolfgang Rosenstiel
1. Berichterstatter:	Prof. Dr. Dominik Hartl
2. Berichterstatter:	Prof. Dr. Andreas Peschel

Table of contents

List of tables

List of figures

Abbreviations

ABCA3	ATP-binding cassette subfamily A member 3
ABC	ATP-binding cassette
ALD	Adrenoleukodystrophy
ALLM	N-Acetyl-Leu-Leu-Met-CHO
apoA-I	Apolipoprotein A-I
ATP	Adenosine triphosphate
BAL	Bronchoalveolar lavage
CA-074ME	L-trans-expoxysuccinyl-Ile-Pro-OH propylamide methyl ester
CFTR	Cystic fibrosis transmembrane conductance regulator
Chol	Cholesterol
CRD	C-terminal regulatory domain
DIP	Desquamative interstitial pneumonitis
DPLD	Diffuse parenchymal lung disease
ER	Endoplasmatic reticulum
FC	Free cholesterol
HDL	High-density lipoprotein
ILD	Interstitial lung disease
IPF	Idiopathic pulmonary fibrosis
kDa	Kilodalton
LB	Lamellar body
LC-MS/MS	Liquid chromatography-mass spectrometry
NapSuI-Ile-Trp-CHO	N-1-naphthalensulfonyl-L-isoleucyl-L-tryptophanal
NBD	Nucleotide-binding domain
PC	Phosphatidylcholine
PC 32:0	Dipalmitoyl-phosphatidylcholine
PE	Phosphatidylethanolamine
PG	Phosphatidylglycerol
PI	Phosphatidylinositol
PIN	Prostatic intraepithelial neoplasia
PL	Phospholipids
PS	Phosphatidylserine

RDS	Respiratory distress syndrome
SBD	Substance-binding domain
SBP	Substance-binding protein
SFTPB	Surfactant protein B (gene)
SFTPC	Surfactant protein C (gene)
SP	Surfactant protein
SPM	Sphingomyelin
TMD	Transmembrane domain
TTF-1	Thyroid transcription facor-1
VLCFA	Very-long-chain fatty acid

Summary

ATP-binding cassette subfamily A member 3 (ABCA3) is a lipid transporter found in type II pneumocytes, where it localizes to the outer membrane of lamellar bodies (LBs). LBs derive from lysosomal origin and are essential for storing phospholipids and surfactant. Mutations in the *ABCA3* gene are the most common known genetic cause of respiratory distress syndrome (RDS) in newborns and of late onset interstitial lung disease (ILD) in children. But the effects of most variations on ABCA3 protein function are still poorly understood. Therefore we looked in detail at different sequence variations of *ABCA3* and their impact on wild type function.

The R288K variation of ABCA3 was found to have an increased frequency in a population of patients suffering from ILD. These patients did not exhibit characteristic features of complete ABCA3 deficiency. Nevertheless, we found strong evidence that R288K variation affects transport function of ABCA3 protein, supported by decelerated detoxification of doxorubicin, reduced dipalmitoyl-phosphatidylcholine (PC 32:0) content, and decreased LB volume.

By contrast, the K1388N variation recently found in a patient suffering from ILD with lethal outcome led to complete ABCA3 deficiency. We showed that this sequence variation of ABCA3 correctly localized to LBs but had a processing defect and a reduced lipid transporter activity, proven by reduced PC 32:0 content and malformed LBs.

Due to existent intracellular processing defects of K1388N sequence variation and other mutations, we particularly looked at potential protease(s) cleaving ABCA3. An identification of these specific proteins may represent a potential therapeutic target. We found that ABCA3 is proteolytically cleaved by cathepsin L and to a lower level by cathepsin B. Furthermore, we identified the exact cleavage site of cathepsin L located after Lys^{174} in the ABCA3 protein.

In summary, the molecular tools used in these studies, together with a close correlation of our *in-vitro* and *ex-vivo* data will allow a better knowledge of ABCA3 wild type function. Besides this, groups of mutations with similar molecular defects can be defined and targeted by specific small molecule correctors for restoring impaired ABCA3 transporter function in the future.

Zusammenfassung

ATP-binding cassette subfamily A member 3 (ABCA3) ist ein Lipidtransporter, der in alveolären Typ II-Pneumozyten in der äußeren Membran der Lamellarkörpcherchen (LBs) zu finden ist. Lamellarkörperchen sind lysosomalen Ursprungs und ein essentielles Organell zur Speicherung von Phospholipiden und Surfactant. Mutationen in der kodierenden Sequenz des *ABCA3*-Gens sind die Hauptursache für das erblich bedingte Atemnotsyndrom (RDS) bei Neugeborenen und für interstitielle Lungenerkrankungen (ILD) bei Kleinkindern. Dennoch sind die Auswirkungen vieler ABCA3-Sequenzvariationen weitgehend unbekannt. Deshalb war es unser Ziel, den Einfluss verschiedener *ABCA3*-Mutationen auf die Wildtypfunktion des Proteins zu untersuchen.

Wir konnten zeigen, dass die ABCA3-Variation R288K gehäuft in einer Patientengruppe mit ILD vorkommt. Diese Patienten zeigten nicht die üblichen Symptome einer kompletten ABCA3-Defizienz. Trotzdem fanden wir starke Hinweise darauf, dass die R288K-Variation des ABCA3-Proteins dessen Transportfunktion beeinflusst. Diese ging mit einer verlangsamten Detoxifizierung von Doxorubicin, einem reduzierten Dipalmitoylphosphatidylcholin (PC 32:0)-Gehalt und einem verminderten LB-Volumen einher.

Im Gegensatz dazu führte die K1388N-Variation, die kürzlich in einem Patienten, der an ILD erkrankte und verstarb, entdeckt wurde, zu einer völligen ABCA3-Defizienz. Wir konnten zeigen, dass diese ABCA3-Sequenzvariation zwar richtig in LBs lokalisiert, aber einen Prozessierungsdefekt und einen verminderten Lipidtransport aufwies, welche durch einen reduzierten PC 32:0-Gehalt und deformierte LBs nachgewiesen worden konnten.

Aufgrund des intrazellulären Prozessierungsdefekts der K1388N-Sequenzvariation und vieler anderer Mutationen fokussierten wir uns genauer auf mögliche Protease(n), die ABCA3 spalten können. Eine Identifikation dieser spezifischen Proteine könnte ein mögliches therapeutisches Ziel darstellen. Wir konnten zeigen, dass ABCA3 durch Cathepsin L und zu einem geringeren Anteil durch Cathepsin B proteolytisch gespalten wird. Zusätzlich konnten wir die genaue Spaltstelle von Cathepsin L identifizieren, die sich hinter dem Lys^{174} im ABCA3-Protein befindet.

Zusammenfassend kann man sagen, dass die hier verwendeten molekularbiologischen Methoden zusammen mit den von uns erhobenen *in-vitro*- und *ex-vivo*-Daten ein besseres Verständnis für die Wildtypfunktion des ABCA3-Proteins aufzeigen. Außerdem können dadurch Mutationen mit ähnlichen molekularen Defekten definiert und gruppiert werden, um in Zukunft die durch Sequenzvariationen verursachte eingeschränkte Transportfunktion von ABCA3 mit spezifischen Korrektoren wiederherzustellen.

Publications

Original publications

Wittmann T., Schindlbeck U., Höppner S., Kinting S., Frixel S., Kröner C., Liebisch G., Hegermann J., Aslanidis C., Brasch F., Reu S., Lasch P., Zarbock R., and Griese M. (2016). *Tools to explore ABCA3 mutations causing interstitial lung disease*. Ped. Pulm. (accepted)

Wittmann T., Frixel S., Höppner S., Schindlbeck U., Schams A., Kappler M., Hegermann J., Wrede C., Liebisch G., Vierzig A., Zacharasiewicz A., Kopp M., Poets CF., Baden W., Hartl D., van Kaam AH., Lohse P., Aslanidis C., Zarbock R., and Griese M. (2016). *Increased risk of interstitial lung disease in children with a single R288K variant of ABCA3*. Mol. Med. (accepted)

Frixel S., Lotz-Havla AS., Kern S., Kaltenborn E., **Wittmann T.**, Gersting SW., Muntau AC., Zarbock R., and Griese M. (2016). *Homooligomerization of ABCA3 and its functional significance for Neonatal Respiratory Distress Syndrome.* Int. J. Mol. Med. (to be submitted)

Hofmann N., Galetskiy D., Rauch D., **Wittmann T.**, Marquardt A., Griese M., and Zarbock R. (2015). *Analysis of the proteolytic processing of ABCA3: identification of cleavage site and involved proteases.* PloS One (accepted)

Griese M., Irnstetter A., Hengst M., Burmester H., Nagel F., Ripper J., Feilcke M., Pawlita I., Gothe F., Kappler M., Schams A., Wesselak T., Rauch D., **Wittmann T.**, Lohse P., Brasch F., and Kröner C. (2015 Sep 25). *Categorizing diffuse parenchymal lung disease in children.* Orphanet J Rare Dis **10**(1): 122.

Griese M., Lorenz E., Hengst M., Schams A., Wesselak T., Rauch D., **Wittmann T.**, Kirchberger V., Escribano A., Schaible T., Baden W., Schulze J., Krude H., Aslanidis C., Schwerk N., Kappler M., Hartl D., Lohse P., and Zarbock R. (2015 Sep 16). *Surfactant proteins in pediatric interstitial lung disease.* Pediatr. Res.

Zarbock R., Kaltenborn E., Frixel S., **Wittmann T.**, Liebisch G., Schmitz G., and Griese M. (2015 Mar 25). *ABCA3 protects alveolar epithelial cells against free cholesterol induced cell death.* Biochim Biophys Acta **1851**(7): 987-995.

Erklärung nach § 5 Abs. 2 Nr. 7 der Promotionsordnung der Math.-Nat. Fakultät

-Anteil an gemeinschaftlichen Veröffentlichungen-
Nur bei kumulativer Dissertation erforderlich!

Declaration according to § 5 Abs. 2 No. 7 of the PromO of the Faculty of Science

-Share in publications done in team work-

Name: Thomas Wittmann

List of publications

1. **Wittmann T.**, Frixel S., Höppner S., Schindlbeck U., Schams A., Kappler M., Hegermann J., Wrede C., Liebisch G., Vierzig A., Zacharasiewicz A., Kopp M., Poets CF., Baden W., Hartl D., van Kaam AH., Lohse P., Aslanidis C., Zarbock R., and Griese M. (2016). *Increased risk of interstitial lung disease in children with a single R288K variant of ABCA3*. Mol. Med. (accepted)

2. **Wittmann T.**, Schindlbeck U., Höppner S., Kinting S., Frixel S., Kröner C., Liebisch G., Hegermann J., Aslanidis C., Brasch F., Reu S., Lasch P., Zarbock R., and Griese M. (2016). *Tools to explore ABCA3 mutations causing interstitial lung disease*. Ped. Pulm. (accepted)

3. Hofmann N., Galetskiy D., Rauch D., **Wittmann T.**, Marquardt A., Griese M., and Zarbock R. (2015). *Analysis of the proteolytic processing of ABCA3: identification of cleavage site and involved proteases.* PloS One (accepted)

Nr.	**Accepted for publication yes/no**	**Number of all authors**	Position of the candidate in list of authors	Scientific ideas of candidate (%)	Data generation by candidate (%)	Analysis and Interpretation by candidate (%)	Paper writing by candidate (%)
			Optional, the declaration of the own share can also be done in words, please add an extra sheet.				
1	yes	20	1				
2	yes	14	1				
3	yes	7	4				

I certify that the above statement is correct.

Date, Signature of the candidate

I/We certify that the above statement is correct.

Date, Signature of the doctoral committee or at least of one of the supervisors

Contributions to publications

Paper 1

Increased risk of interstitial lung disease in children with a single R288K variant of ABCA3

I performed the *in-vitro* assays with assistance of S. Frixel and S. Höppner. I also performed data analyses, created figures and wrote the manuscript. M. Griese designed the study, supervised the experiments and co-wrote the manuscript. Other authors provided various important materials and contributed to the manuscript.

Paper 2

Tools to explore ABCA3 mutations causing interstitial lung disease

Along with U. Schindlbeck, I performed experiments for this study, analyzed data, created figures and wrote the manuscript. Other authors provided related materials and contributed to the manuscript. M. Griese co-wrote the manuscript.

Paper 3

Analysis of the proteolytic processing of ABCA3: identification of cleavage site and involved proteases

I supported the *in-vitro* assays for this study, discussed the data and created figures. R. Zarbock designed the study and wrote the manuscript.

1. Introduction

1.1. Interstitial lung diseases in children

Interstitial lung diseases (ILD) also referred to as diffuse parenchymal lung diseases (DPLD), encompass a huge heterogeneous group of chronic respiratory disorders leading to dysfunction of gas exchange and restrictive lung physiology [1]. This entity involves the distal air spaces as well as the interstitium consisting of connective tissue elements, extracellular matrix structures with complex polysaccharides, and small numbers of cells such as macrophages [2].

ILD is reported in childhood and adults, although prognosis, causes, and severity vary in a great manner [3,4]. Idiopathic pulmonary fibrosis (IPF) displays the most prominent ILD in adults and is not diagnosed in children [5]. In addition, desquamative interstitial pneumonitis (DIP) occurs in both children and adults, but differs in clinical and histological features and shows better prognosis in adulthood [6]. The main causes and the molecular pathways of ILD development are still poorly understood, and further studies have to be performed assuring further insights into each entity [7-9].

1.2. Pulmonary surfactant and surfactant dysfunction disorders

The respiratory tract represents a complex biological system consisting of 300 million alveolar sacs, which ensure gas exchange of oxygen and carbon dioxide [10]. The alveolar epithelium is lined by two different cell types, the alveolar type I and type II pneumocytes (AT I or II respectively, Figure 1 A) [11]. The flattened, non-dividing AT I cells constitute 90% of the alveolar surface and facilitate gas exchange, while the cuboidal AT II cells play an important role in alveolar homeostasis [12]. Therefore, AT II cells produce, store, and secret pulmonary surfactant into the alveolar space [13]. Once secreted, the surfactant rapidly spreads across the alveolar surface and forms a monolayer at the gaseous-aqueous interface in order to lower surface tension and prevent alveolar collapse at the end of expiration [14,15].

Surfactant is a heterogenous mixture of lipids (90%) and proteins (10%) [16]. Most of the lipids are phospholipids (PL), mainly phosphatidylcholine (PC), dipalmityol-phosphatidylcholine (PC 32:0), phosphatidylglycerol (PG), phosphatidylinositol (PI),

phosphatidylethanolamine (PE), phosphatidylserine (PS), and sphingomyelin (SPM), whereas PC 32:0 is the most abundant [14,17]. Due to its chemical property, PC 32:0 can be packed at high density onto the air-water interface thus lowering alveolar surface tension during inspiration [18,19]. Next to phospholipids, surfactant also contains neutral lipids like cholesterol (Chol) [14,17].

The surfactant proteins are mainly composed of surfactant protein (SP)-A, SP-B, SP-C, and SP-D. The large and hydrophilic SP-A and SP-D proteins belong to the family of collectins thereby opsonising pathogens and contributing to host-defence [20,21]. SP-B and SP-C proteins are small hydrophobic polypeptides packed into organelles called lamellar bodies (LBs), which produce and store pulmonary surfactant.

LB biogenesis is a complex process with a number of intermediate steps. LBs derive from lysosomes and late endosomes by redistributing membrane phospholipids and fusion, resulting in multivesicular bodies (MVB) and composite bodies (CB) (Figure 1 B) [21,22]. Moreover, surfactant lipids are likely transported by ABC transporters into LBs, especially by ATP-binding cassette subfamily A member 3 (ABCA3) [23]. Despite having an acidic pH and lysosomal features, LBs are secretory organelles and may therefore fuse with the plasma membrane of AT II cells [21]. After releasing the pulmonary surfactant into the alveolar space, the LBs are converted to tubular myelin, a defined lattice-like structure [19]. During inspiration, PL rapidly adsorb from tubular myelin to the air-water interface forming a functional surfactant film [19,24]. Interestingly, a proportion of 25-90% of pulmonary surfactant is recycled, suggesting a reinternalization into LBs followed by an eventual resecretion [25].

Recently, genetic disorders disrupting the surfactant metabolism have been recognized and identified in newborns and infants [26-30]. Despite its rarity, morbidity and mortality is considerable [3,31]. Sequence variations were found in genes involved in surfactant homeostasis, including SP-B gene (*SFTPB*), SP-C gene (*SFTPC*), and ABCA3 gene (*ABCA3*) [3]. Those inborn errors in newborns lead to severe RDS and of late onset ILD in children [14]. This entity represents one of the best molecularly characterized subgroup of ILD in childhood [32-34], while *ABCA3* gene variants are the most frequent cause [10,35].

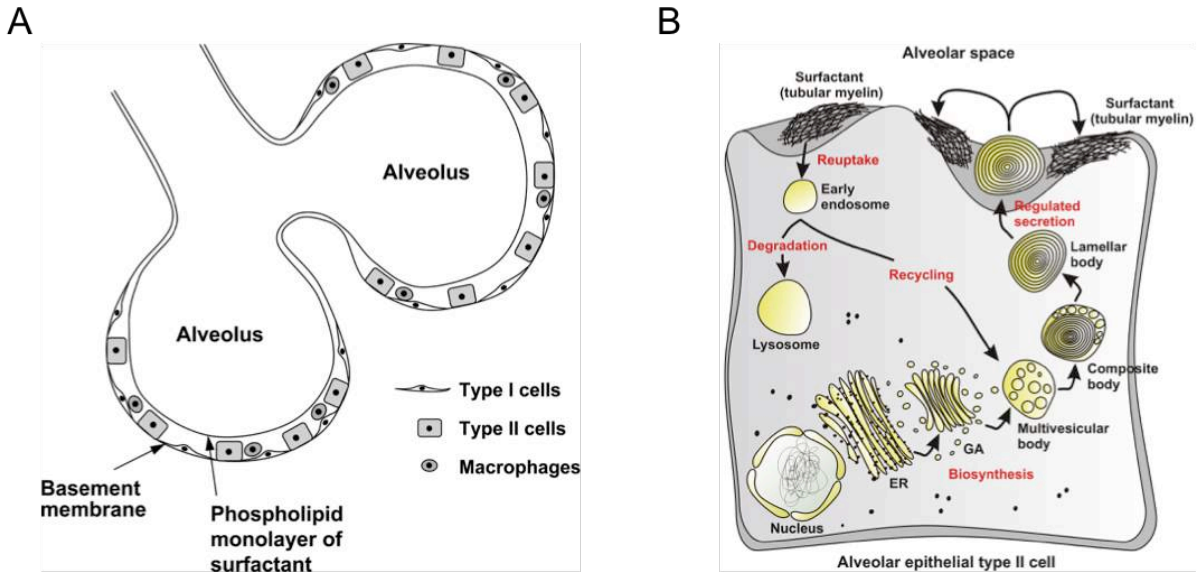

Figure 1: Schematic representation of a pulmonary alveolus (A) and of lamellar body formation and pulmonary surfactant secretion in AT II cells (B)
(A) adapted from [21]; (B) adapted from [36]

1.3. The ABC transporter superfamily

ATP-binding cassette (ABC) transporters are a large group of membrane proteins widely distributed among living organisms, such as bacteria, plants, and animals [37,38]. ABC proteins hydrolyze adenosine triphosphate (ATP), which provides the driving force for translocating molecules across membranes. These ATP-powered pumps cover a broad spectrum of substrates, including lipids, ions, xenobiotics, drugs, and hydrophobic compounds [39].

Functional ABC proteins contain two transmembrane domains (TMDs) and two nucleotide-binding domains (NBDs) [37]. Each TMD consists of six membrane-spanning α-helices forming a cavity for substrate transport [40]. The NBDs, which bind and hydrolyze ATP, contain highly conserved domains: the Walker A and Walker B motifs found in all ABC transporters, and a unique signature motif located upstream of the Walker B domain [41,42].

Based on TMD folds and direction of transport relative to cytoplasm, four different ABC transporters were identified (Figure 2). Type I and type II importers together with ECF-transporters (type III importer) are exclusively expressed in prokaryotes, while exporters are found in both prokaryotes and eukaryotes [43]. Type I and II

importers depend on substance-binding proteins (SBP) or substance-binding domains (SBD), delivering molecules to the respective TMDs [44,45]. Type III importers possess specialized TMDs called S-components, which bind substrates with high affinity [46,47]. Exporters are involved in multidrug resistances, facilitating the export through cell membranes [48].

The human ABC superfamily comprises 49 *ABC* genes divided into seven subfamilies, termed A to G [49] (Table 1). Furthermore, defects in human ABC transporters were shown to cause genetic disorders [50,51] (Table 2).

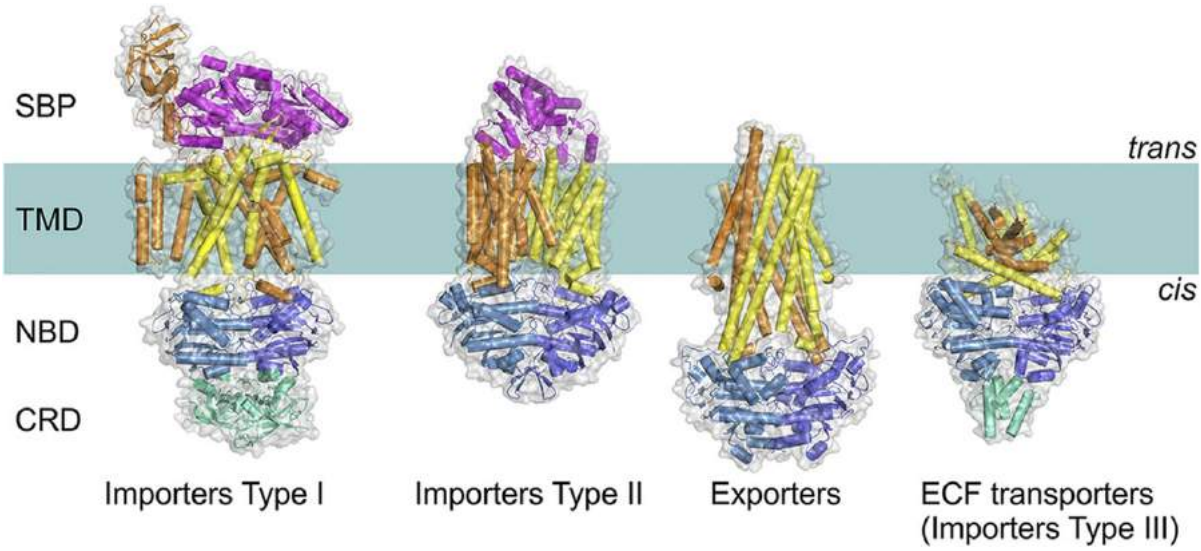

Figure 2: Overview of different ABC transporters

Figure adapted from [43]
SBP: Substrate-binding protein; TMD: Tansmembrane domain; NBD: Nucleotide-binding domain; CRD: C-terminal regulatory domain

Table 1: The superfamily of ABC transporters

Subfamily name	Aliases	Gene	Chromosome location	Expression	Function
ABCA	ABC1	ABCA1	9q31.1	Ubiquitous	Cholesterol efflux onto HDL
		ABCA2	9q34	Brain	Drug resistance
		ABCA3	16p13.3	Lung	Multidrug resistance
		ABCA4	1p22	Rod photoreceptors	N-retinylidene-phosphatidylethanolamine (PE) efflux
		ABCA5	17q24.3	Muscle, heart, testes	Urinary diagnostic marker for prostatic intraepithelial neoplasia (PIN)
		ABCA6	17q24.3	Liver	Multidrug resistance
		ABCA7	19p13.3	Spleen, thymus	Cholesterol efflux
		ABCA8	17q24	Ovary	Transports certain lipophilic drugs
		ABCA9	17q24.2	Heart	Might play a role in monocyte differentiation and macrophage lipid homeostasis
		ABCA10	17q24	Muscle, heart	Cholesterol-responsive gene
		ABCA12	2q34	Stomach	Has implications for prenatal diagnosis
		ABCA13	7p12.3	Low in all tissues	Inherited disorder affecting the pancreas
ABCB	MDR	ABCB1	7q21.1	Adrenal, kidney, brain	Multidrug resistance
		ABCB2	6p21.3	All cells	Peptide transport
		ABCB3	6p21.3	All cells	Peptide transport
		ABCB4	7q21.1	Liver	Phosphatidylcholine (PC) transport
		ABCB5	7p15.3	Ubiquitous	Melanogenesis
		ABCB6	2q36	Mitochondria	Iron transport
		ABCB7	Xq12-q13	Mitochondria	Fe/S cluster transport
		ABCB8	7q36	Mitochondria	Intracellular peptide trafficking across membranes
		ABCB9	12q24	Heart, brain	Located in lysosomes
		ABCB10	1q42.13	Mitochondria	Export of peptides derived from proteolysis of inner-membrane proteins

Subfamily name	Aliases	Gene	Chromosome location	Expression	Function
		ABCB11	2q24	Liver	Bile salt transport
ABCC	MRP	ABCC1	16p13.1	Lung, testes, PBMC	Drug resistance
		ABCC2	10q24	Liver	Organic anion efflux
		ABCC3	17q22	Lung, intestine, liver	Drug resistance
		ABCC4	13q32	Prostate	Nucleoside transport
		ABCC5	3q27	Ubiquitous	Nucleoside transport
		ABCC6	16p13.1	Kidney, liver	Expressed primarily in liver and kidney
		ABCC7	7q31.2	Exocrine tissues	Chloride ion channel (same as *CFTR* gene in cystic fibrosis)
		ABCC8	11p15.1	Pancreas	Sulfonylurea receptor
		ABCC9	12p12.1	Heart, muscle	Encodes the regulatory SUR2A subunit of the cardiac K^+ (ATP) channel
		ABCC10	6p21.1	Low in all tissues	Multidrug resistance
		ABCC11	16q12.1	Low in all tissues	Drug resistance in breast cancer
		ABCC12	16q21.1	Low in all tissues	Multidrug resistance
		ABCC13	21q11.2	Unknown	Encodes a polypeptide of unknown function
ABCD	ALD	ABCD1	Xq28	Peroxisomes	Very-long chain fatty acid (VLCFA) transport
		ABCD2	12q11-q12	Peroxisomes	Major modifier locus for clinical diversity in X-linked ALD
		ABCD3	1p22-p21	Peroxisomes	Involved in import of fatty acids and/or fatty acyl-coenzyme As into the peroxisome
		ABCD4	14q24	Peroxisomes	May modify ALD phenotype
ABCE	OABP	ABCE1	4q31	Ovary, testes, spleen	Oligoadenylate-binding protein

Subfamily name	Aliases	Gene	Chromosome location	Expression	Function
ABCF	GGN20	ABCF1	6p21.33	Ubiquitous	Susceptibility to autoimmune pancreatitis
		ABCF2	7q36	Ubiquitous	Tumour suppression at metastatic sites and in endocrine pathway for breast cancer/drug resistance
		ABCF3	3q27.1	Ubiquitous	Also present in promastigotes (one of five forms in the life cycle of trypanosomes)
ABCG	White	ABCG1	21q22.3	Ubiquitous	Cholesterol transport
		ABCG2	4q22	Placenta, intestine	Toxicant efflux, drug resistance
		ABCG4	11q23.3	Liver	Found in macrophage, eye, brain and spleen
		ABCG5	2p21	Liver, intestine	Sterol transport
		ABCG8	2p21	Liver, intestine	Sterol transport

Table adapted from [49]and [52].

Table 2: Diseases caused by mutations in *ABC* genes

Transporter name	Disease
ABCA1	Tangier disease; Familial hypoapoproteinemia
ABCA4	Stargradt/fundus flavimaculatis; Retinitis pigmentosa; Cone-rod dystrophy; Age-related macular degeneration
ABCB2	Immune deficiency
ABCB3	Immune deficiency
ABCB4	Progressive familial intrahepatic cholestasis-3
ABCB7	X-linked sideroblastosis and anemia
ABCB11	Progressive familial intrahepatic cholestasis-2
ABCC2	Dubin-Johnson Syndrome
ABCC6	Pseudoxanthoma elasticum
ABCC7	Cystic fibrosis
ABCD1	Adrenoleukodystrophy
ABCG5	Sitosterolemia
ABCG8	Sitosterolemia

Table adapted from [50,53] and [51]

1.3.1. The ABCA subfamily

The ABCA subfamily comprises 12 transporters organised both as head-to-tail cluster on chromosome 17q24 and dispersed on six different chromosomes (Table 1, ABCA subfamily) [52,54]. Furthermore, ABCA transporters are widely expressed in different tissues and primarily involved in lipid trafficking (Table 1) [49,55].

Several inherited diseases are caused by variations in the *ABCA* genes. Mutations in the *ABCA1* gene are linked to Tangier disease, which is characterized by severe plasma deficiency or absence of high-density lipoprotein (HDL) and apolipoprotein A-I [56]. The ABCA1 transporter plays a key role in the efflux of PL and free cholesterol (FC) from peripheral cells to lipid-poor apo A-I proteins [52,57].

Another member of the ABCA family, the ABCA4 transporter, is mainly expressed in rod photoreceptors of the retina [58]. The ABCA4 transporter is thought to mediate the transport of modified PE across the cellular plasma membrane [59]. Variations in

the *ABCA4* gene are associated with Stargardt disease, a retinal degeneration syndrome in childhood [58].

1.3.2. ABCA3

The *ABCA3* gene located on chromosome 16p13.3 encodes for a 1704 amino acid-long protein and covers 80 kb of genomic DNA. ABCA3 is mainly expressed in the lungs, but also in liver, kidney, stomach, brain, and pancreas (Figure 3) [60,61]. Similar to SP-B and SP-C, ABCA3 expression is induced by thyroid transcription facor-1 (TTF-1) [62,63]. Usually, the ABCA3 protein is located to the limiting membrane of LBs, regulating LB biogenesis and pulmonary surfactant homeostasis [23,64,65]. Furthermore, the ABCA3 transporter is thought to exocytose PC and PG into the alveolar space [60,66].

Previous studies showed a link of mutations in the *ABCA3* gene with surfactant disorders in children, implicating a significant relevance to ILD [29,35,67]. Moreover, homozygous ABCA3$^{-/-}$ knock-out mice, which were unable to release surfactant into the alveolar space, soon died after birth. By contrast, heterozygous ABCA3$^{-/+}$ knock-out mice survived [68]. To date, more than 180 various *ABCA3* mutations were found, resulting in trafficking, localization, and transport defects [60,69]. However, the precise mechanisms by which ABCA3 transporters act on surfactant metabolism remain unclear.

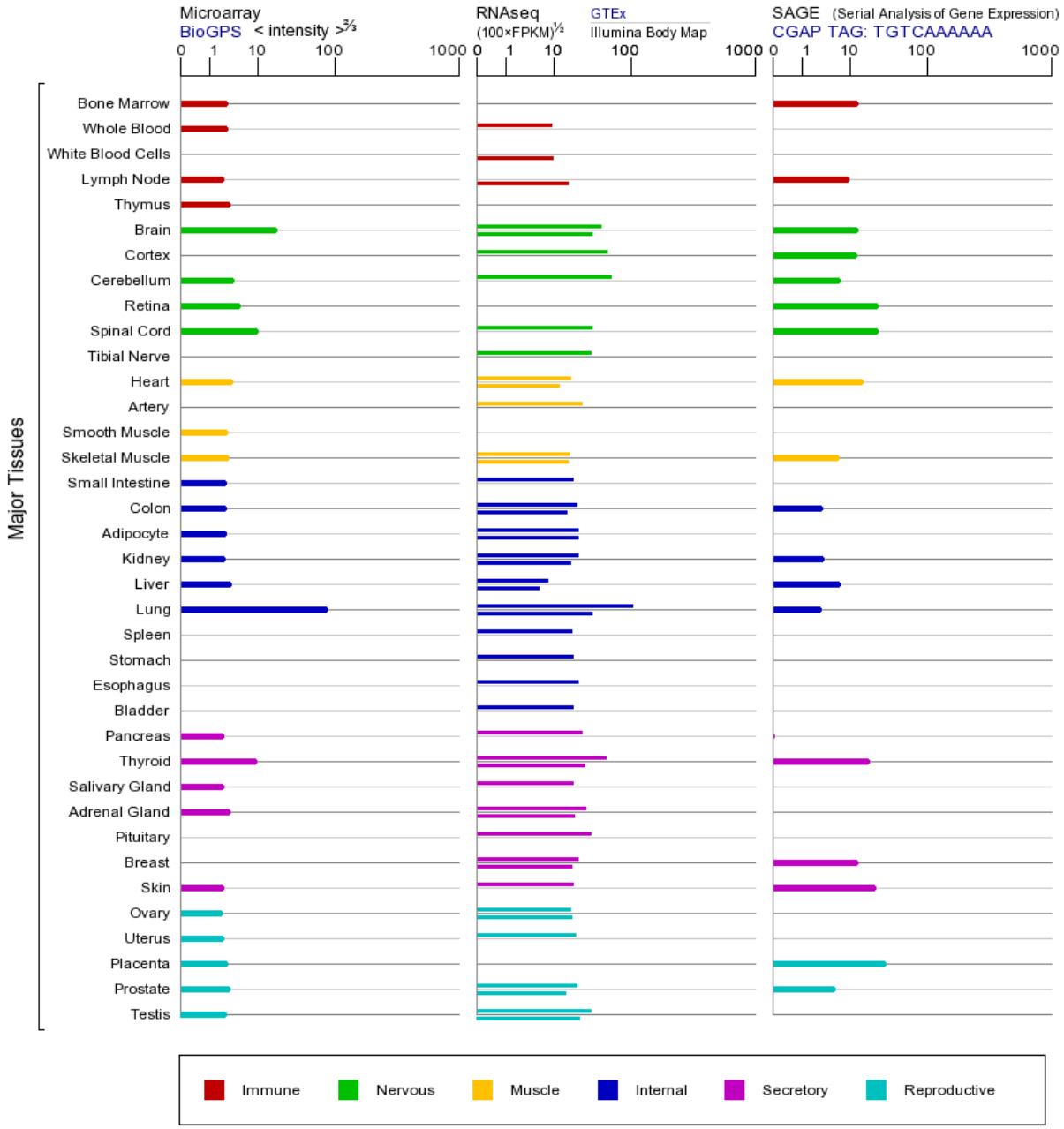

Figure 3: *ABCA3* RNA expression in different tissues

Adapted from [70]

2. Aims of the study

The major aim of the study was to establish a system for characterizing and classifying different ABCA3 variations causing ILD. Therefore, we used a broad set of molecular tools to acquire knowledge about ABCA3 wild type protein. Based upon this, we analyzed *ABCA3* mutations and compared them to the wild type protein.

First, we explored cellular processing, trafficking, and intracellular localization of ABCA3 wild type protein and sequence variations in a reliable cellular model. Next, we analyzed LB morphogenesis in cells stably expressing ABCA3 wild type and protein variants. Furthermore, we investigated lipid transport function of ABCA3 wild type protein and different mutations. To proof its relevance, the *in-vitro* data were related to the respective *ex-vivo* data collected from patients carrying the same ABCA3 variations.

3. Results and Discussion

ILD comprise a huge entity of diseases with mostly unknown cause. The inherited surfactant disorders as a subgroup of ILD are mainly caused by mutations in the *ABCA3* gene. ABCA3 is a lipid transporter found in AT II cells, where it localizes to the limiting membrane of LBs, the intracellular production and storage organelles for pulmonary surfactant. To date, more than 180 different ABCA3 variants were found in patients suffering from ILD, but the molecular mechanisms of interacting with surfactant metabolism and homeostasis are still poorly understood.

The central aims of the study were to explore wild type function of ABCA3, and to characterize and classify different ABCA3 variants causing ILD. Based on *in-vitro* assays and patient studies, we established a broad set of molecular tools, which allowed a detailed insight into ABCA3 function.

3.1. Increased risk of interstitial lung diseases in children with a single R288K variant of ABCA3

In this study we investigated the impact of the ABCA3 variant R288K on ILD. In our study cohort of 228 children suffering from ILD, we found nine patients harbouring the R288K mutation in a heterozygous state. The carrier frequency of R288K variant was enriched over that in the general Caucasian population [71]. Moreover, the patients had non-consanguineous parents and carried no sequence variations in *SFTPB* and *SFTPC*. All children with a single heterozygous R288K variant of ABCA3 developed neonatal respiratory distress and recurrent airway infections followed by chronic pediatric ILD. However, the patients did not exhibit characteristic features of complete ABCA3 deficiency. Two of nine patients displayed mild phenotypes of respiratory distress, suggesting additional factors involved in surfactant dysfunction. Moreover, correlation of prematurity in our patient cohort with single ABCA3 variations was proven and confirmed [72].

We provided evidence that the R288K variant reduces lipid transport activity of ABCA3 in the affected infants, proven by reduced levels of PC and PC 32:0 in bronchoalveolar lavage (BAL) fluids. In addition, decelerated detoxification

capacity for doxorubicin and reduced LB volume was shown in an appropriate cell model caused by functionally impaired ABCA3-R288K protein.

Since expression of ABCA3 protein is a developmentally regulated process towards birth [61], prematurity has a pronounced effect resulting in elevated surfactant dysfunction. Previous studies demonstrated an increased susceptibility to lung injury in the presence of ABCA3 variations and respiratory tract infections, which was also a consistent feature in our patients [73,74].

Taken together, we showed that the R288K variant in combination with prematurity or respiratory infections could lead to respiratory distress in newborns and ILD in children.

3.2. Tools to explore ABCA3 mutations causing interstitial lung disease

In the present study we used a set of molecular tools for characterization and classification different ABCA3 mutations according to their impact on ABCA3 activity. The ABCA3 variant K1388N was exemplarily used to investigate molecular pathomechansims affecting pulmonary surfactant metabolism. Moreover, we aimed to correlate *in-vitro* and *in-vivo* findings.

The homozygous K1388N variant was found in a patient suffering from severe respiratory distress, progressing to ILD with lethal outcome at the age of nine weeks. Furthermore, the K1388N mutation led to complete ABCA3 deficiency, which is incompatible with life [68].

Our study revealed that the K1388N variant was correctly localized to LBs *in-vitro* and was not retained in the endoplasmatic reticulum (ER). Moreover, ABCA3-K1388N protein showed trafficking through ER and Golgi apparatus, which is consistent with ABCA3 wild type protein. We showed that K1388N mutation led to impaired cellular processing of ABCA3 protein. ABCA3 is normally processed from a 190 kDa form to a 150 kDa form [69,75]. The 190 kDa was clearly enriched in the sequence variant K1388N *in-vitro*. In addition, the replaced lysine to asparagine introduces a possible further N-glycosylation side on position K1388N; this may lead to decreased protein stability [76].

Furthermore, we showed an induction of LBs in our cell model stably expressing ABCA3 wild type protein. By contrast, expression of ABCA3-K1388N resulted in malformed LBs with decreased vesicle volume *in-vitro* and *ex-vivo*.

Next, we assessed the impact of the K1388N variant on ABCA3 protein function by measuring lipid composition. PC and PC 32:0 content was both reduced in BAL of the patient and in our cell model stably expressing ABCA3-K1388N, which is in concordance with previous studies [62,77].

In summary, the K1388N variant was defined as a processing mutation with normal intracellular localization and a reduced lipid transporter activity for PC 32:0. The used molecular tools allow a detailed classification of different ABCA3 mutations, thereby facilitating the screening for small molecule correctors in order to restore wild type function of ABCA3.

3.3. Analysis of the proteolytic processing of ABCA3: identification of cleavage site and involved proteases

Since the K1388N variation and other ABCA3 mutations lead to intracellular processing defects, we had a detailed look at the potential protease(s) cleaving ABCA3 from 190 kDa to 150 kDa form. Based on liquid chromatography–mass spectrometry (LC-MS/MS), we identified a proposed cleavage site of ABCA3 in proximity to Lys^{174}, which was only detectable in the 190 kDa processing form. Analysis of a topological model of ABCA3 generated by TOPCONS indicated a localization of the potential cleavage site inside the vesicular lumen [78].

Moreover, previous studies revealed a N-terminally cleavage of ABCA3 protein in CD63-positive vesicles, which can be blocked by inhibition of vesicle acidification [79]. Furthermore, we showed that cleavage of ABCA3 proteins is blocked by E-64, a cysteine protease inhibitor [79]. Therefore, the spectrum of proteases can be limited to lysosomal cysteine proteases acting at acidic pH.

We narrowed down the list of proteases involved in ABCA3 cleavage using ALLM (N-Acetyl-Leu-Leu-Met-CHO), an inhibitor of calpains I and II, and cathepsins B and L [80]. We revealed an enrichment of the 190 kDa processing form compared to the 150 kDa form, which was diminished. Since the potential cleavage site of

ABCA3 protein is located in the vesicular lumen with acidic pH, calpains can be excluded.

We next applied inhibitors specific for cathepsin B and cathepsin L. The cathepsin B inhibitor L-trans-expoxysuccinyl-Ile-Pro-OH propylamide methyl ester (CA-074Me, [81]) led to an accumulation of the 190 kDa form, but had a weaker effect than ALLM, suggesting a lower activity of cathepsin B on ABCA3 protein cleavage.

The inhibition of cathepsin L with N-1-napthalenesulfonyl-L-isoleucyl-L-tryptophanal (NapSul-Ile-Trp-CHO, [82]) did not lead to an accumulation of the 190 kDa form. Instead, both bands disappeared due to effects on cell viability. This is in concordance with previous reports [83].

These findings were verified by specific siRNA-mediated knockdown of cathepsin L and B expression [84], revealing an accumulation of the 190 kDa processing form. The effect was enhanced by combination of both cathepsin B and L knockdown. Moreover, synthesized peptides comprising residues 151-194 were cleaved by cathepsin L and to a lower content by cathepsin B after Lys^{174}.

Furthermore, we aimed to abolish the specific cleavage site for cathepsin L in the ABCA3 protein. Replacement of Leu^{173} and Lys^{174} by alanine residues resulted in an accumulation of the 190 kDa processing form of ABCA3.

Taken together, we identified the specific cleavage site of ABCA3 protein at Lys^{174}, which is processed by cathepsin L and to a lower level by cathepsin B. Since both processing forms seem to be necessary for normal function of ABCA3 protein, the identified proteases represent a potential target to therapeutically influence ABCA3 activity in ABCA3-associated surfactant disorders.

4. References

1. Schwarz MI and King TE, *Intersitital lung disease, 5th ed.* 2011: Pub. House, Shelton, Conn.
2. Cosgrove GP and Schwarz MI, *Approach to the Evaluation and Diagnosis of Interstitial Lung Disease*, in *Interstitial Lung Disease*. 2010, People's Medical Publishing House-USA. p. 3.
3. Deutsch GH, Young LR, Deterding RR, Fan LL, Dell SD, Bean JA, et al., *Diffuse lung disease in young children: application of a novel classification scheme.* Am J Respir Crit Care Med, 2007. **176**(11): p. 1120-8.
4. Glasser SW, Hardie WD, and Hagood JS, *Pathogenesis of Interstitial Lung Disease in Children and Adults.* Pediatr Allergy Immunol Pulmonol, 2010. **23**(1): p. 9-14.
5. Vece TJ and Fan FL, *Interstitial Lung Disease in Children Older Than 2 Years.* Pediatr. Allergy Immunol. Pulmonol., 2010. **23**(1): p. 33-41.
6. Nicholson AG, Kim H, Corrin B, Bush A, du Bois RM, Rosenthal M, et al., *The value of classifying interstitial pneumonitis in childhood according to defined histological patterns.* Histopathology, 1998. **33**(3): p. 203-11.
7. Fan LL, Deterding RR, and Langston C, *Pediatric interstitial lung disease revisited.* Pediatr Pulmonol, 2004. **38**(5): p. 369-78.
8. Ryu JH, Colby TV, Hartman TE, and Vassallo R, *Smoking-related interstitial lung diseases: a concise review.* Eur Respir J, 2001. **17**(1): p. 122-32.
9. Cho JH, Gelinas R, Wang K, Etheridge A, Piper MG, Batte K, et al., *Systems biology of interstitial lung diseases: integration of mRNA and microRNA expression changes.* BMC Med Genomics, 2011. **4**: p. 8.
10. Whitsett JA, Wert SE, and Weaver TE, *Alveolar surfactant homeostasis and the pathogenesis of pulmonary disease.* Annu Rev Med, 2010. **61**: p. 105-19.
11. Ward HE and Nicholas TE, *Alveolar type I and type II cells.* Aust N Z J Med, 1984. **14**(5 Suppl 3): p. 731-4.
12. Witherden IR and Tetley TD, *Isolation and Culture of Human Alveolar Type II Pneumocytes.* Methods Mol Med, 2001. **56**: p. 137-46.
13. Kuroki Y, Mason RJ, and R. VD, *Alveolar typeII cells express a high-affinity receptor for pulmonary surfactant protein A.* Proc. Natl. Acad. Sci. USA, 1988. **85**: p. 5566-70.
14. Wert SE, Whitsett JA, and Nogee LM, *Genetic disorders of surfactant dysfunction.* Pediatr Dev Pathol, 2009. **12**(4): p. 253-74.
15. Akella A and Deshpande SB, *Pulmonary surfactants and their role in pathophysiology of lung disorders.* Indian J Exp Biol, 2013. **51**(1): p. 5-22.
16. Weaver TE and Whitsett JA, *Function and regulation of expression of pulmonary surfactant-associated proteins.* Biochem J, 1991. **273(Pt 2)**: p. 249-64.
17. Serrano AG and Perez-Gil J, *Protein-lipid interactions and surface activity in the pulmonary surfactant system.* Chem Phys Lipids, 2006. **141**(1-2): p. 105-18.
18. Perez-Gil J, *Structure of pulmonary surfactant membranes and films: the role of proteins and lipid-protein interactions.* Biochim Biophys Acta, 2008. **1778**(7-8): p. 1676-95.
19. Goerke J, *Pulmonary surfactant: functions and molecular composition.* Biochim Biophys Acta, 1998. **1408**(2-3): p. 79-89.

20. Wright JR, *Immunoregulatory functions of surfactant proteins.* Nat Rev Immunol, 2005. **5**(1): p. 58-68.
21. Andreeva AV, Kutuzov MA, and Voyno-Yasenetskaya TA, *Regulation of surfactant secretion in alveolar type II cells.* Am J Physiol Lung Cell Mol Physiol, 2007. **293**(2): p. L259-71.
22. Weaver TE, Na CL, and Stahlman M, *Biogenesis of lamellar bodies, lysosome-related organelles involved in storage and secretion of pulmonary surfactant.* Semin Cell Dev Biol, 2002. **13**(4): p. 263-70.
23. Ban N, Matsumura Y, Sakai H, Takanezawa Y, Sasaki M, Arai H, et al., *ABCA3 as a lipid transporter in pulmonary surfactant biogenesis.* J Biol Chem, 2007. **282**(13): p. 9628-34.
24. Griese M, *Pulmonary surfactant in health and human lung diseases: state of the art.* Eur Respir J, 1999. **13**(6): p. 1455-76.
25. Schmitz G and Muller G, *Structure and function of lamellar bodies, lipid-protein complexes involved in storage and secretion of cellular lipids.* J Lipid Res, 1991. **32**(10): p. 1539-70.
26. Whitsett JA and Weaver TE, *Hydrophobic surfactant proteins in lung function and disease.* N Engl J Med, 2002. **347**(26): p. 2141-8.
27. Nogee LM, *Alterations in SP-B and SP-C expression in neonatal lung disease.* Annu Rev Physiol, 2004. **66**: p. 601-23.
28. Hartl D and Griese M, *Interstitial lung disease in children -- genetic background and associated phenotypes.* Respir Res, 2005. **6**: p. 32.
29. Bullard JE, Wert SE, and Nogee LM, *ABCA3 deficiency: neonatal respiratory failure and interstitial lung disease.* Semin Perinatol, 2006. **30**(6): p. 327-34.
30. Hamvas A, Cole FS, and Nogee LM, *Genetic disorders of surfactant proteins.* Neonatology, 2007. **91**(4): p. 311-7.
31. Griese M, Haug M, Brasch F, Freihorst A, Lohse P, von Kries R, et al., *Incidence and classification of pediatric diffuse parenchymal lung diseases in Germany.* Orphanet J Rare Dis, 2009. **4**: p. 26.
32. Hildebrandt J, Yalcin E, Bresser HG, Cinel G, Gappa M, Haghighi A, et al., *Characterization of CSF2RA mutation related juvenile pulmonary alveolar proteinosis.* Orphanet J Rare Dis, 2014. **9**: p. 171.
33. Kroner C, Reu S, Teusch V, Schams A, Grimmelt AC, Barker M, et al., *Genotype alone does not predict the clinical course of SFTPC deficiency in paediatric patients.* Eur Respir J, 2015. **46**(1): p. 197-206.
34. Whitsett JA, Wert SE, and Weaver TE, *Diseases of pulmonary surfactant homeostasis.* Annu Rev Pathol, 2015. **10**: p. 371-93.
35. Brasch F, Schimanski S, Muhlfeld C, Barlage S, Langmann T, Aslanidis C, et al., *Alteration of the pulmonary surfactant system in full-term infants with hereditary ABCA3 deficiency.* Am J Respir Crit Care Med, 2006. **174**(5): p. 571-80.
36. Kern S, *Lamellar body formation and pulmonary surfactant secretion in AT II cells*. p. Adapted from Kern S (AG Griese).
37. Linton KJ and Higgins CF, *The Escherichia coli ATP-binding cassette (ABC) proteins.* Mol Microbiol, 1998. **28**(1): p. 5-13.
38. Zolnerciks JK, Andress EJ, Nicolaou M, and Linton KJ, *Structure of ABC transporters.* Essays Biochem, 2011. **50**(1): p. 43-61.
39. Hediger MA, Romero MF, Peng JB, Rolfs A, Takanaga H, and Bruford EA, *The ABCs of solute carriers: physiological, pathological and therapeutic implications of human membrane transport proteinsIntroduction.* Pflugers Arch, 2004. **447**(5): p. 465-8.

40. Higgins CF, *ABC transporters: from microorganisms to man.* Annu Rev Cell Biol, 1992. **8**: p. 67-113.
41. Hyde SC, Emsley P, Hartshorn MJ, Mimmack MM, Gileadi U, Pearce SR, et al., *Structural model of ATP-binding proteins associated with cystic fibrosis, multidrug resistance and bacterial transport.* Nature, 1990. **346**(6282): p. 362-5.
42. Ambudkar SV, Kim IW, Xia D, and Sauna ZE, *The A-loop, a novel conserved aromatic acid subdomain upstream of the Walker A motif in ABC transporters, is critical for ATP binding.* FEBS Lett, 2006. **580**(4): p. 1049-55.
43. ter Beek J, Guskov A, and Slotboom DJ, *Structural diversity of ABC transporters.* J Gen Physiol, 2014. **143**(4): p. 419-35.
44. Quiocho FA and Ledvina PS, *Atomic structure and specificity of bacterial periplasmic receptors for active transport and chemotaxis: variation of common themes.* Mol Microbiol, 1996. **20**(1): p. 17-25.
45. Berntsson RP, Smits SH, Schmitt L, Slotboom DJ, and Poolman B, *A structural classification of substrate-binding proteins.* FEBS Lett, 2010. **584**(12): p. 2606-17.
46. Duurkens RH, Tol MB, Geertsma ER, Permentier HP, and Slotboom DJ, *Flavin binding to the high affinity riboflavin transporter RibU.* J Biol Chem, 2007. **282**(14): p. 10380-6.
47. Berntsson RP, ter Beek J, Majsnerowska M, Duurkens RH, Puri P, Poolman B, et al., *Structural divergence of paralogous S components from ECF-type ABC transporters.* Proc Natl Acad Sci U S A, 2012. **109**(35): p. 13990-5.
48. Dawson RJ and Locher KP, *Structure of a bacterial multidrug ABC transporter.* Nature, 2006. **443**(7108): p. 180-5.
49. Vasiliou V, Vasiliou K, and Nebert DW, *Human ATP-binding cassette (ABC) transporter family.* Hum Genomics, 2009. **3**(3): p. 281-90.
50. Dean M, Rzhetsky A, and Allikmets R, *The Human ATP-Binding Cassette (ABC) Transporter Superfamily.* Genome Res., 2001. **11**: p. 1156-66.
51. Quazi F and Molday RS, *Lipid transport by mammalian ABC proteins.* Essays Biochem, 2011. **50**(1): p. 265-90.
52. Dean M, Hamon Y, and Chimini G, *The human ATP-binding cassette (ABC) transporter superfamily.* J Lipid Res, 2001. **42**(7): p. 1007-17.
53. Stefkova J, Poledne R, and Hubacek JA, *ATP-binding cassette (ABC) transporters in human metabolism and diseases.* Physiol Res, 2004. **53**(3): p. 235-43.
54. Broccardo C, Luciani M, and Chimini G, *The ABCA subclass of mammalian transporters.* Biochim Biophys Acta, 1999. **1461**(2): p. 395-404.
55. Tusnady GE, Sarkadi B, Simon I, and Varadi A, *Membrane topology of human ABC proteins.* FEBS Lett, 2006. **580**(4): p. 1017-22.
56. Puntoni M, Sbrana F, Bigazzi F, and Sampietro T, *Tangier disease: epidemiology, pathophysiology, and management.* Am J Cardiovasc Drugs, 2012. **12**(5): p. 303-11.
57. Kang MH, Singaraja R, and Hayden MR, *Adenosine-triphosphate-binding cassette transporter-1 trafficking and function.* Trends Cardiovasc Med, 2010. **20**(2): p. 41-9.
58. Allikmets R, Singh N, Sun H, Shroyer NF, Hutchinson A, Chidambaram A, et al., *A photoreceptor cell-specific ATP-binding transporter gene (ABCR) is mutated in recessive Stargardt macular dystrophy.* Nat Genet, 1997. **15**(3): p. 236-46.

59. Molday RS, Zhong M, and Quazi F, *The role of the photoreceptor ABC transporter ABCA4 in lipid transport and Stargardt macular degeneration.* Biochim Biophys Acta, 2009. **1791**(7): p. 573-83.
60. Paolini A, Baldassarre A, Del Gaudio I, and Masotti A, *Structural Features of the ATP-Binding Cassette (ABC) Transporter ABCA3.* Int J Mol Sci, 2015. **16**(8): p. 19631-44.
61. Stahlman MT, Besnard V, Wert SE, Weaver TE, Dingle S, Xu Y, et al., *Expression of ABCA3 in developing lung and other tissues.* J Histochem Cytochem, 2007. **55**(1): p. 71-83.
62. Garmany TH, Moxley MA, White FV, Dean M, Hull WM, Whitsett JA, et al., *Surfactant composition and function in patients with ABCA3 mutations.* Pediatr Res, 2006. **59**(6): p. 801-5.
63. DeFelice M, Silberschmidt D, DiLauro R, Xu Y, Wert SE, Weaver TE, et al., *TTF-1 phosphorylation is required for peripheral lung morphogenesis, perinatal survival, and tissue-specific gene expression.* J Biol Chem, 2003. **278**(37): p. 35574-83.
64. Yamano G, Funahashi H, Kawanami O, Zhao LX, Ban N, Uchida Y, et al., *ABCA3 is a lamellar body membrane protein in human lung alveolar type II cells.* FEBS Lett, 2001. **508**(2): p. 221-5.
65. Mulugeta S, Gray JM, Notarfrancesco KL, Gonzales LW, Koval M, Feinstein SI, et al., *Identification of LBM180, a lamellar body limiting membrane protein of alveolar type II cells, as the ABC transporter protein ABCA3.* J Biol Chem, 2002. **277**(25): p. 22147-55.
66. Agassandian M and Mallampalli RK, *Surfactant phospholipid metabolism.* Biochim Biophys Acta, 2013. **1831**(3): p. 612-25.
67. Doan ML, Guillerman RP, Dishop MK, Nogee LM, Langston C, Mallory GB, et al., *Clinical, radiological and pathological features of ABCA3 mutations in children.* Thorax, 2008. **63**(4): p. 366-73.
68. Fitzgerald ML, Xavier R, Haley KJ, Welti R, Goss JL, Brown CE, et al., *ABCA3 inactivation in mice causes respiratory failure, loss of pulmonary surfactant, and depletion of lung phosphatidylglycerol.* J Lipid Res, 2007. **48**(3): p. 621-32.
69. Matsumura Y, Ban N, Ueda K, and Inagaki N, *Characterization and classification of ATP-binding cassette transporter ABCA3 mutants in fatal surfactant deficiency.* J Biol Chem, 2006. **281**(45): p. 34503-14.
70. Available from: http://www.genecards.org/cgi-bin/carddisp.pl?gene=ABCA3&keywords=abca3.
71. National Heart, Lung, and Blood Institute Exome Variant Server: http://evs.gs.washington.edu/EVS/.
72. Naderi HM, Murray JC, and Dagle JM, *Single mutations in ABCA3 increase the risk for neonatal respiratory distress syndrome in late preterm infants (gestational age 34-36 weeks).* Am J Med Genet A, 2014. **164A**(10): p. 2676-8.
73. Herber-Jonat S, Mittal R, Huppmann M, Hammel M, Liebisch G, Yildirim AO, et al., *Abca3 haploinsufficiency is a risk factor for lung injury induced by hyperoxia or mechanical ventilation in a murine model.* Pediatr Res, 2013. **74**(4): p. 384-92.
74. Kaltenborn E, Kern S, Frixel S, Fragnet L, Conzelmann KK, Zarbock R, et al., *Respiratory syncytial virus potentiates ABCA3 mutation-induced loss of lung epithelial cell differentiation.* Hum Mol Genet, 2012. **21**(12): p. 2793-806.

75. Campo I, Zorzetto M, Mariani F, Kadija Z, Morbini P, Dore R, et al., *A large kindred of pulmonary fibrosis associated with a novel ABCA3 gene variant.* Respir Res, 2014. **15**: p. 43.
76. Beers MF, Zhao M, Tomer Y, Russo SJ, Zhang P, Gonzales LW, et al., *Disruption of N-linked glycosylation promotes proteasomal degradation of the human ATP-binding cassette transporter ABCA3.* Am J Physiol Lung Cell Mol Physiol, 2013. **305**(12): p. L970-80.
77. Griese M, Kirmeier HG, Liebisch G, Rauch D, Stuckler F, Schmitz G, et al., *Surfactant lipidomics in healthy children and childhood interstitial lung disease.* PLoS One, 2015. **10**(2): p. e0117985.
78. Bernsel A, Viklund H, Hennerdal A, and Elofsson A, *TOPCONS: consensus prediction of membrane protein topology.* Nucleic Acids Res, 2009. **37**(Web Server issue): p. W465-8.
79. Weichert N, Kaltenborn E, Hector A, Woischnik M, Schams A, Holzinger A, et al., *Some ABCA3 mutations elevate ER stress and initiate apoptosis of lung epithelial cells.* Respir Res, 2011. **12**: p. 4.
80. Sasaki T, Kishi M, Saito M, Tanaka T, Higuchi N, Kominami E, et al., *Inhibitory effect of di- and tripeptidyl aldehydes on calpains and cathepsins.* J Enzyme Inhib, 1990. **3**(3): p. 195-201.
81. Buttle DJ, Murata M, Knight CG, and Barrett AJ, *CA074 methyl ester: a proinhibitor for intracellular cathepsin B.* Arch Biochem Biophys, 1992. **299**(2): p. 377-80.
82. Yasuma T, Oi S, Choh N, Nomura T, Furuyama N, Nishimura A, et al., *Synthesis of peptide aldehyde derivatives as selective inhibitors of human cathepsin L and their inhibitory effect on bone resorption.* J Med Chem, 1998. **41**(22): p. 4301-8.
83. Zheng X, Chu F, Mirkin BL, Sudha T, Mousa SA, and Rebbaa A, *Role of the proteolytic hierarchy between cathepsin L, cathepsin D and caspase-3 in regulation of cellular susceptibility to apoptosis and autophagy.* Biochim Biophys Acta, 2008. **1783**(12): p. 2294-300.
84. Schroder BA, Wrocklage C, Hasilik A, and Saftig P, *The proteome of lysosomes.* Proteomics, 2010. **10**(22): p. 4053-76.

5. Curriculum vitae

Personal data

Name:	Thomas Wittmann
Date of birth:	02.06.1987
Place of birth:	Neumarkt in der Oberpfalz

Contact information

Residence:	Alfred-Bischoff-Straße 11
	92318 Neumarkt
Email address:	T.Wittmann@gmx.net

Education

01/2013 - present: Doctoral thesis, LMU Munich, Hauner Children's Hospital, Pneumology I

- Thesis: "Categorization and classification of different ABCA3 variants causing interstitial lung disease"
- Supervision: Prof. Dr. med. Dominik Hartl and Prof. Dr. med. Matthias Griese

10/2010 - 09/2012: Master of Science (M.Sc.) in Cell and Molecular Biology, Friedrich-Alexander University of Erlangen

- Master thesis: "Expression and Function of SPARCL1 in Colorectal Carcinoma"

10/2007 - 09/2010: Bachelor of Science (B.Sc.) in Biology, Friedrich-Alexander University of Erlangen

- Bachelor thesis: "Charakterisierung eines Saccharose- und Citrattransporters aus *Xanthomonas campestris* pv. *vesicatoria*"

09/1995 - 06/2006: Grammar school, Willibald-Gluck-Gymnasium Neumarkt in der Oberpfalz

- Final exam: Abitur

6. Acknowledgements

An erster Stelle möchte ich mich bei Prof. Dr. Dominik Hartl und Prof. Dr. Matthias Griese für die persönliche und fachkompetente Betreuung und Unterstützung bedanken.

Des Weiteren bedanke ich mich recht herzlich bei Prof. Dr. Andreas Peschel für die Übernahme und Erstellung des Zweitgutachtens.

Außerdem danke ich unserem Postdoc Dr. Ralf Zarbock, der mir mit hilfreichen Ratschlägen zur Seite stand und immer ein offenes Ohr für neue Ideen hatte.

Traudl Wesselak, Kathrin Schiffl und Andrea Schams danke ich für die Mithilfe bei experimentellen Arbeiten.

Ein besonderer Dank gilt allen Kooperationspartnern, Dr. Jan Hegermann für die Anfertigung der elektronenmikroskopischen Aufnahmen, Dr. Gerhard Liebisch für die Messung und Analyse der Lipiddaten und Dr. Simone Reu für die Durchführung der immunhistochemischen Färbungen.

Einen herzlichen Dank an alle Mitarbeiter der AG Griese, im Besonderen an Daniela Rauch und Sabrina Frixel, die immer lustigen Gespräche im und außerhalb des Labors sowie unseren produktiven Kaffeepausen. Ohne euch wäre diese Arbeit unvorstellbar gewesen.

Abschließend möchte ich mich bei meinen Eltern, Geschwistern und insbesondere meiner Freundin Johanna für ihre großartige Unterstützung bedanken! Dafür, dass sie großes Interesse für meine Arbeit zeigten und immer für mich da waren.

7. Appendix

Paper 1

Wittmann T., Frixel S., Höppner S., Schindlbeck U., Schams A., Kappler M., Hegermann J., Wrede C., Liebisch G., Vierzig A., Zacharasiewicz A., Kopp M., Poets CF., Baden W., Hartl D., van Kaam AH., Lohse P., Aslanidis C., Zarbock R., and Griese M. (2016). *Increased risk of interstitial lung disease in children with a single R288K variant of ABCA3*. Mol. Med. (accepted)

Increased risk of interstitial lung disease in children with a single R288K variant of ABCA3

Thomas Wittmann[1#], Sabrina Frixel[1#], Stefanie Höppner[1], Ulrike Schindlbeck[1], Andrea Schams[1], Matthias Kappler[1], Jan Hegermann[2], Christoph Wrede[2], Gerhard Liebisch[3], Anne Vierzig[4], Angela Zacharasiewicz[5], Matthias Kopp[6], Christian F. Poets[7], Winfried Baden[7], Dominik Hartl[7], Anton H. van Kaam[8], Peter Lohse[9], Charalampos Aslanidis[3], Ralf Zarbock[1], and Matthias Griese[1,*]

[1]Dr. von Hauner Children's Hospital, Ludwig-Maximilians University, German Centre for Lung Research (DZL), Lindwurmstraße 2a, 80337 Munich, Germany

[2]Institute of Functional and Applied Anatomy, Hannover Medical School, Carl-Neuberg-Straße 1, German Center for Lung Research (DZL), Hannover, Germany

[3]Institute for Clinical Chemistry and Laboratory Medicine, University of Regensburg, Franz-Josef-Strauss-Allee 11, 93053 Regensburg, Germany

[4]Paediatric Intensive Care, University Children's Hospital, University of Cologne, Kerpener Straße 62, 50937 Cologne, Germany

[5]Department of Pediatrics, Wilhelminenspital, Montleartstraße 35 Pav. 21, 1160 Vienna, Austria

[6]Department of Pediatric Allergy and Pulmonology, University Luebeck, Airway Research Center North (ARCN), Ratzeburger Allee 160 23538, Lübeck

[7]Children's Hospital, University of Tuebingen, Hoppe-Seyler-Str. 1, 72076 Tuebingen, Germany.

[8]Department of Neonatology, Emma Children's Hospital, Academic Medical Center, Meibergdreef 9,1105 AZ Amsterdam, The Netherlands

[9]Doctor's Office for Human Genetics, CeGaT GmbH, Paul-Ehrlich-Straße 23, 72076 Tübingen, Germany.

Running head:

ABCA3 in children's interstitial lung disease

Key words:

Diffuse parenchymal lung disease; ABC transporter; ABCA3 carrier frequency; dipalmitoyl-phosphatidylcholine; lamellar bodies

This paper has supplementary material.

E-mail addresses

Thomas.Wittmann@med.uni-muenchen.de

Sabrina.Frixel@med.uni-muenchen.de

Stefanie.Hoeppner@med.uni-muuenchen.de

Ulrike.Schindlbeck@med.uni-muenchen.de

Andrea.Schams@med.uni-muenchen.de

Matthias.Kappler@med.uni-muenchen.de

Hegermann.Jan@mh-hannover.de

wrede.christoph@mh-hannover.de

Gerhard.Liebisch@klinik.uni-regensburg.de

anne.vierzig@uk-koeln.de

angela.zacharasiewicz@wienav.at

Matthias.Kopp@uksh.de

christian-f.poets@med.uni-tuebingen.de

winfried.baden@med.uni-tuebingen.de

dominik.hartl@med.uni-tuebingen.de

a.h.vankaam@amc.uva.nl

charalampos.aslanidis@klinik.uni-regensburg.de

peter.lohse@cegat.de

Ralf.Zarbock@med.uni-muenchen.de

Matthias.Griese@med.uni-muenchen.de

#contributed equally

*to whom correspondence should be addressed

Matthias Griese

Matthias.Griese@med.uni-muenchen.de

Phone 0049/(0)89/4400-57870

Fax 0049/(0)89/4400-57872

ABSTRACT

Rationale: The *ABCA3* gene encodes a lipid transporter in type II pneumocytes critical for survival and normal respiratory function. The frequent ABCA3 variant R288K increases the risk for neonatal respiratory distress syndrome among term and late preterm neonates, but its role in children´s interstitial lung disease has not been studied in detail.

Objectives: In a retrospective cohort study of 228 children with interstitial lung disease related to the alveolar surfactant system, the frequency of R288K was assessed and the phenotype of patients carrying a single R288K variant further characterized by clinical course, lung histology, computed tomography, and bronchoalveolar lavage phosphatidylcholine PC 32:0. Cell lines stably transfected with ABCA3-R288K were analysed for intracellular transcription, processing, and targeting of the protein. ABCA3 function was assessed by detoxification assay of doxorubicin, and the induction and volume of lamellar bodies.

Results: We found 9 children with interstitial lung disease carrying a heterozygous R288K variant, a frequency significantly higher than in the general Caucasian population. All identified patients had neonatal respiratory insufficiency, recovered, and developed chronic interstitial lung disease with intermittent exacerbations during early childhood. *In-vitro* analysis showed normal transcription, processing, and targeting of ABCA3-R288K, but impaired detoxification function and smaller lamellar bodies.

Conclusions: We propose that the R288K variant can underlie interstitial lung disease in childhood due to reduced function of ABCA3, demonstrated by decelerated detoxification of doxorubicin, reduced PC 32:0 content, and decreased lamellar body volume.

Abstract word count: 229 (250 Molecular Medicine)

INTRODUCTION

Interstitial lung diseases (ILD) encompass a large number of diffuse parenchymal lung disorders involving the lung parenchyma and the alveolar interstitium [1]. The disease spectrum is much broader in childhood, as many diseases primarily manifest during infancy [2]. The surfactant dysfunction disorders are the best molecularly characterized subgroups of ILD [3–5], and among these, variants in the ATP-binding cassette sub-family A member 3 (*ABCA3*) are the most frequent cause [6–8].

The carrier frequency of heterozygous ABCA3 variants in the population predicts disease prevalence of 1 in ~3100 European-descent and a total of ~750 homozygous newborns annually in the United States [9]. This incidence is in the range of that for cystic fibrosis (about 1 in 2500 European-descent infants) [10]. However sick patients carrying ABCA3 variants are not as frequently identified as could be expected based on these numbers. The main reason for this is the relatively large and thus costly analysis of the *ABCA3* gene, which is assessed mainly in very severe, frequently lethal courses of respiratory distress syndrome in the mature neonate [11, 12]. Additional reasons include many not or only poorly defined ABCA3 variants with unclear pathogenic significance [9, 13]. Some variants lead to rare but well characterized chronic children's interstitial lung disease with a firm histopathological pattern, including desquamative interstitial pneumonitis or non-specific interstitial pneumonitis [14, 15]. The ABCA3 variant R288K (c.863G>A) has been previously associated with pediatric respiratory disease [6] and a single copy was threefold to fourfold enriched among the European-descent infants with neonatal respiratory distress [9, 16, 17], although it is predicted to be benign and tolerated by the algorithms Polyphen and SIFT.

ABCA3 is a lipid transporter in alveolar type II cells, where it localizes to the outer membrane of lamellar bodies (LBs) which store surfactant. Variants in the *ABCA3* gene can impair the intracellular localization, processing and transport activity of the ABCA3 protein. For instance, ABCA3 with the variants L101P, L982P, L1553P, Q1591P, and Ins1518fs/ter1519 was retained in the endoplasmatic reticulum, whereas N568D, G1221S, and L1580P mutant ABCA3 proteins were correctly localized in the LB limiting membrane, but showed decreased ATP hydrolysis activity compared to wild type protein [12]. ABCA3 activity is also linked to LB biogenesis. Heterozygous $ABCA3^{+/-}$ knockout mice had fewer LB in their lungs [18]. Radiolabeled substrates, which were incorporated into newly synthesized disaturated phosphatidylcholine, phosphatidylglycerol, phosphatidylethanolamine and phosphatidylserine molecules, were lower in both LB and surfactant when compared to $ABCA3^{+/+}$ mice [18]. Additionally, inherited ABCA3 variants caused a decrease of total phosphatidylcholine content in bronchoalveolar lavage of infants and raised surface tension compared to control group [19, 20]. Molecular species patterns of phosphatidylcholine, i.e. dipalmitoyl-phosphatidylcholine (PC 32:0), were also decreased in lavage of affected children [20].

In this study we investigated the hypothesis that the ABCA3 variant R288K may be permissive for children´s interstitial lung disease. Supportive of such a connection would be an increased frequency of this variant in a population of patients affected by ILD over the general population, *ex-vivo* evidence from these subjects for a certain functional impairment related to ABCA3, and *in-vitro* data from cells expressing this variant and proving functionally concordant cellular abnormalities.

METHODS

Cohort

Between 2003 and 2012, 377 infants and children were diagnosed in the program for rare lung diseases of the Kids-Lung Register as suffering from ILD related to the alveolar surfactant region on a clinical, radiological and sometimes histological basis [21]. 228 of these patients were sequenced for variants in the *ABCA3* gene. In 62 patients possibly disease causing variants were identified and R288K was present in 11 cases. The latter patients were analysed in more detail (Supplemental tables 1, 2, 3). Two of these children (patients 10 and 11 in Suppl. Table 1) had additional damaging homozygous ABCA3 variants very likely to cause ABCA3 insufficiency and determine their clinical course. These subjects were considered separately in further analysis as we intended to understand the role of heterozygous R288K alone or in association with non-damaging variants. As control cohorts for the sequence variant frequencies the Caucasian collections were used (National Heart, Lung, and Blood Institute Exome Variant Server (EVS)).

Ethics Statement

All parents or the guardians of the children gave their informed consent; an older youth assented. The retrospective analysis of the data was approved by the institutional review board (EK 026-06) of the University of Munich. Prospective collection and analysis of data was performed under (EK 257-10) and the FP7-305653 project chILD-EU (EK 111-13).

Genetic analysis for *ABCA3, SFTPC* and *SFTPB*

Patients were investigated for variants in exons 4-33 of the *ABCA3* gene (NM_001089), in exons 1-11 of the *SFTPB* gene (NM_000542), and in exons 1-5 of the *SFTPC* gene (NM_003018) [22]. Genomic DNA was amplified by PCR using the primers listed (Suppl. Tab. 4). Electrophoresis of sequenced products was performed on an Applied Biosystems 3130xl Genetic Analyzer (Applied Biosystems, Darmstadt, Germany).

Plasmids

pT2/HB transposon vector was purchased from Addgene (Cambridge, United States, plasmid #26557). First, the puromycin resistance gene with corresponding PGK promoter elements was amplified from pLKO.1puro vector (purchased from Addgene, plasmid #8453) and cloned into the pT2/HB vector using EcoRI and HindIII restriction sites, yielding pT2/HB-puro. Second, *ABCA3* cDNA fused to a C-terminal HA-tag was amplified with corresponding CMV promoter elements from pcDNA4TO-*ABCA3*-HA vector and cloned into pT2/HB-puro using NheI and NotI restriction sites, yielding pT2/HB-puro-*ABCA3*-HA. The R288K point variant was introduced into pT2/HB-puro-*ABCA3*-HA using the Q5® site-directed mutagenesis kit (NEB, Massachusetts, United States) with following primers: R288K-for *5'-GAGAAGGAAAAGAGGCTGAAGGAGTAC-3'* and R288K-rev *5'-CTGCACGACAGCACGGGC-3'*. pCMV(CAT)T7-SB100 transposase was ordered from Addgene (plasmid #34879). All resulting vector constructs were verified using Sanger sequencing. Sequence analysis and alignment was done using Clone Manager Suite (Version 6.00).

Antibodies

The following antibodies were used: rabbit anti-HA (Sigma, Taufkirchen, Germany), rat anti-HA (Roche, Mannheim, Germany), mouse anti-CD63 (Abcam, Cambridge, United Kingdom), mouse anti-Calnexin (Novus Biologicals, Cambridge, United Kingdom), chicken horse radish peroxidase (HRP)-conjugated anti-β-Actin (Santa Cruz, Heidelberg, Germany), Alexa Fluor 488 goat anti-rabbit IgG and Alexa Fluor 555 goat anti-mouse IgG (Life Technologies, Darmstadt, Germany).

Cell culture

Human A549 and HEK293 cells were purchased from the German Collection of Microorganisms and Cell Cultures (DSMZ, Braunschweig, Germany). Both cell lines were maintained in RPMI 1640 medium (Gibco, Darmstadt, Germany) supplemented with 10% fetal calf serum (FCS) (Sigma) at 37°C and 5% CO_2.

Generation of single clones stably expressing ABCA3-HA

To evaluate the effect of the R288K point variant *in-vivo*, ABCA3-HA wildtype (WT) and mutated protein were stably transfected using the *"Sleeping Beauty"* transposon system into A549 cells and HEK293 cells, respectively. Therefore cells were seeded into 6-well plates and cotransfected with pCMV(CAT)T7-SB100 and pT2/HB-puro-*ABCA3*-HA WT or R288K respectively in the ratio of 2:5 using X-tremeGENE HP DNA transfection reagent (Roche). 48 hours post transfection, selection of stable cells were started by addition of 1 µg/ml Puromycin (Sigma). Single cell clones were obtained by transferring single cells into the wells of a 96-well plate.

Immunofluorescence staining

Stable A549 cells grown in 8-well slides (Ibidi, Martinsried, Germany) were washed twice with PBS (Sigma) and fixed with 4% paraformaldehyde (Sigma) for 20 min. After treating with 0.1 M glycine (Sigma) in PBS, cells were permeabilized with 0.1% TritonX 100 (Sigma) for 10 min. Unspecific binding sites were blocked with 3% BSA (Sigma) and 10% FCS in PBS for 30 minutes. Labelling with primary antibodies was carried out for 1 h at room temperature. Cells were washed three times with PBS and stained with the appropriate Alexa Fluor secondary antibodies. After washing three times with PBS, cells were stained with 0.1 µg/ml DAPI (Sigma) for 10 minutes and washed with PBS. The cells were immediately covered with mounting medium (90% glycerine in PBS and 2% DABCO (Sigma)). Objects were viewed with an Olympus IX81/Fluoview FV1000 confocal laser scanning microscope and imaged with the Olympus Fluoview version 4.2 software.

Real-time PCR

Total RNA was collected from cells grown for 48h in 6-well plates using the High-Pure RNA Isolation Kit (Roche) according to the manufacturer's instructions. RNA concentrations were determined with a NanoDrop spectrophotometer (Thermo Scientific, Darmstadt, Germany). One microgram of total RNA was transcribed into cDNA with the Tetro cDNA Synthesis Kit (Bioline, Luckenwalde, Germany). Real-time PCR was carried out on a 7900HT Fast Real-Time PCR System (Bioline) using SYBR green (Life Technologies) and following primers: ABCA3-for *5'-CATGGTCAGCACCTTCTTCA-3'*, ABACA3-rev *5'-TTCTGGCTCAGAGTCATCCA-3*', HPRT-for *5'-GCTGACCTGCTGGATTAC-3'* HPRT-rev *5'-TGCGACCTTGACCATCTT*. Relative changes in gene expression caused by ABCA3-WT

or R288K variant were calculated using the $2^{-\Delta\Delta CT}$ method with hypoxanthine-guanine phosphoribosyltransferase (HPRT) as housekeeper.

Immunoblotting

Cells were seeded in 6-well plates for 48h and then rinsed with PBS once and subsequently trypsinized and again washed with PBS. After that, cells were lysed with radioimmunoprecipitation assay (RIPA) buffer containing 0.15 M sodium chloride, 1% Triton-X 100, 0.5% sodium deoxycholate, 0.1% sodium dodecylsulfate, 5 mM ethylene diamine tetraacetic acid (EDTA) and 50 mM Tris pH 8 (Sigma). RIPA buffer was accomplished by complete protease inhibitor (Roche). The lysate was centrifuged for 30 min at 1000 x g and 4°C. The Protein concentration of the post-nuclear supernatant (i.e. whole-cell lysate) was determined with the Pierce BCA protein assay using bovine serum albumin (BSA) as the protein standard. Totally, 20 µg of cell lysates in 4xLDS buffer (Invitrogen, Darmstadt, Germany) were loaded onto NuPage Mini Tris-Acetate gels (Invitrogen). Following gel electrophoresis, proteins were blotted to polyvinylidene fluoride membranes (Millipore, Darmstadt, Germany). After transfer, membranes were blocked with 5% skim milk in TBS-T (Sigma). Membranes were incubated over night with primary antibodies in blocking solution. After washing the membranes three times with TBS-T, HRP-conjugated secondary antibodies were applied 1 h at room temperature. Detection was performed using ECL reagent (GE Healthcare, Munich, Germany).

Viability assay

Cell viability was assessed by determining cleavage of 2,3-bis (2-methoxy-4-nitro-sulfophenyl)-2H-tetrazolium-5-carboxyanilide (XTT, Sigma) in the presence of phenazine

methosulfate. For XTT assay, cells were seeded in 96-well plates in RPMI medium containing 10% FCS and no phenol red. After different points of time, absorbance was measured at 490 nm and 650 nm using a spectrophotometer.

Cytotoxicity assay

Triplicates of A549 cells stably transfected with ABCA3-WT and ABCA3-R288K and cells transfected with mock control were seeded into 6-well plates. After an incubation time of 96h, cell supernatants were harvested and the amount of the lactate dehydrogenase (LDH) enzyme was quantified colorimetrically at 490 nm using the CytoTox 96® Non-Radioactive Cytotoxicity Assay (Promega, Mannheim, Germany) according to the manufacturer's instructions. The resulting optical densities were referred to numbers of cells counted with the Cellometer Auto T4 Cell Viability Counter (Nexcelom, Bramsche, Germany).

Lipid analyses of human bronchoalveolar lavages

After protein level determination, lipids of bronchoalveolar lavages (BALs) obtained from the patients were analysed by ESI-MS/MS in positive ion mode as described [20].

Doxorubicin assay

For doxorubicin assay HEK293 cells stably expressing ABCA3 wild type protein or R288K variant were seeded as octuplicate in 96-well plates at a density of 1 x 10^5 cells per well. After attaching to 96-well plate HEK293 cells were treated with different concentrations of doxorubicin for 3h. Cells were washed subsequently with PBS and incubated for further 24h in RPMI medium containing 10 % FCS and no phenol red under normal conditions. Viability was measured with XTT assay (as previously described).

Electron microscopy

Cells were fixed in 150 mM HEPES, pH 7.35, containing 1.5 % formaldehyde and 1.5 % glutaraldehyde (Sigma) at room temperature for 30 min and then at 4°C overnight. After dehydration in acetone, cells were embedded in EPON. 50 nm sections were stained with 4 % uranyl acetate and lead citrate and observed in a Morgagni TEM (FEI). Images were taken with a 2 K side mounted Veleta CCD camera.

Calculation of vesicle volume

A549 cells containing either ABCA3 wild type or R288K protein variant were seeded in 8-well slides (Ibidi). After an incubation time of 48h, cells were fixed as described above and immunostained against HA-tag. Cells were imaged with the confocal laser scanning microscope. Diameter of each ABCA3-HA containing vesicle was determined with ImageJ software tool. Vesicle volume was calculated with formula: $V = \frac{4}{3} * \pi * r^3$. 60 different ABCA3-HA containing vesicles were randomly chosen from three distinct experiments, thus analysing 20 vesicles per condition and experiment.

Statistical analyses

Dependency on gestational age of the different ABCA3 variants was analysed using Fisher's exact test. Comparisons of two groups were done using student's t-test. Comparisons of multiple groups were done using one-way repeated measure ANOVAs with Tuckey's post hoc test. Doxorubicin assay, phospholipid (PL) classes and phosphatidylcholine (PC) species were analyzed using two-way repeated measure ANOVAs with Sidak's post hoc test. Results were presented as mean ± SEM of a minimum of three different experiments. P-values < 0.05 were considered to be statistically significant. All tests were performed using Graph-Pad Prism 6.0 (GraphPad Software).

RESULTS

Clinical characterization of children with interstitial lung disease and R288K

In our cohort of 228 children with ILD and ABCA3 sequenced, we identified 11 subjects as carriers of R288K. This frequency of R288K was clearly enriched over that in the general Caucasian population (71 R288K in 4229 Caucasian subjects of the Exom variant server (National Heart, Lung, and Blood Institute Exome Variant Server (EVS)) (P=0.0014)). We next analysed the dependency on gestational age of the different ABCA3 variants identified. Whereas all the other possibly disease causing ABCA3 variants were evenly distributed among mature and immature infants, R288K was found more frequently in premature infants (Table 1).

All our patients carrying a single heterozygous R288K variant were Caucasians, had non-consanguineous parents and did not carry known disease-causing genetic variants in *SFTPC* and *SFTPB* (Suppl. Table 1). In all children, the initial manifestation of lung disease was during the neonatal period, only 5 were premature infants (median gestational age 30 weeks, range 27 to 32). 6 children were mechanically ventilated; most recovered and had chronic or intermittent episodes with respiratory symptoms during infancy and childhood. Those old enough to perform lung function tests had restrictive lung disease (Suppl. Table 2). The CT pattern was consistent with ILD in 6 of the 9 children. In 2 where no CT scan was available histology documented ILD. Six of the 9 children had lung biopsies, always showing ILD alone or in combination with emphysematous areas (Suppl. Table 3).

No evidence for impaired ABCA3 transport activity in children with chronic ILD and heterozygous for R288K

Initially, we excluded severe ABCA3 deficiency as the molecular cause of the diseases by excluding complete ABCA3 deficiency and demonstrating evidence for some ABCA3 function (Table 2). The subjects had regular ABCA3 histopathologic staining (available in 4 subjects), had normally formed lamellar bodies (available in 3 subjects) or had a dipalmitoyl-phosphatidylcholine (PC 32:0) content in bronchoalveolar lavage (in 6 subjects available) that was on average a little higher than typically found in infants with ABCA3 deficiency, but significant lower than in healthy children (Figure 1). In 3 other subjects, no such investigations were done due to mild and improving course.

It was of interest that all patients heterozygous for R288K presented to us, as infants or children, rather than as neonates, with an unusual course of ILD, and which, their treating physicians could not explain by prematurity or perinatal lung injury. All surviving children improved, but their ILD was not cured at follow up. Despite broad clinical investigations, no other causes of their ILD could be identified.

To summarize, these children with chronic ILD had enrichment of the R288K variant in ABCA3 and somewhat reduced dipalmitoyl-phosphatidylcholine in the alveolar space, i.e. strong epidemiologic and biochemical evidence for an involvement of ABCA3 in their pathogenesis. Although the R288K variant was predicted not to be detrimental to protein function by SIFT and Polyphen, our data nonetheless suggest impairment of ABCA3 function due to the presence of this particular variant. Therefore, we performed detailed studies on the cellular effects of the R288K variant.

Transcription, intracellular processing, and cellular targeting of R288K in ABCA3-transfected lung cells

Stable transfection of A549 cells with DNA coding for ABCA3-WT or ABCA3-R288K induced *ABCA3*-mRNA transcription of 200-fold compared to mock transfected cells (Supplemental Figure 1A). Intracellular processing as assessed by Western immunoblotting did not differ between ABCA3-WT and ABCA3-R288K. Both proteins were present as the 190 and 170 kDa processing forms (Supplemental Figure 1B) and their intensity ratios did not differ (Supplemental Figure 1C). Cell growth and proliferation were unaffected in comparison to mock controls (Supplemental Figure 1D, 1E). Intracellular localization was investigated by immunofluorescence staining and revealed normal colocalization of both, the wild type and the R288K mutated ABCA3 protein with CD63, a marker for late endosomes and lamellar bodies (Supplemental Figure 1F). Obvious protein misfolding was ruled out by lack of colocalization with the ER-resident chaperone calnexin (Supplemental Figure 1G). These findings were confirmed independently in HEK293 cells. Whereas there was no difference in protein expression, mRNA expression differed between ABCA3-WT and ABCA3-R288K expressing cells (Supplemental figure 2).

Impaired ABCA3-dependent doxorubicin detoxification in R288K variants

ABCA3 transport activity was analysed in HEK293 cells stably transfected with ABCA3-WT or ABCA3-R288K by means of their ability to detoxify doxorubicin (Supplemental Figure 2). High activity of the transporter, i.e. overexpression of ABCA3 protein in childhood acute myeloic leukaemia patients, induced resistance against doxorubicin [23]. HEK293 cells stably expressing R288K mutated ABCA3 protein had a diminished viability compared to cells expressing WT protein when treated with 5,10 or 20 μM of doxorubicin respectively (Figure 2A). In concordance, the morphology of the cells expressing ABCA3-R288K was altered to a

round-shaped appearance compared to ABCA3-WT expressing cells (Figure 2B; 10 μM Doxo). These results point to a reduced ABCA3 transport activity as a result of the R288K variant.

Lamellar bodies of ABCA3 with the R288K variant

Electron microscopy of A549 cells stably expressing ABCA3-WT or R288K mutated protein revealed an induction of lamellar body (LB)-like structures in A549 cells (Figures 3A, 3B). LB-like structures of both cell lines showed well-formed organelles containing concentric membranes arranged in parallel. Volumes of LB-like structures in cells expressing ABCA3-R288K were quantitatively compared to cells expressing ABCA3-WT protein. Using immunofluorescence staining of A549 cells stably expressing ABCA3-R288K, smaller ABCA3-positive vesicles were found compared to cells expressing ABCA3-WT protein (Figure 4).

DISCUSSION

In this study we present a cohort of children with chronic ILD characterized by their carriage of a single R288K variant of ABCA3. All children suffered from a mainly restrictive lung disease with the typical histological and chest CT imaging pattern of chronic pediatric ILD. However, they did not exhibit the generic features of complete ABCA3 deficiency. We present evidence that the presence of the R288K variant interferes with ABCA3's transport activity. Therefore, we propose that the development and long term persistence of chronic ILD in our cohort was due to the presence of a single R288K variant of ABCA3 and not a result of their neonatal history of respiratory distress following either term or preterm birth.

Manifestation of ABCA3 deficiency due to homozygous or compound heterozygous variants causes severe respiratory distress in mature infants, frequently leading to early death [11, 12] or chronic ILD in a small number of older children and young adults [14, 15]. In this study, we characterize subjects carrying the R288K variant on a single allele and suffering from a characteristic chronic pediatric ILD phenotype. Whereas the individual course of their lung disease was quite variable, all patients had a characteristic diffuse parenchymal lung disease. Histology of lung biopsies demonstrated ILD present with almost the entire spectrum of histologic patterns known for these conditions, including pulmonary alveolar proteinosis (PAP), non-specific interstitial pneumonitis (NSIP), desquamative interstitial pneumonitis (DIP), chronic pneumonitis of infancy (CPI), interstitial emphysema, dystelectasis and eosinophilia, often in combination. Such heterogeneity is not unusual, even in the presence of the same disease causing variants [2, 4, 21], and likely represents the morphologic response of lung parenchyma to variable injuries in different individuals.

Our data suggest that heterozygous R288K variants in ABCA3 are not strong enough determinants permitting the manifestation of ILD in the absence of additional factors. This is supported by the fact that only two out of nine parents carrying the variant had some, but not severe respiratory symptoms. However, the precise nature of their conditions was not investigated to great detail. In our patients, neonatal respiratory distress was a consistent feature, together with injury from recurrent airway infections. The strong interaction of single ABCA3 variants and prematurity was previously demonstrated [17] and confirmed here. Other modifying factors may be present like cis-acting elements, introns or non-translated regions within the *ABCA3* gene, which were not covered by our sequencing strategy [24]. Whereas variants in *SFTPC* or *SFTPB* were excluded, variants in other genes not directly related to ABCA3 expression, epigenetic regulation, and additional environmental or developmental factors are also conceivable. Furthermore, previous studies showed that some ABCA3 variants had a mild cellular effect, associated with increased inflammation [25].

Lower levels of phosphatidylcholine and dipalmitoyl-phosphatidylcholine in the alveolar space of the infants are likely to be a result of functional impairment of ABCA3-R288K. The other phospholipid species (lyso-phosphatidylcholine, phosphatidylglycerol, sphingomyelin, phosphatidylethanolamine, phosphatidylserine) were not different. Additionally, a reduced capacity for detoxification of doxorubicin and a smaller volume of ABCA3-positive vesicles provide *in-vitro* evidence for reduced ABCA3 transport function due to the presence of the R288K variant. Taken together these data point to a causative role of the R288K variant. Although the functional impairment of ABCA3-R288K is likely too small to induce lung disease on its own, when acting in combination with significant respiratory stress at birth or later in life during respiratory tract infections, its effects will become amplified and will cause notable clinical symptoms.

As there is a strong developmental dependency of ABCA3 expression with an increase towards birth [26], an increased vulnerability in premature infants is expected. The strong association of the R288K variant with respiratory distress obviously results from a partially defective surfactant lipid transport, which will have a more pronounced effect the more immature the baby.

Mice carrying *ABCA3* knockout on a single allele show an increased susceptibility to injury [27]. Similarly, single point variants in the *ABCA3* gene can reduce the expression of mature protein, presumably by increasing ER-associated degradation of misfolded protein [28]. Beyond the neonatal period, infants carrying a single R288K variant of ABCA3 may be more vulnerable to lung injury affecting the alveolar space, resulting in an increased risk of chronic pediatric ILD involving surfactant dysfunction. Among the most likely mechanisms triggering ILD in our patients were the frequently observed viral and other respiratory tract infections, which put an enormous burden on the ABCA3-dependent lung surfactant system. As demonstrated previously and in agreement with our *ex-vivo* measurements, infection with respiratory syncytial virus strongly impaired the expression of alveolar type 2 cell differentiation marker SP-C and other key epithelial cell proteins in the presence of ABCA3 varints. Simultaneously, a mesenchymal phenotype was acquired, indicating development of pulmonary fibrosis [29].

Our observations imply that the presence of a single mutated allele is permissive to cause symptoms in conjunction with common and usually well-tolerated burdens of the respiratory system. This is in concordance with findings in individuals with single allele variants in another ABC transporter, i.e. ABCA7 also called cystic fibrosis transmembrane regulator (CFTR). The expression of single alleles increases the risk for bronchiectasis [30, 31] and rhinosinusitis [32], as well as extra pulmonary manifestations of cystic fibrosis like

pancreatitis [33, 34] or azoosermia [35]. In the case of ABCA3-R288K, it remains to be elucidated whether the effects of the variants can be explained by haploinsufficiency alone or if the variant exerts a dominant-negative effect.

Whereas a major strength of our study is the detailed cellular analysis of the R288K variant, identifying mechanisms by which it may exert its disadvantageous effects, there are some weaknesses in our study, including its retrospective design resulting in variable follow up, a relatively low number of cases due to the rarity of pediatric ILD, and the fact that biopsies were obtained in many but not all cases. In addition the cellular model is not perfect as clonal differences might account in part for the results; the transfection is homozygous since either ABCA3-WT or R288K variant were introduced and, although we used two different cell lines yielding similar results, these are still different from primary type II cells. On the other hand, this is a third and independent cohort demonstrating some pathogenic potential of R288K, showing for the first time a role in pediatric ILD, and providing detailed cell biological analysis.

Taken together, we show that the presence of the ABCA3-R288K variant on a single allele, when acting together with aggravating external stressors like prematurity or recurrent respiratory infections, can cause respiratory insufficiency and ILD. We also demonstrate that in spite of R288K having been predicted to be neutral by *in-silico* prediction algorithms, this particular variant indeed may cause functional impairment of ABCA3 leading to clinically relevant consequences. This finding also highlights the notion that results from prediction algorithms for variants identified during analysis of next generation sequencing data need to be backed by clinical and experimental data.

Acknowledgements: The authors thank all patients and their proxies who participated in the study. The work of M.G. was supported by DFG-970/8-1, chILD-EU (FP7, No. 305653), and the BMBF (German center for lung research (DZL)).

Disclosure: The authors declare they have no competing interests as defined by *Molecular Medicine*, or other interests that might be perceived to influence the results and discussion reported in this paper.

REFERENCES

1. Schwarz MI, King TE (2011) Interstitial lung disease, 5th ed. People's Medical Pub. House, Shelton, Conn.
2. Deutsch GH, Young LR, Deterding RR, Fan LL, Dell SD, Bean JA, Brody AS, Nogee LM, Trapnell BC, Langston C et al. (2007) Diffuse lung disease in young children: application of a novel classification scheme. Am J Respir Crit Care Med 176(11): 1120–1128
3. Hildebrandt J, Yalcin E, Bresser H, Cinel G, Gappa M, Haghighi A, Kiper N, Khalilzadeh S, Reiter K, Sayer J et al. (2014) Characterization of CSF2RA mutation related juvenile pulmonary alveolar proteinosis. Orphanet J Rare Dis 9: 171. DOI:10.1186/s13023-014-0171-z
4. Kröner C, Reu S, Teusch V, Schams A, Grimmelt A, Barker M, Brand J, Gappa M, Kitz R, Kramer BW et al. (2015) Genotype alone does not predict the clinical course of SFTPC deficiency in paediatric patients. Eur. Respir. J. DOI:10.1183/09031936.00129414
5. Whitsett JA, Wert SE, Weaver TE (2015) Diseases of pulmonary surfactant homeostasis. Annual review of pathology 10: 371–393. DOI:10.1146/annurev-pathol-012513-104644
6. Brasch F, Schimanski S, Mühlfeld C, Barlage S, Langmann T, Aslanidis C, Boettcher A, Dada A, Schroten H, Mildenberger E et al. (2006) Alteration of the Pulmonary Surfactant System in Full-Term Infants with Hereditary ABCA3 Deficiency. Am J Respir Crit Care Med 174: 571–580
7. Nogee LM, Garnier G, Dietz HC, Singer L, Murphy AM, deMello DE, Colten HR (1994) A mutation in the surfactant protein B gene responsible for fatal neonatal respiratory disease in multiple kindreds. J Clin Invest 93(4): 1860–1863

8. Whitsett JA, Wert SE, Weaver TE (2010) Alveolar surfactant homeostasis and the pathogenesis of pulmonary disease. Annu Rev Med 61: 105–119

9. Wambach JA, Wegner DJ, Depass K, Heins H, Druley TE, Mitra RD, An P, Zhang Q, Nogee LM, Cole FS et al. (2012) Single ABCA3 mutations increase risk for neonatal respiratory distress syndrome. Pediatrics 130(6): e1575-e1582

10. Hodson ME, Geddes DM (1995) Cystic fibrosis, 1st ed. Chapman & Hall Medical, London, New York

11. Cheong N, Madesh M, Gonzales LW, Zhao M, Yu K, Ballard PL, Shuman H (2006) Functional and trafficking defects in ATP binding cassette A3 mutants associated with respiratory distress syndrome. J Biol Chem 281(14): 9791–9800

12. Matsumura Y, Ban N, Ueda K, Inagaki N (2006) Characterization and classification of ATP-binding cassette transporter ABCA3 mutants in fatal surfactant deficiency. J Biol Chem 281(45): 34503–34514

13. Doan ML, Guillerman RP, Dishop MK, Nogee LM, Langston C, Mallory GB, Sockrider MM, Fan LL (2008) Clinical, radiological and pathological features of ABCA3 mutations in children. Thorax 63(4): 366–373

14. Bullard JE, Wert SE, Whitsett JA, Dean M, Nogee LM (2005) ABCA3 mutations associated with pediatric interstitial lung disease. Am J Respir Crit Care Med 172(8): 1026–1031

15. Campo I, Zorzetto M, Mariani F, Kadija Z, Morbini P, Dore R, Kaltenborn E, Frixel S, Zarbock R, Liebisch G et al. (2014) A large kindred of pulmonary fibrosis associated with a novel ABCA3 gene variant. Respir. Res. 15(1): 43. DOI:10.1186/1465-9921-15-43

16. Wambach JA, Casey AM, Fishman MP, Wegner DJ, Wert SE, Cole FS, Hamvas A, Nogee LM (2014) Genotype-phenotype correlations for infants and children with ABCA3 deficiency. Am J Respir Crit Care Med 189(12): 1538–1543. DOI:10.1164/rccm.201402-0342OC

17. Naderi HM, Murray JC, Dagle JM (2014) Single mutations in ABCA3 increase the risk for neonatal respiratory distress syndrome in late preterm infants (gestational age 34-36 weeks). American journal of medical genetics. Part A 164A(10): 2676–2678. DOI:10.1002/ajmg.a.36660

18. Cheong N, Zhang H, Madesh M, Zhao M, Yu K, Dodia C, Fisher AB, Savani RC, Shuman H (2007) ABCA3 is critical for lamellar body biogenesis in vivo. J Biol Chem 282(33): 23811–23817

19. Garmany TH, Moxley MA, White FV, Dean M, Hull WM, Whitsett JA, Nogee LM, Hamvas A (2006) Surfactant composition and function in patients with ABCA3 mutations. Pediatr Res 59(6): 801–805

20. Griese M, Kirmeier HG, Liebisch G, Rauch D, Stückler F, Schmitz G, Zarbock R (2015) Surfactant lipidomics in healthy children and childhood interstitial lung disease. PLoS One 10(2): e0117985. DOI:10.1371/journal.pone.0117985

21. Griese M, Irnstetter A, Hengst M, Burmester H, Nagel F, Ripper J, Feilcke M, Pawlita I, Gothe F, Kappler M et al. (2015) Categorizing diffuse parenchymal lung disease in children. Orphanet J Rare Dis 10(1): 122. DOI:10.1186/s13023-015-0339-1

22. Griese M, Lorenz E, Hengst M, Schams A, Wesselak T, Rauch D, Wittmann T, Kirchberger V, Escribano A, Schaible T et al. (2015) Surfactant proteins in pediatric interstitial lung disease. Pediatr. Res. DOI:10.1038/pr.2015.173

23. Steinbach D, Gillet J, Sauerbrey A, Gruhn B, Dawczynski K, Bertholet V, de Longueville F, Zintl F, Remacle J, Effert T (2006) ABCA3 as a Possible Cause of Drug Resistance in Childhood Acute Myeloid Leukemia. Clin Cancer Res 12(14): 4357–4363

24 Agrawal A, Hamvas A, Cole FS, Wambach JA, Wegner D, Coghill C, et al. (2012) An intronic ABCA3 mutation that is responsible for respiratory disease. Pediatr Res. 71(6): p. 633-7

25. Flamein F, Riffault L, Muselet-Charlier C, Pernelle J, Feldmann D, Jonard L, Durand-Schneider AM, Coulomb A, Maurice M, Nogee LM, et al. (2012) Molecular and cellular characteristics of ABCA3 mutations associated with diffuse parenchymal lung diseases in children. Hum Mol Genet. 21(4): p. 765-75.

26. Stahlman MT, Besnard V, Wert SE, Weaver TE, Dingle S, Xu Y, Zychlin K von, Olson SJ, Whitsett JA (2007) Expression of ABCA3 in developing lung and other tissues. J Histochem Cytochem 55(1): 71–83

27. Herber-Jonat S, Mittal R, Huppmann M, Hammel M, Liebisch G, Yildirim AÖ, Eickelberg O, Schmitz G, Hrabé de Angelis, Martin, Flemmer AW et al. (2013) Abca3 haploinsufficiency is a risk factor for lung injury induced by hyperoxia or mechanical ventilation in a murine model. Pediatr. Res. 74(4): 384–392. DOI:10.1038/pr.2013.127

28. Weichert N, Kaltenborn E, Hector A, Woischnik M, Schams A, Holzinger A, Kern S, Griese M (2011) Some ABCA3 mutations elevate ER stress and initiate apoptosis of lung epithelial cells. Respir Res. 2011 Jan 7;12:4. doi: 10.1186/1465-9921-12-4.

29. Kaltenborn E, Kern S, Frixel S, Fragnet L, Conzelmann KK, Zarbock R, Griese M (2012) Respiratory syncytial virus potentiates ABCA3 mutation-induced loss of lung epithelial cell differentiation. Hum Mol Genet. DOI:10.1093/hmg/dds107

30. Ziedalski TM, Kao PN, Henig NR, Jacobs SS, Ruoss SJ (2006) Prospective analysis of cystic fibrosis transmembrane regulator mutations in adults with bronchiectasis or pulmonary nontuberculous mycobacterial infection. Chest 130(4): 995–1002. DOI:10.1378/chest.130.4.995

31. Casals T, De-Gracia J, Gallego M, Dorca J, Rodríguez-Sanchón B, Ramos MD, Giménez J, Cisteró-Bahima A, Olveira C, Estivill X (2004) Bronchiectasis in adult patients: an expression of heterozygosity for CFTR gene mutations? Clinical genetics 65(6): 490–495. DOI:10.1111/j.0009-9163.2004.00265.x

32. Wang X, Kim J, McWilliams R, Cutting GR (2005) Increased prevalence of chronic rhinosinusitis in carriers of a cystic fibrosis mutation. Archives of otolaryngology--head & neck surgery 131(3): 237–240. DOI:10.1001/archotol.131.3.237

33. Ooi CY, Durie PR (2012) Cystic fibrosis transmembrane conductance regulator (CFTR) gene mutations in pancreatitis. J. Cyst. Fibros. 11(5): 355–362. DOI:10.1016/j.jcf.2012.05.001

34. Sharer N, Schwarz M, Malone G, Howarth A, Painter J, Super M, Braganza J (1998) Mutations of the cystic fibrosis gene in patients with chronic pancreatitis. N Engl J Med 339(10): 645–652. DOI:10.1056/NEJM199809033391001

35. Sharma H, Mavuduru RS, Singh SK, Prasad R (2014) Increased frequency of CFTR gene mutations identified in Indian infertile men with non-CBAVD obstructive azoospermia and spermatogenic failure. Gene 548(1): 43–47. DOI:10.1016/j.gene.2014.07.005

LEGENDS TO THE FIGURES

Fig 1: **Levels of phosphatidylcholine and dipalmitoyl-phosphatidylcholine in bronchoalveolar lavage fluid of infants heterozygous for R288K in ABCA3.**

A. Phosphatidylcholine of patients carrying heterozygote R288K variant (n=4) compared to healthy control group (n=11). Data are shown in % of all analyzed PL classes measured in BAL. **B.** Dipalmitoyl-phosphatidylcholine amounts of healthy patients (n=11) and patients with R288K variant (n=4) measured in BAL. Data are shown in % of total PC. All results were expressed as mean ± SEM. *$p < 0.05$; ***$p < 0.001$

Fig 2: **Induction of cellular multidrug resistance *in-vitro* by ABCA3. A.** Effects of soluble doxorubicin on viability of HEK293 cells stably expressing ABCA3-WT or ABCA3-R288K protein. Different concentrations of doxorubicin were used and viability was measured with XTT assay. Values are displayed as means ± SEM of HEK293 cells stably expressing either ABCA3 wild type protein (solid line) or R288K mutated ABCA3 protein (dashed line). *$P < 0.05$; ****$P < 0.0001$. **B.** Light microscopy of HEK293 cells stably expressing ABCA3-WT and ABCA3-R288K protein respectively. Additionally cells were treated with 10µM doxorubicin for 3h and displayed after 24h of growth in RPMI medium supplemented with 10% FCS under normal conditions.

Fig. 3: Transmission electron microscopy. Electron Microscopy of A549 cells expressing ABCA3-WT (**A**) or ABCA3-R288K (**B**). Several lamellar bodies are visible in the overviews. These exhibit concentric lamellae, as distinguishable in the higher magnifications (insets). Scale bars are 1 µm for overviews and 0.5 µm for insets.

Fig. 4: **Determination of vesicle volumes in A549 cells with ABCA3-WT or ABCA3-R288L protein**. **A.** Immunofluorescence staining of HA-tagged ABCA3 vesicles imaged with a confocal microscope. Shown is either ABCA3-WT (left) or ABCA3-R288K containing vesicles (right). **B.** Volumes of ABCA3 containing vesicles harbouring either ABCA3-WT or ABCA3-R288K were calculated on the basis of vesicle diameters determined with ImageJ software tool. ***P<0.001

TABLES

Table 1: Frequencies of ABCA3 variants among 228 neonates and infants (mean gestational age 35.4 weeks) sequenced for ABCA3 variants and interstitial lung disease.

Gestational age (wks)	< 37		≥ 37		
Mean gestational age (wks)	31.6	31.3	39.4	39.4	
ABCA3 variant present	Yes	No	Yes	No	P#
Any variants	15	48	47	118	0.5106
R288K	6	8	5	43	0.0012
R288K without other disease causing ABCA3 variant (n=2)	6	8	3	43	0.0001

Fisher's exact test

Table 2: *Ex-vivo* evidence for functionality of ABCA3 transport activity

Patient	Code	Immunohistologic staining for ABCA3	Electron-microscopy	Dipalmitoyl-phosphatidylcholine (PC 32:0) (% total PC) in BAL	Overall evidence for ABCA3 transport activity
	Expected normal result[#]:	Type 2 cells with granular ring like structures	Concentric lamellar	45.8 ± 3.6[##]	
1	199	N.a.	Yes, normal	40.8	Yes
2	652	N.a.	N.a.	40.7	Yes
3	1300	Yes, normal	Yes, normal	41.1	Yes
4	1468	Yes, normal	N.a.	42.1[###]	Yes
5	1479	Yes, normal	N.a.	23.5	Yes, marginal
6	1601	N.a.	N.a.	n.a.	Yes, no investigations as mild course
7	2253	Yes, normal	Yes, normal	30.6[###]	Yes
8	2405	N.a.	N.a.	n.a.	Yes, no investigations as mild course
9	2741	N.a.	N.a.	n.a.	Yes, no investigations as mild course

[#]Griese, Kiermeier et al 2015; [##]Dipalmitoyl-phosphatidylcholine (PC 32:0) was 12.7 ± 4.2 % of total PC in 4 subjects with severe neonatal disease causing ABCA3 variants; [###]Lung tissue. N.a. = Not available

FIGURES

Figure 1

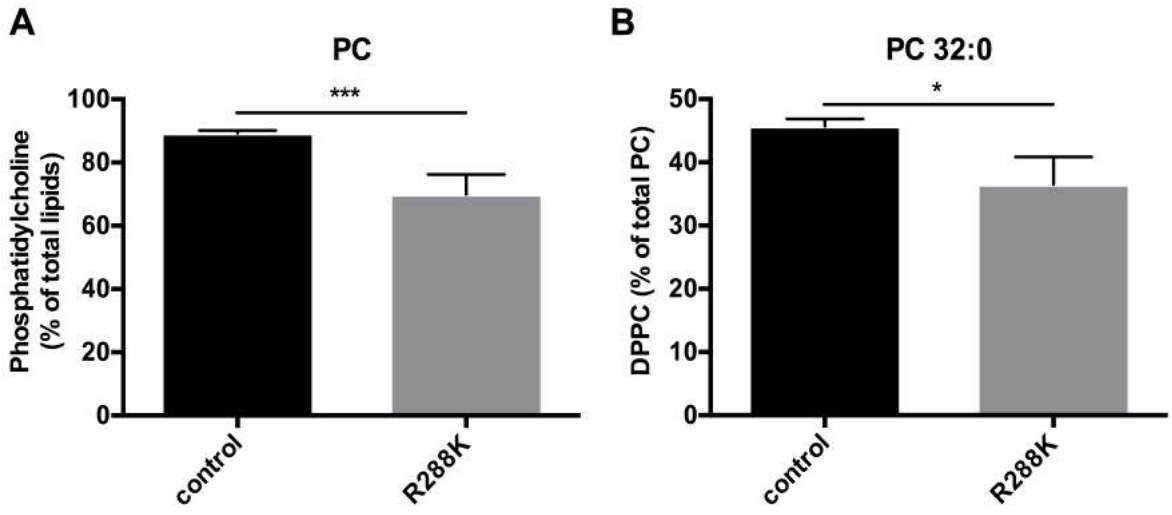

Figure 2

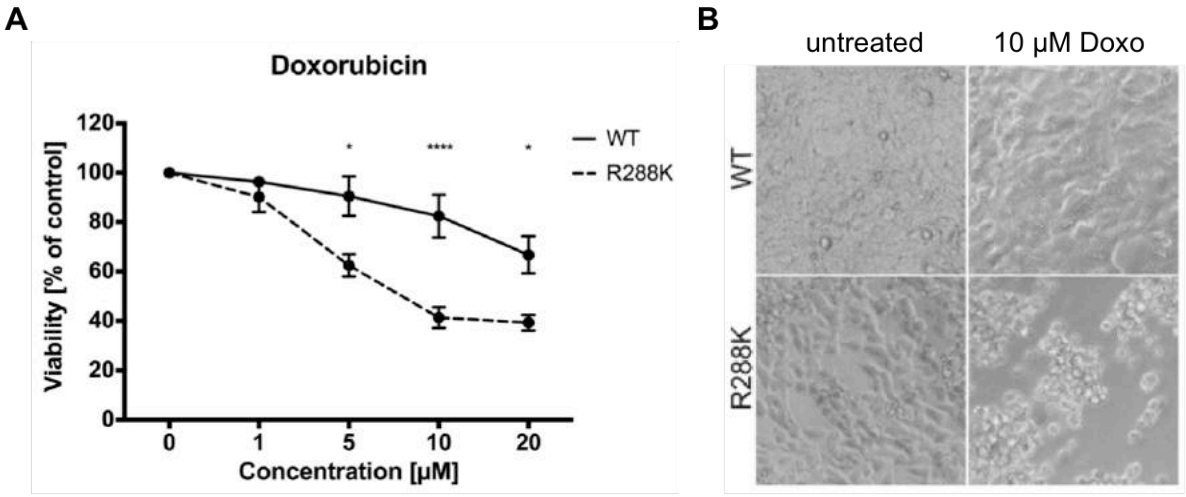
A
Doxorubicin
Viability [% of control]
120
100
80
60
40
20
0
0
1
5
10
20
Concentration [µM]
*
****
*
WT
R288K
B
untreated
10 µM Doxo
WT
R288K

Figure 3

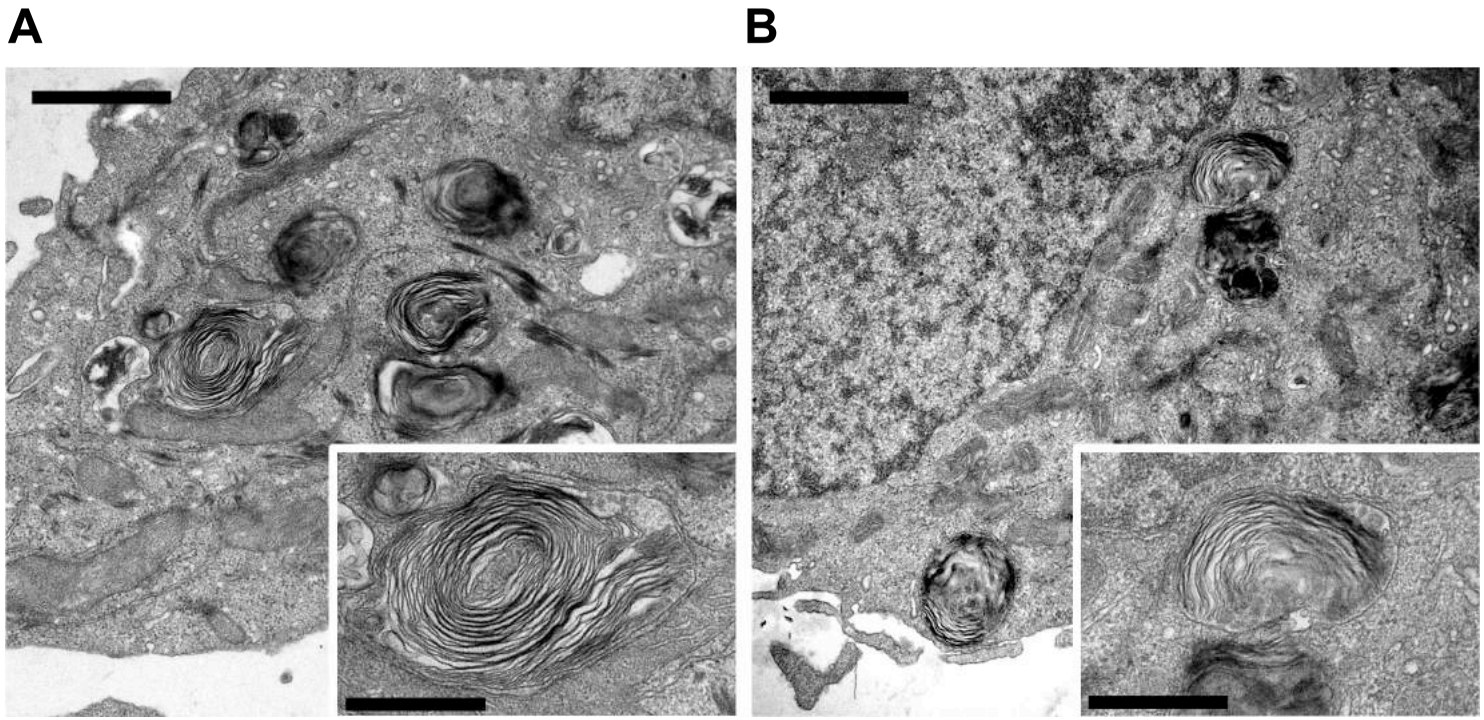

Figure 4

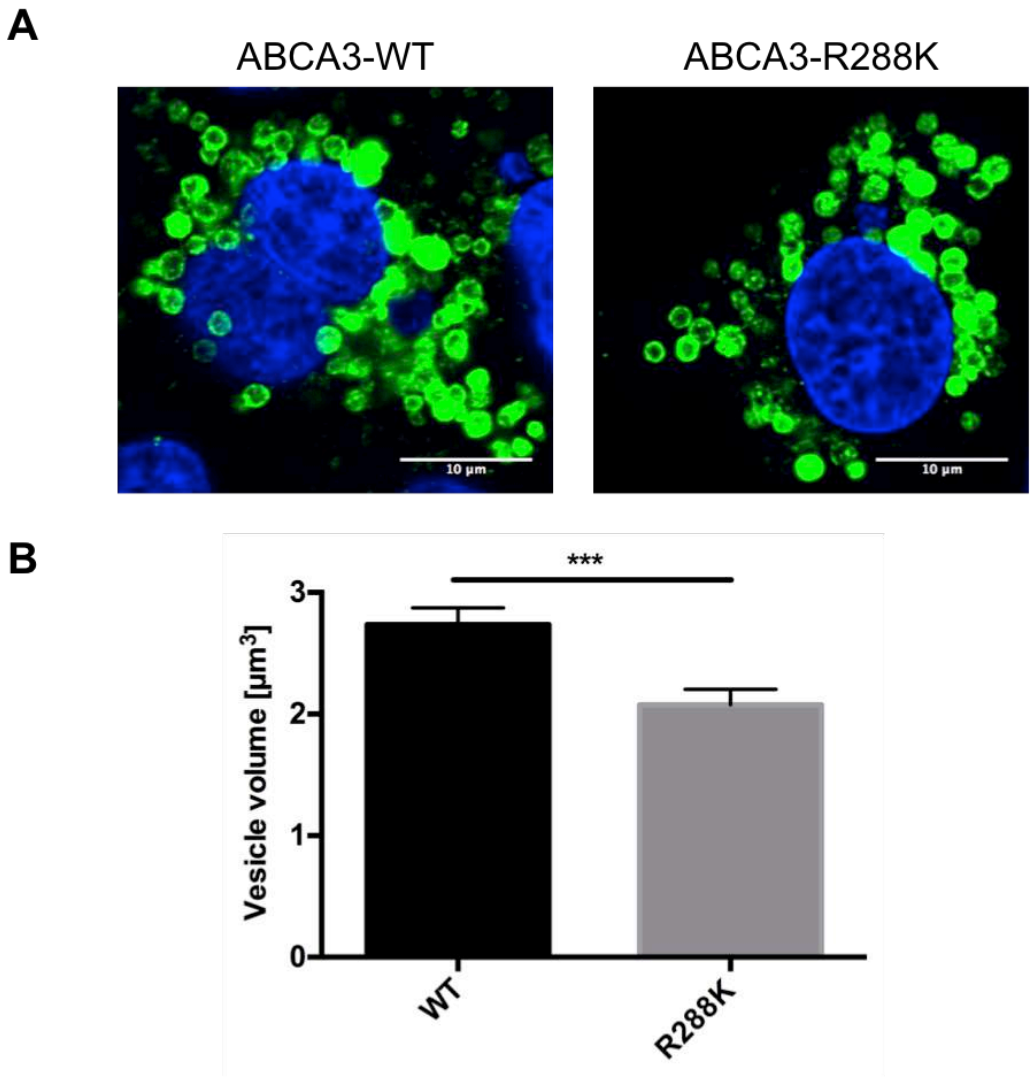
A
ABCA3-WT
ABCA3-R288K
10 µm
10 µm
B
***
Vesicle volume [µm³]
3
2
1
0
WT
R288K

Supplemental Material

Supplemental table 1. Genetic data of the patients

Patient	Sex	Ethnics	Family history	ABCA3 sequence variant	SFTPB	SFTPC
1	Female	Caucasian	Mother 33y, I grav, I para	R288K heterozygous	nl	nl
2	Female	Caucasian	Mother IV grav, III para	R288K heterozygous	nl	nl
3	Male	Caucasian (f) Pacific Islander Polynesian (m),	Mother, brother: bronchial asthma, Father: lung problems	R288K heterozygous	nl	nl
4	Male	Caucasian	Geminus I, 22 gest wk death of sibling	R288K heterozygous	nl	nl
5	Female	Caucasian	Parental smoking	R288K heterozygous	+/- Pos -384	nl
6	Male	Caucasian	Mother healthy, no lung symptoms	R288K heterozygous	nl	CC to GT substitution at -92 to -91 to ATG start codon, heterozygous
7	Male	Caucasian	Twin died short after birth due to lung failure	R288K heterozygous, P766S heterozygous, (trans)	nl	nl
8	Female	Caucasian	Mother: hemithyroidectomy; father: bronchial asthma, suspected ILD, no biopsy taken	R288K heterozygous, S693L heterozygous (both cis)	nl	nl
9	Female	Caucasian	None	R288K heterozygous	n.d.	nl
10	Female	Caucasian	None	R43L/R288K+c4751 delT (frameshift) compound heterozygous (trans)	nl	nl
11	Male	African	None	Q215K homozygous, R288K homozygous	nl	nl

nl = normal, n.d. = not done

Supplemental table 2. Neonatal history, lung function and CT scan of the children with chronic interstitial lung disease and R288K in ABCA3

Patient	Gest. Age	Oxygen neo. Period	Mech. Ventilation neo. Period	Onset lung disease (y)	Course lung disease	Lung function	CT scan
1	39	Yes	Yes	0.1	6 wks: tachydyspnea, cyanosis, wheezing;	N.a.	4 months: bilateral interstitial diffuse infiltration
2	36	Yes	Yes	0.0	Postpartal tachypnea; 6 mon RDS due to bronchopneumonia; 8 mon RDS due to UTI; bronchial hyperreactivity	7y: FEV1 54%, FVC 56%	13 mon: ground glass attenuation; 6y:bronchopneumonia, hilar lymphadenopathy
3	32	Yes	No	0.1	RDS, persistent need of oxygen	N.a.	Interstitial changes, thickened septa, air trapping, emphysema
4	27	Yes	Yes	0.0	RDS	N.a.	N.d.
5	30	Yes	Yes	0.0; 4.3	RDS 3d ventilated, 8 d CPAP, 4.25y dyspnea, cyanosis, coughing attacks, tachypnea, wheezing; 8y rec. respir.infections	8y: no desaturation under physical performance	4.5y: honey comb pattern bilateral, ground glass attenuation; 7y: bronchiectasis
6	30	Yes	No	0.0	Congenital lobar emphysema and interstitial lung disease	11y: FEV1 58%, FVC 52%	3 months: emphysema and mosaic pattern in under-developed lung. 7 y: basal thickened and rarefied interlobar septa; mosaic perfusion; emphysema
7	29	Yes	Yes	0.0	RDS 26d ventilated, BPD, pulmonary hypertension	N.a.	N.a.
8	37	Yes	Yes	0.0	0.2y: oxygen need, deteriorations of saturation; 1.8y: obstructive episodes	N.a.	1 mon: diminished ventilation, ground-glass attenuation bilateral
9	37	No	No	0.0	Tachydypnea since birth, 2.0 y recurrent broncho-pulmonary infections	1st lung function: LCI 9.5, central obstruction, lung compliance decreased 8.7ml/kPa/kg 2nd lung function , at 7mo LCI normal, compliance improved 10 ml/kPa/kg	1st CT: Mosaic pattern, ventilation inhomogeneities, no tracheobronchial malacia, ectasy of LAD-coronary artery 2nd CT, at 7 mo, normal lung parenchyma, no ventilation inhomogeneity, constant ectatic LM, LAD, RCA after Kawasaki's disease
10	42	Yes	Yes	0.0	Postpartal tachydyspnea, cyanosis	N.a.	N.a.

11	40	No	No	0.0	No information	N.a.	N.a.

BPD = Bronchopulmonary dysplasia; CPAP = continuous positive airway pressure; FEV1 = forced expiratory volume in 1 second; FVC = forced vital capacity; LCI = lung clearance index; RDS = respiratory distress syndrome. N.a. = not available

Supplemental table 3. Lung biopsy and other diagnosis, treatment, outcome of children with chronic interstitial lung disease and R288K in ABCA3

Patient	Lung biopsy	Final pulmonary and additional diagnosis	Treatment	Follow up if alive or age of death (y)	Long term outcome
1	y	ILD with PAP pattern, mild lymphocytic infiltration	Prednisolone	0.4	dead
2	n	ILD with ground glass attenuation and septal thickening Arnold-Chiari malformation Typ II; recurrent airway infections	Prednisolone, antibiotics, long term oxygen (until age 7, now)	7.0	sick-better
3	y	ILD, Wilson Mikity Syndrome	Diuretics, inhalation, oxygen	3.9	sick-better
4	y	ILD / BPD, interstitial emphysema, dystelectasis, bronchiolitis	Surfactant	0.1	dead
5	y	ILD with NSIP, DIP pattern; eosinophilia	Hydroxychloroquine, azathioprine until 6.5y; steroid boosts until 8y, azithromycin	8.0	sick-better
6	y	Thickened and rarefied interlobar septa; mosaic perfusion; emphysema; dysalbuminemic hyperthyroxinemia, short stature	Inhaled steroids, diuretics, systemic steroids, theophylline; somatotropin	9.0	sick-better
7	y	ILD with CPI, NSIP, and DIP pattern	Oxygen, corticosteroids	0.5	dead
8	n	ILD, chronic respiratory symptoms; has healthy twin	Surfactant, dexamethasone; 1.8y: montelukast, salbutamol	3.0	sick-better
9	n	ILD with ground glass attenuation, Kawasaki syndrome, aneurysm LCX	Oxygen, aspirin	4.0	sick-better
10	y	ILD previously published (case 3)#	Oxygen, mechanical ventilation	0.2	dead
11	y	ILD previously published (case 5)#	Oxygen, mechanical ventilation	0.3	dead

BPD = Bronchopulmonary dysplasia; CPI = chronic pneumonitis of infancy; DIP = desquamative interstitial pneumonitis; NSIP = non-specific interstitial pneumonitis; ILD = interstitial lung disease; PAP = pulmonary alveolar proteinosis; RDS = respiratory distress syndrome. # Brasch et al 2007.

Supplemental table 4. Primers used for analysis of ABCA3, SFTPC and SFTPB. The sequence of all PCR primers is given in the 5′ to 3′ direction.

ABCA3 gene

A3-4-1	CCAAATCCCCACTCTGCGTG
A3-5-2	CAGCTGCTTCGCACATCCTG
A3-6-1	CAAAGCCCTAGAGGATTTGCC
A3-6-2	CAGACCCAAAGGAGTGACTGC
A3-7-1	CTCTCCCACTCCACCCTGTTG
A3-7-2	CTGCTATAAGGACACATGCACACG
A3-8-1	TCTCATTTGCTGTCAGTGTGTGG
A3-8-2	CTAAAACACCAAGCCTTTGGACATG
A3-9-1	CTGCTGGGACAGTCGGACTC
A3-9-2	CTGACCATCCCTGGTCACAGG
A3-10-1	CTCTTGGGAAGAACTTTGTGGTCAG
A3-10-2	GCTGACTTTCCTCCTTCCAGTCC
A3-11-1	GTGTAGATGGCAAGTGCCAGGAG
A3-11-2	CAGCTATCCAGCCCACACTCAG
A3-12-1	CATGCCAACCAAGCAGTGG
A3-12-2	CTCTCTCTGAACCAGTCCCAAGG
A3-13-1	CTGCATGGCTGTGTGCATCTAG
A3-13-2	CTATGAGGTCTCACTGCCGTGC
A3-14-1	CTAGGCTTGGTTCCTTCTGAGACG
A3-14-2	GTGCATCTCCTGCCGCTGTG
A3-15-1	CAGGGTCCTCAGAGGAAATTAGG
A3-15-2	CTCAGAACCCTGGCTCCTGC
A3-16-1	CAGCTACGTCAAGGAGAGGTTCC
A3-16-2	GCTCGTCCAGTATCAGCACCTG
A3-17-1	CCATCCTTGGAGGACTCAAGC
A3-17-2	CAGAGGCAACAGACAGGAAGTCTAG
A3-18-1	CAAGACACATTCATTCTGCTTCAGC
A3-18-2	GCAGATTCATCTGGGCTGATG
A3-19-1	GTTCAAGTGTTCTCCTGCCTCTG
A3-19-2	CTGGGCAACTAGAGTGAAACTCC
A3-20-1	CATAAGCAGATGCATGAGCAAGC
A3-20-2	CTCGCAGACTCTCCTCTGCATG
A3-21-1	GCTGGCGTCACACAGAACAG
A3-21-2	CATTCGGAACAGCCAAGAACC
A3-22-1	GTCCCTGATTAGCCATGCTCAG
A3-22-2	GCAGACACAATGCTCTATCTATGGG
A3-23-1	GTGCTTGTGCTCTCCCATAAGC
A3-23-2	CAGCTGGTTCCGGTTCTGC
A3-24-1	GTCTGAGGACCTCCAAATGCTC
A3-24-2	CATGAACTGGGCCCATTGC
A3-25-1	CTCCACACAGCACGGATAAGG
A3-25-2	CCACTCAGACGCAGAGGAGC
A3-26-1	GTCTGCCATGTCGCTCATGG

A3-26-2	GAGACCATCTGGTGCAGGAGC
A3-27-1	GATTGGGACGAGAAGCCTTG
A3-27-2	GCAAAGCAGAGCAGTCTGAGC
A3-28-1	CTGATTATCAAGGAGCTCTCCAAGG
A3-28-2	CAAGCCACAGATGCAGCAGC
A3-29-1	CACTGGCAGGAACCACAG
A3-29-2	CTCCATCCTGGAGCCACAAG
A3-30-1	CTGTTCTGCAATTGCTGGGTG
A3-30-2	GACTCTGCACCAGATGCTGATG
A3-31-1	GAGAGCCAATGCCTTCCTGTC
A3-31-2	GTGCTCAGCACTGGAGTCCTC
A3-32-1	GAGGACTCCAGTGCTGAGCAC
A3-32-2	GTGACTCCTCTGTGGAAAGAGCC
A3-33-1	CTATTGCCAGAGGACTCCCAGG
A3-33-2	GAGTGCCTGGAGAAATTCAACC

SFTPB gene

SB-1-1	GCCACAGAAATCTTGTCTCTGACTC
SB-1-2	TTACCACCTGTCCTGGCTGATG
SB-2-1	GTTGGAGGAAGCCACAAGTCC
SB-2-2	GTTAATGCCTAGCACAAAGCAGTG
SB-3-1	AGAGCTGTCTGACGTCCACATG
SB-3-2	ATCGCATCCATCCCATTCC
SB-4-1	AGCTGCATGTGCCTTGGAGTG
SB-4-2	CTCAGCTCTTCCCTGCTCTGTC
SB-5-1	TGCCCAACTACTTAACTCCTTGGC
SB-5-2	CTCCCCATGGGTGGGCACAG
SB-6-1	AGTGGTCCCTGAGCCCTTG
SB-6-2	GCTTCGGAGGTGGCTCTAGC
SB-7-1	CTAGAGCCACCTCCGAAGCC
SB-7-2	GTGTGAGTTGGGAGAGAGGTGG
SB-8-1	CTGGACTCTCTGATCCCCAGTG
SB-8-2	CAGAGGTGTTTGGTTTCTGTCCTC
SB-9-1	TCTGTGGTCCCACTGCAATG
SB-9-2	ACATCCTGTCTGCCTGTCTGTG
SB-10-1	TGATCCAGAGATGTGGAGAGGC
SB-10-2	GAGTGAGGCCTCTGAGGATCAC
SB-11-1	GTGGAGTGAGTGCTGTTCTTTCC
SB-11-2	TCTTCCTGCTTGGGGAGCAG

SFTPC gene

SC-1-1	CAGCAAGGAAGGCAGGCAC
SC-1-2	GAATGGATCTGGATAAGGAAACAGG
SC-2-1	TCCCTGTCCATCCATCGCATC
SC-2-2	GACAGTTTCCTATCGCCCATCC
SC-3-1	GAAAGAGGGAAGCGCATTTGAG

SC-3-2	CTCTAGGTTGGGCACGGGAGTC
SC-4-1	CAGATTCTAGTATGACTCCCGTGC
SC-4-2	GAGGAACAGTGCTTTACAGGTGAC
SC-5-1	CTGGTGGCTTCTGACTCTAGCAC
SC-5-2	GAGTGGGAAGTACCGGTCTGTGAG

Supplemental figure 1

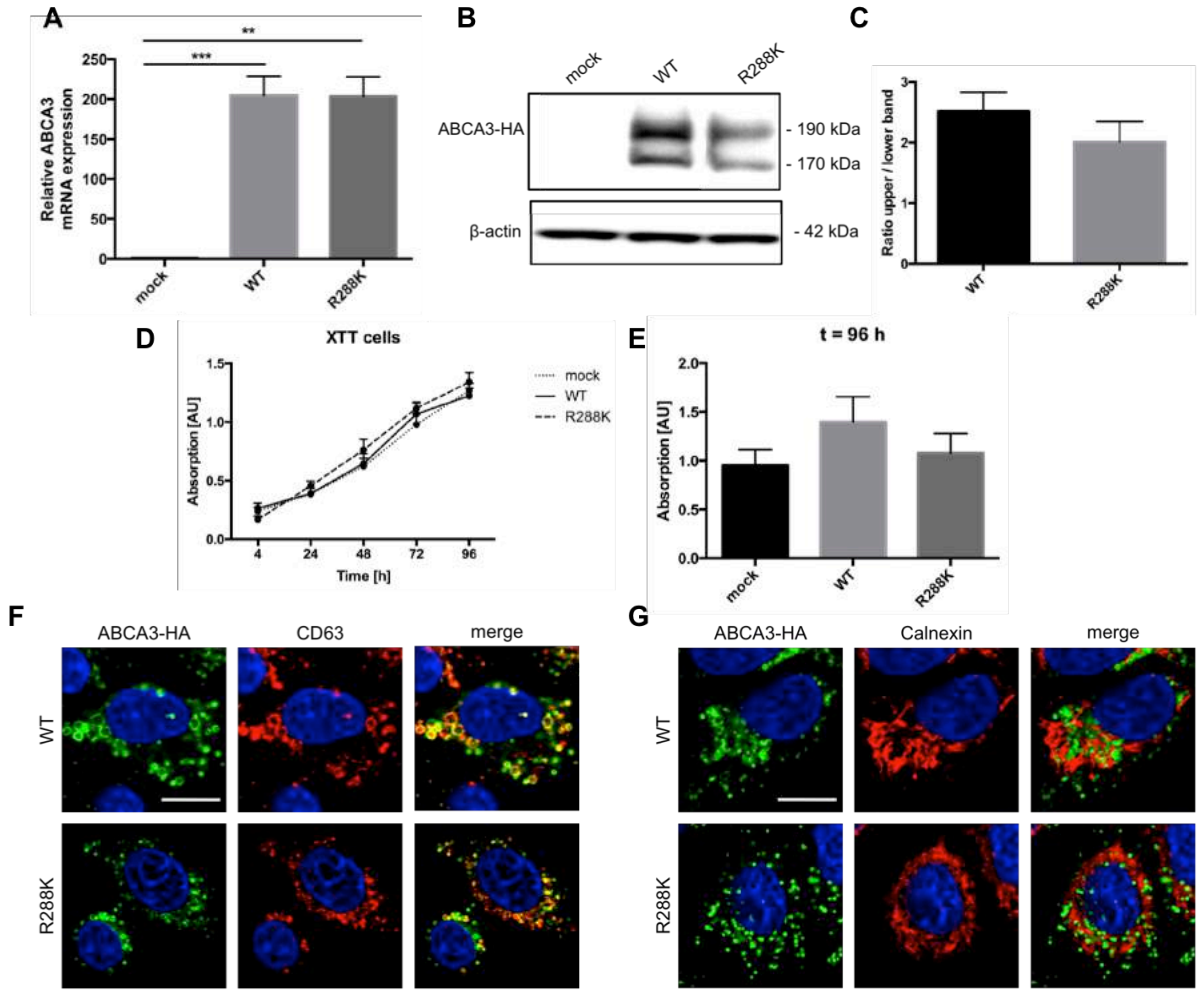

Legend to Supplemental figure. 1: **Cellular effects of ABCA3-WT and ABCA3-R288K stably expressed in A549 cells. A.** *ABCA3* mRNA levels analyzed by quantitative real time PCR ($p<0.001$ for WT/mock and $p< 0.01$ for R288K/mock). **B.** Western immunoblot analysis of HA-tagged ABCA3 in total cell lysates. β-actin was used as a loading control. **C.** Ratio of upper/lower ABCA3 processing form. **D.** Cell proliferation assay of A549 cells stably transfected with ABCA3-WT protein of R288K variant compared to mock control. XTT tetrazolium salt was used for absolute quantification. **E.** Impact of stably transfection method on cell cytotoxicity. Therefore lactate dehydrogenase was quantified in cell supernatants. **F.**

Co-immunostaining of HA-tagged ABCA3 with the lysosomal (lamellar body) marker CD63. **G.** Co-immunostaining of HA-tagged ABCA3 with the ER marker calnexin. Scale: 10 μm. Merge images present the overlay from green and red fluorescence. All results were expressed as mean ± SEM.

Supplemental figure 2

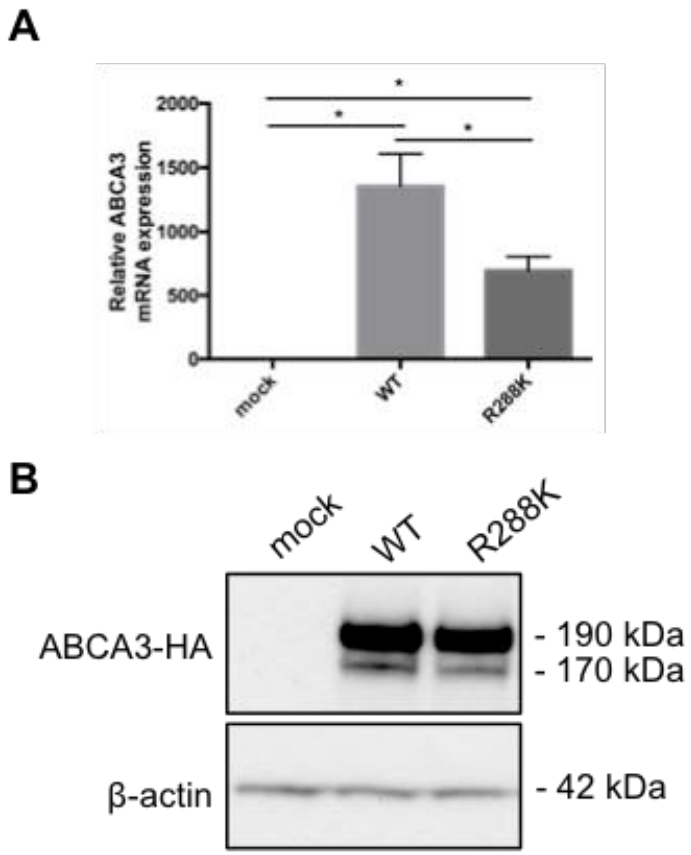

Legend to Supplemental figure 2: **Stably expression of ABCA3-WT and ABCA3-R288K protein in HEK293 cells**: **A:** Relative mRNA levels of HEK293 stably expressing ABCA3-WT and ABCA3-R288K analyzed by quantitative real time PCR compared to mock control. *P<0.05. **B:** Immunoblot analysis of ABCA3-WT and ABCA3-R288K stably expressed in HEK293 cells. ß-actin was used as loading control.

Paper 2

Wittmann T., Schindlbeck U., Höppner S., Kinting S., Frixel S., Kröner C., Liebisch G., Hegermann J., Aslanidis C., Brasch F., Reu S., Lasch P., Zarbock R., and Griese M. (2016). *Tools to explore ABCA3 mutations causing interstitial lung disease*. Ped. Pulm. (accepted)

Tools to explore ABCA3 mutations causing interstitial lung disease

Thomas Wittmann[1#], Ulrike Schindlbeck[1#], Stefanie Höppner[1], Susanna Kinting[1], Sabrina Frixel[1], Carolin Kröner[1], Gerhard Liebisch[2], Jan Hegermann[3], Charalampos Aslanidis[2], Frank Brasch[4], Simone Reu[5], Peter Lasch[6], Ralf Zarbock[1], Matthias Griese[1,*]

[1]Dr. von Hauner Children's Hospital, Ludwig-Maximilians University, German Centre for Lung Research, 80337 Munich, Germany

[2]Institute for Clinical Chemistry and Laboratory Medicine, University of Regensburg, Franz-Josef-Strauss-Allee 11, D-93053 Regensburg, Germany

[3]Institute of Functional and Applied Anatomy, Hannover Medical School, Carl-Neuberg-Straße 1, German Center for Lung Research (DZL), Hannover, Germany

[4]Academic Teaching Hospital Bielefeld, Department of Pathology, Teutoburger Straße 50, 33604 Bielefeld, Germany

[5]Ludwig-Maximilians University, Department of Pathology, Thalkirchner Straße 36, 80337 Munich, Germany

[6]Pediatric Intensive Care, Hospital Bremen-Mitte, Sankt-Jürgen-Straße 1, 28205 Bremen, Germany

#contributed equally

*to whom correspondence should be addressed

This paper has supplementary material.

Key words: Interstitial lung disease (ILD), Respiratory Distress Syndrome & ARDS, Surfactant Biology and Pathophysiology, Neonatal Pulmonary Medicine

Running head: Molecular tools for ABCA3 mutations causing ILD

Prof. Dr. Matthias Griese

Matthias.Griese@med.uni-muenchen.de

Phone 0049/(0)89/4400-57870

Fax 0049/(0)89/4400-57872

E-mail addresses:

Thomas.Wittmann@med.uni-muenchen.de

Ulrike.Schindlbeck@med.uni-muenchen.de

Stefanie.Hoeppner@med.uni-muenchen.de

Susanna.Kinting@med.uni-muenchen.de

Sabrina.Frixel@med.uni-muenchen.de

Carolin.Kroener@med.uni-muenchen.de

Gerhard.Liebisch@klinik.uni-regensburg.de

Hegermann.Jan@mh-hannover.de

charalampos.aslanidis@klinik.uni-regensburg.de

frank.brasch@klinikumbielefeld.de

Simone.Reu@med.uni-muenchen.de

Peter.Lasch@Klinikum-Bremen-Mitte.de

Ralf.Zarbock@med.uni-muenchen.de

Matthias.Griese@med.uni-muenchen.de

ABSTRACT

Background: Interstitial lung diseases (ILD) comprise disorders of mostly unknown cause. Among the few molecularly defined entities, mutations in the gene encoding the ATP-binding cassette (ABC), subfamily A, member 3 (ABCA3) lipid transporter represent the main cause of inherited surfactant dysfunction disorders, a subgroup of ILD. Whereas many cases are reported, specific methods to functionally define such mutations are rarely presented.

Materials and methods: In this study, we exemplarily utilized a set of molecular tools to characterize the mutation K1388N, which had been identified in a patient suffering from ILD with lethal outcome. We also aimed to correlate *in-vitro* and *ex-vivo* findings.

Results: We found that presence of the K1388N mutation did not affect protein expression, but resulted in functional impairment of ABCA3 as demonstrated by reduced transport of dipalmitoyl-phosphatidylcholine (PC 32:0) and malformed lamellar bodies.

Conclusions: Here we present a set of tools useful for categorizing different ABCA3 mutations according to their impact upon ABCA3 activity. Knowledge of the molecular defects and close correlation of *in-vitro* and *ex-vivo* data will allow us to define groups of mutations that can be targeted by small molecule correctors for restoring impaired ABCA3 transporter in the future.

Word count abstract: 194

Word count total: 2858

INTRODUCTION

ATP-binding cassette (ABC), subfamily A, member 3 (ABCA3) is an intracellular lipid transporter containing two transmembrane domains each consisting of six membrane helices and two nucleotide binding domains (NBDs) hydrolyzing ATP.[1,2] In the lungs the transporter localizes to the outer membrane of lamellar bodies (LBs) of type II pneumocytes. LBs derive from lysosomal origin and serve as production and storage organelles for pulmonary surfactant, which is then secreted into the alveolar space. ABCA3 transports phospholipids and cholesterol into the LB lumen and is therefore essential for LB biogenesis and homeostasis of pulmonary surfactant and normal lung function.[1,3,4]

All these processes are delicately disturbed by sequence variations of *ABCA3*. A broad spectrum of mutations has recently been shown to cause pulmonary ABCA3 deficiency followed by early death or fibrotic lung disease in survivors.[5-8]

The deficiency of another ABC transporter, ABCC7 (Cystic fibrosis transmembrane conductance regulator, CFTR), shows many interesting similarities to ABCA3 deficiencies. The availability of cellular assays to characterize the CFTR phenotype *in-vitro* and tight correlations to *ex-vivo* patient data have led to the precise molecular classification of CFTR mutations,[9,10] successful correction of mutations in cell models with small molecules identified by high throughput screening and rapid transfer into patients.[11,12]

To acquire similar knowledge for ABCA3 deficiency, many intermediate steps need to be realized including stable and readily available cellular models, assays to characterize the cellular phenotype of the different mutations, and in particular close correlation of such measurements to *ex-vivo* patient data. ABCA3 mutations, which were predicted to result in truncated or non-functional proteins were classified as “null/null” mutations and affected infants presented respiratory failure at birth and all had died by 1 year of age if not lung transplanted.[8] Mutations affecting protein function in any way were termed “other”.[8] From a

cellular perspective mutations were previously distinguished between those with abnormal localization of the ABCA3 protein in the cells and those with ATP hydrolysis defects.[1] The major role of ABCA3 in LB biogenesis and surfactant lipid synthesis, i.e. dipalmitoyl-phosphatidylcholine (PC 32:0) content of the cells, must also be considered.[13,14]

Such cellular classifications of ABCA3 mutations have to be linked to the clinical characterizations of affected subjects carrying different types of *ABCA3* gene sequence variations to build up a consistent and reliable model.

In this study we used a broad range of experiments to assess *in-vitro* and *ex-vivo* characteristics of wild type and a mutated ABCA3 protein. Our results demonstrate a very close connection between the results obtained in the cell model applied and the findings from a patient harbouring the same homozygous ABCA3 variant. The molecular tools defined here allow a classification of ABCA3 mutations; this will be of use when searching for new molecules to restore genetically disturbed ABCA3 function.

MATERIALS and METHODS (see detailed descriptions in the supplemental material)

Plasmids and antibodies

ABCA3 cDNA (NM_001089) fused to a C-terminal HA-tag and puromycin resistance gene were cloned into pT2/HB transposon vector (Addgene, Cambridge, United States, plasmid #26557). ABCA3-K1388N point mutation (c. 4164G>C; AAG/AAC) was introduced using Q5® site-directed mutagenesis kit (NEB, Massachusetts, United States) with following primers: K1388N-for *5'-AGCTCTCCAACGTGTACGAGC-3'* and K1388N-rev *5'-CCTTGATAATCAGAGGTGTG-3'*. pCMV(CAT)T7-SB100 transposase was ordered from Addgene (plasmid #34879).

Used antibodies are listed in the supplement.

Cell culture

A549 cells were purchased from the German Collection of Microorganisms and Cell Cultures (DSMZ, Braunschweig, Germany) and maintained in RPMI 1640 medium (Gibco, Darmstadt, Germany) supplemented with 10% fetal bovine serum (FBS) (Sigma, Taufkirchen, Germany) at 37°C with 5% CO_2.

Generation of stable cell clones

ABCA3-HA wild type (WT) and K1388N variation were stably transfected using the *"Sleeping Beauty"* transposon system.[15] Therefore A549 cells were cotransfected with pCMV(CAT)T7-SB100 and pT2/HB-puro-ABCA3-HA WT or K1388N variation using X-tremeGENE HP DNA transfection reagent (Roche, Mannheim, Germany). Selection of stable cells was started by addition of 1µg/ml puromycin.

Viability and cytotoxicity assay

Cell viability was assessed by specific cleavage of 2,3-bis (2-methoxy-4-nitro-sulfophenyl)-2H-tetrazolium-5-carboxyanilide (XTT, Sigma) in the presence of phenazine methosulfate. Absorbance was measured at 490 nm and 650 nm using a spectrophotometer.

For cytotoxic effects of stable transfection, the amount of lactate dehydrogenase (LDH) was determined in cell supernatants according to the manufacturer's instructions (Promega, Mannheim, Germany).

Real-time PCR/ Immunoblotting/ Immunofluorescence staining/ Oil Red O staining

Real-time PCR, immunoblotting, immunofluorescence staining and oil red O staining were performed as previously described.[16] To determine cellular oil red O volume, Z stacks image series were generated with an Olympus IX81/Fluoview FV1000 confocal laser scanning microscope (Olympus, Tokyo, Japan). Data were analysed with the 3D object counter software plugin in ImageJ.

Glycosylation analysis/ Lipid analysis / Electron microscopy

Glycosylation analysis was done as previously described.[1] Lipid analysis was performed as previously reported.[14] Electron microscopy was performed as described.[7]

Vesicle volume

A549 cells containing either ABCA3-WT or K1388N variation were immunostained against HA-tag and imaged with an Olympus IX81/Fluoview FV1000 confocal laser scanning microscope. Diameter of ABCA3-HA containing vesicle was determined with ImageJ software. Volumes of 60 different randomly chosen vesicles were calculated, thus analysing 20 vesicles per condition and experiment.

Immunohistochemistry

Slides were pretreated with Target Unmasking Fluid (Panpath, Amsterdam, The Netherlands) at 90°C followed by an incubation of primary antibody against ABCA3 protein (diluted 1:1800) for 60 min at RT. Detection was done using Vectastain ABC-Kit Elite Universal (Vector Laboratories, Burlingame, United States) and AEC+ chromogen as substrate (Dako, Santa Clara, United States). Slides were counterstained with Hematoxylin Gill's Formula (Vector Laboratories). Microscopic pictures were taken with a Leica DM4000 (Leica, Wetzlar, Germany)

***In-vivo* and *ex-vivo* analysis of patient materials**

Bronchoalveolar lavage (BAL), lung tissue and blood were investigated from an infant. Informed consent of the parents and approval of the institutional review board (EK 026-06) were obtained. Analysis of data was performed under the FP7-305653 project chILD-EU (EK 111-13).

Statistical analysis

Comparison of two groups was done using Student's t-test. Comparisons of multiple groups were done using one-way repeated measure ANOVAs with Tuckey's post hoc test. Lipid contents were analysed using two-way ANOVA with Sidak's post hoc test. Ratios of phosphatidylcholine species were analysed using one-sample t test comparing to the hypothetical value of 1. Significance levels for ratios were corrected according to Benjamini and Hochberg.[17] Results were presented as mean ± S.E.M. of a minimum of three different experiments. P-values < 0.05 were considered to be statistically significant.

RESULTS

The homozygous K1388N variant of ABCA3 protein leads to complete ABCA3 deficiency resulting in lethal interstitial lung disease

The homozygous ABCA3 variation K1388N was found in a patient presenting typically for complete ABCA3 deficiency with severe respiratory distress (Figure 1 A-B), a brief period of recovery with interstitial lung disease and the typical histological pattern of chronic pneumonitis of infancy and abnormal LB on electron microscopy (Figure 1 C-F), progressing to respiratory insufficiency and death at the age of 9 weeks. BAL content of SP-C was reduced and showed some higher molecular weight forms at relatively low concentration (Figure 1 G). The K1388N mutation was predicted to be malign and not tolerated by the algorithms Polyphen and SIFT. A topological model of ABCA3 protein predicts a localisation of K1388N variant in proximity to the nucleotide-binding domain 2 (NBD2) (Figure 1 H), which comprises two Walker motives.[18] Furthermore partial alignment of codons 1348-1429 of the ABCA3 coding sequence demonstrates an extremely conserved region including Lys1388 between different species (Figure 1 I).

Impaired intracellular processing of K1388N variation

A549 lung epithelial cells stably expressing ABCA3-WT and ABCA3-K1388N variant showed an increased *ABCA3*-mRNA expression of 200-fold as compared to mock transfected cells (Figure 2 A). Furthermore cell growth and proliferation were unaffected in both cell lines either expressing ABCA3-K1388N or ABCA3-WT protein in comparison to mock control cells (Figure 2 D+E). But intracellular processing examined by Western immunoblotting revealed an alteration of K1388N variant compared to wild type protein (Figure 2 B). Both proteins were present as the 190 and 150 kDa processing forms, but band intensities differed. The 190 kDa processing form of the mutated K1388N protein was

enriched considerably. Therefore the band ratio of 190 kDa to 150 kDa was increased up to 20-fold in ABCA3-K1388N expressing cells as compared to A549 cells with ABCA3-WT protein (Figure 2 C). Intracellular processing examined by co-localization studies with the immunofluorescent marker CD63, a marker for late endosomes and lamellar bodies, revealed localization within CD63 positive vesicles of both wild type and K1388N protein variant (Figure 2 G). Furthermore neither ABCA3 wild type protein nor K1388N mutated protein showed a co-localization with the ER-resident chaperone calnexin (Figure 2 H). Additional N-glycosylation studies revealed that ABCA3 wild type protein as well as K1388N mutated protein showed equal processing from high-mannose oligosaccharides to complex-type oligosaccharides (Figure 2 F). This further supports the view that both proteins undergo correct folding in the ER and further processing within the Golgi apparatus.

K1388N variation results in smaller lamellar bodies with abnormal morphology

Analysis of ABCA3-K1388N containing lamellar bodies revealed a significant decrease of volume compared to lamellar body volume of A549 cells expressing ABCA3-WT (Figure 3 A). Lamellar body morphology of ABCA3-K1388N expressing cells was altered as compared to ACBCA3-WT expressing cells. Mock control cells contained no lamellar bodies (Figure 3 B, left), whereas ABCA3-WT expressing cells showed well-structured lamellar bodies with concentric membranes arranged in parallel (Figure 3 B, middle). ABCA3-K1388N containing lamellar bodies showed abnormal morphology with fried-egg-like structures (Figure 3 B, right). Additional analysis of lung tissue from a patient carrying homozygous K1388N variant showed a very weak expression and a high dispersed ABCA3 protein in type II pneumocytes, whereas ABCA3 is strongly expressed in healthy lung tissue (Figure 3 C). Control tissue displayed a typical pattern of LBs with ring-like structures,

whereas LBs in lung tissue with ABCA3-K1388N variant were absent (compare Figure 3 C left to right).

Reduction of phosphatidylcholine and dipalmitoyl-phosphatidylcholine content due to K1388N mutation

Measurement of intracellular lipid classes from A549 cells expressing ABCA3-K1388N mutated protein exhibits a reduction of phosphatidylcholine content as the major lipid in surfactant compared to A549 cells expressing ABCA3-WT (Figure 4 A, left). Other lipid classes were not affected by this mutation (Supplemental figure 1 A, right). Free cholesterol content and cholesteryl esters were significantly reduced in K1388N expressing A549 cells, whereas lipid droplet volume and lipid droplet number showed no differences compared to A549 expressing ABCA3-WT cells (Supplemental figure 2 A+B). On the detailed PC species level short-chained lipid contents were reduced in contrast to long-chained species, which were increased (Supplemental figure 1 B, right). PC 32:0 as the most abundant PC species in surfactant was also reduced to a third (Figure 4 A, right). These findings can also be verified in BAL isolated from the homozygous carrier of the K1388N variant. PC content was also lowered as compared to BALs of control group (Figure 4 B, left). Additionally sphingomyelin (SPM), PE based plasmalogens (PE P) and phosphatidylglycerol (PG) content were decreased, whereas ceramide (Cer) content was slightly increased (Supplemental figure 1 A, left). Furthermore molecular PC species composition showed a similar distribution with a lower fraction of PC 30 and 32 species and more PC 36 and 38 species compared to controls (Supplemental figure 1 B, left). PC 32:0 content of a patient with K1388N variation was diminished by half of it as compared to controls (Figure 4 B, right).

DISCUSSION

In this study we present a broad set of experiments to assess the function of wild type ABCA3 protein in comparison to the specific features of ABCA3 with the mutation K1388N, which was found in a patient suffering from respiratory distress syndrome (Table 1). Our goal was to establish different molecular tools for the characterization and classification of newly described ABCA3 variants and to test the tightness of correlation between the *in-vitro* data raised in stably transfected A549 cells and *ex-vivo* data collected from an affected subject.

The K1388N variation of the ABCA3 transporter caused severe respiratory neonatal distress followed by a brief period of recovery with interstitial lung disease, progressing to respiratory insufficiency and death at the age of 9 weeks. Obviously, this newly described homozygous mutation led to complete ABCA3 deficiency, which is incompatible with life.[19] *In-silico* analysis predicted these damaging consequences of this mutation, which is localized in proximity of the functional critical nucleotide-binding domain 2 (NBD2). Lys1388 is a highly conserved position among various species, further supporting its role for normal function of ABCA3 protein.

It could be shown for some ABC transporters like ABCC7 (CFTR) that certain mutations induce intracellular mislocalization of the protein.[20,21] Our data clearly show that ABCA3-K1388N is correctly localized to lamellar bodies and was not retained in the ER. The processing of its oligosaccharides from the high mannose type to the complex type showed trafficking through ER and Golgi apparatus. This follows the cellular path of ABCA3-WT protein, which also passes through these two organelles. Nevertheless, cellular processing of K1388N is impaired compared to WT protein, as the 190 kDa processing form of the protein is enriched in A549 cells stably expressing the variant. Previous studies showed that N-glycosylation is essential for the stability of ABCA3 protein.[18] Introducing a further N-glycosylation site due to another asparagine instead of a lysine on position 1388 may lead

to elevated protein instability. Thus several lines of evidence support impaired processing of the K1388N variant, resulting in less active transporter available and leading to reduced volume and structurally altered LBs. Whereas ABCA3-WT expression led to the prominent induction of well-shaped LBs in A549 cells, expression of ABCA3-K1388N induced the formation of abnormal LBs. This notion supports the concept that ABCA3 wild type function is indispensable for normal LB production and that this ability is severely impaired in the K1388N variant.

Analysis of lung tissue from the child carrying the homozygous K1388N variant demonstrated an altered expression pattern of ABCA3 protein in type II pneumocytes. This was identified by a weak immunohistochemical staining of ABCA3 and only rather small protein agglomerations compared to normal well-shaped LBs detectable in tissues from healthy children. Similarly, in lung tissue from the affected child, the characteristic fried-egg-shaped and functionally inactive LBs were demonstrated. Together, we show a close recapitulation of morphological LB dysfunction in our stable cell model and the patient.

To directly assess the functional impact of the K1388N variant compared to ABCA3-WT protein, lipid composition was measured. Previous studies showed that the amount of PC 32:0 is significantly reduced in BALs of children carrying interstitial lung disease causing mutations on both alleles.[13,14] Both total PC and PC 32:0 were reduced in A549 cells stably expressing ABCA3-K1388N and in BAL of the child with homozygous K1388N variant compared to respective controls. This provides direct *in-vitro* and *ex-vivo* evidence for reduced ABCA3 lipid transporter function. Furthermore the K1388N variant led to an elevation of long-chained PC species content in both A549 cells and in BAL of the patient compared to controls.

Whereas a major strength of our study was to correlate the *in-vitro* data from our model system for lung epithelial cells and *ex-vivo* data from a patient in relation to the

K1388N variant, there are some weaknesses. We assessed intracellular lipid composition; however the surfactant lipids are usually exocytosed into the alveolar space *in-vivo* and thus represent just a subfraction. We found a tight correlation for PC 32:0 which, as the major surfactant phosphatidylcholine species is enriched in lamellar bodies.[22] We expected this *in-vitro*, but the sensitivity of mass spectrometry to determine unlabelled PC 32:0 directly in the supernatant of cells cultured in dishes was too low. However an enrichment of intracellular PC 32:0 was shown in our model system.

Patient-derived type-II-pneumocytes would be most helpful for *in-vitro* studies on specific mutations; however such lines are not available for most rare mutations.[23,24] The A549 cell-line used here was formerly derived from lung adenocarcinoma and lost its ability to form LBs with normal structure and characteristic surfactant composition.[25] However, this may even be of advantage to demonstrate transport of surfactant lipids into such organelles *in-vitro*. Here we show that the expression of ABCA3-WT protein at a constantly high level led to the formation of well-shaped LBs with an enrichment of PC and PC 32:0 content. This morphological feature has previously been shown for HEK293 cells[3,7] and represents an elegant functional assay for intact ABCA3 transporter activity.

Collecting further clinical data from patients with this mutation linked to laboratory-based experiments to understand how a particular mutation works will be necessary and will be of use for allocating mutations into groups with the same class of a molecular defect in the future. This is essential in face of the large number of different ABCA3 mutations identified, as those from the same class might be targeted by the same group of small molecules for restoring the wild type function of the protein.

In summary, we characterized the K1388N variant of ABCA3 as a processing mutation with normal intracellular localisation and a reduced lipid transporter activity for PC

32:0. This led to LBs with a reduced volume and an abnormal morphology. Thus this mutation can be classified as a functional mutation.

Acknowledgements:

The work of M.G. was supported by DFG-970/8-1 and chILD-EU (FP7, No. 305653).

Conflict of interests:

The authors declare to have no conflict of interests.

Contributions:

Thomas Wittmann, Ulrike Schindlbeck, Ralf Zarbock and Matthias Griese designed the study, analyzed data and wrote the manuscript. Thomas Wittmann, Ulrike Schindlbeck, Stefanie Höppner, Susanna Kinting, Sabrina Frixel, Simone Reu, Gerhard Liebisch and Jan Hegermann performed research, contributed important reagents, and analyzed data. Matthias Griese, Peter Lasch, Charalampos Aslanidis, Frank Brasch and Carolin Kröner evaluated the patient, made chart reviews and organized the study logistics. All authors approved the final manuscript. Matthias Griese is responsible for the study content and validity of the data.

REFERENCES

1. Matsumura Y, Ban N, Ueda K, and Inagaki N, Characterization and classification of ATP-binding cassette transporter ABCA3 mutants in fatal surfactant deficiency. J Biol Chem, 2006. 281(45): p. 34503-14.
2. Peca D, Cutrera R, Masotti A, Boldrini R, and Danhaive O, ABCA3, a key player in neonatal respiratory transition and genetic disorders of the surfactant system. Biochem Soc Trans, 2015. 43(5): p. 913-9.
3. Cheong N, Zhang H, Madesh M, Zhao M, Yu K, Dodia C, Fisher AB, Savani RC, and Shuman H, ABCA3 is critical for lamellar body biogenesis in vivo. J Biol Chem, 2007. 282(33): p. 23811-7.
4. Besnard V, Matsuzaki Y, Clark J, Xu Y, Wert SE, Ikegami M, Stahlman MT, Weaver TE, Hunt AN, Postle AD, et al., Conditional deletion of Abca3 in alveolar type II cells alters surfactant homeostasis in newborn and adult mice. Am J Physiol Lung Cell Mol Physiol, 2010. 298(5): p. L646-59.
5. Shulenin S, Nogee LM, Annilo T, Wert SE, Whitsett JA, and Dean M, ABCA3 gene mutations in newborns with fatal surfactant deficiency. N Engl J Med, 2004. 350(13): p. 1296-303.
6. Saugstad OD, Hansen TW, Ronnestad A, Nakstad B, Tollofsrud PA, Reinholt F, Hamvas A, Coles FS, Dean M, Wert SE, et al., Novel mutations in the gene encoding ATP binding cassette protein member A3 (ABCA3) resulting in fatal neonatal lung disease. Acta Paediatr, 2007. 96(2): p. 185-90.
7. Campo I, Zorzetto M, Mariani F, Kadija Z, Morbini P, Dore R, Kaltenborn E, Frixel S, Zarbock R, Liebisch G, et al., A large kindred of pulmonary fibrosis associated with a novel ABCA3 gene variant. Respir Res, 2014. 15: p. 43.

8. Wambach JA, Casey AM, Fishman MP, Wegner DJ, Wert SE, Cole FS, Hamvas A, and Nogee LM, Genotype-phenotype correlations for infants and children with ABCA3 deficiency. Am J Respir Crit Care Med, 2014. 189(12): p. 1538-43.

9. Sosnay PR, Siklosi KR, Van Goor F, Kaniecki K, Yu H, Sharma N, Ramalho AS, Amaral MD, Dorfman R, Zielenski J, et al., Defining the disease liability of variants in the cystic fibrosis transmembrane conductance regulator gene. Nat Genet, 2013. 45(10): p. 1160-7.

10. Okiyoneda T, Veit G, Dekkers JF, Bagdany M, Soya N, Xu H, Roldan A, Verkman AS, Kurth M, Simon A, et al., Mechanism-based corrector combination restores DeltaF508-CFTR folding and function. Nat Chem Biol, 2013. 9(7): p. 444-54.

11. Ramsey BW, Davies J, McElvaney NG, Tullis E, Bell SC, Drevinek P, Griese M, McKone EF, Wainwright CE, Konstan MW, et al., A CFTR potentiator in patients with cystic fibrosis and the G551D mutation. N Engl J Med, 2011. 365(18): p. 1663-72.

12. Wainwright CE, Elborn JS, and Ramsey BW, Lumacaftor-Ivacaftor in Patients with Cystic Fibrosis Homozygous for Phe508del CFTR. N Engl J Med, 2015. 373(18): p. 1783-4.

13. Garmany TH, Moxley MA, White FV, Dean M, Hull WM, Whitsett JA, Nogee LM, and Hamvas A, Surfactant composition and function in patients with ABCA3 mutations. Pediatr Res, 2006. 59(6): p. 801-5.

14. Griese M, Kirmeier HG, Liebisch G, Rauch D, Stuckler F, Schmitz G, Zarbock R, and Kids-Lung-Register I-Bwgot, Surfactant lipidomics in healthy children and childhood interstitial lung disease. PLoS One, 2015. 10(2): p. e0117985.

15. Geurts AM, Yang Y, Clark KJ, Liu G, Cui Z, Dupuy AJ, Bell JB, Largaespada DA, and Hackett PB, Gene transfer into genomes of human cells by the sleeping beauty transposon system. Mol Ther, 2003. 8(1): p. 108-17.

16. Zarbock R, Kaltenborn E, Frixel S, Wittmann T, Liebisch G, Schmitz G, and Griese M, ABCA3 protects alveolar epithelial cells against free cholesterol induced cell death. Biochim Biophys Acta, 2015. 1851(7): p. 987-95.

17. Benjamini Y and Hochberg Y, Controlling the False Discovery Rate: a Practical and Powerful Approach to Multiple Testing. J R Statist Soc B, 1995. 57(1): p. 289-300.

18. Beers MF, Zhao M, Tomer Y, Russo SJ, Zhang P, Gonzales LW, Guttentag SH, and Mulugeta S, Disruption of N-linked glycosylation promotes proteasomal degradation of the human ATP-binding cassette transporter ABCA3. Am J Physiol Lung Cell Mol Physiol, 2013. 305(12): p. L970-80.

19. Fitzgerald ML, Xavier R, Haley KJ, Welti R, Goss JL, Brown CE, Zhuang DZ, Bell SA, Lu N, McKee M, et al., ABCA3 inactivation in mice causes respiratory failure, loss of pulmonary surfactant, and depletion of lung phosphatidylglycerol. J Lipid Res, 2007. 48(3): p. 621-32.

20. He L, Kota P, Aleksandrov AA, Cui L, Jensen T, Dokholyan NV, and Riordan JR, Correctors of DeltaF508 CFTR restore global conformational maturation without thermally stabilizing the mutant protein. FASEB J, 2013. 27(2): p. 536-45.

21. Phuan PW, Veit G, Tan J, Roldan A, Finkbeiner WE, Lukacs GL, and Verkman AS, Synergy-based small-molecule screen using a human lung epithelial cell line yields DeltaF508-CFTR correctors that augment VX-809 maximal efficacy. Mol Pharmacol, 2014. 86(1): p. 42-51.

22. Schlame M, Casals C, Rustow B, Rabe H, and Kunze D, Molecular species of phosphatidylcholine and phosphatidylglycerol in rat lung surfactant and different pools of pneumocytes type II. Biochem J, 1988. 253(1): p. 209-15.

23. Kurmann AA, Serra M, Hawkins F, Rankin SA, Mori M, Astapova I, Ullas S, Lin S, Bilodeau M, Rossant J, et al., Regeneration of Thyroid Function by Transplantation of Differentiated Pluripotent Stem Cells. Cell Stem Cell, 2015. 17(5): p. 527-42.

24. Hawkins F and Kotton DN, Embryonic and induced pluripotent stem cells for lung regeneration. Ann Am Thorac Soc, 2015. 12 Suppl 1: p. S50-3.

25. Shapiro DL, Nardone LL, Rooney SA, Motoyama EK, and Munoz JL, Phospholipid biosynthesis and secretion by a cell line (A549) which resembles type II aleveolar epithelial cells. Biochim Biophys Acta, 1978. 530(2): p. 197-207.

LEGENDS TO THE FIGURES

Figure 1: Clinical characterization of a child carrying homozygous K1388N variation of ABCA3 protein. A. Chest x-ray. Initial chest x-ray showing homogenous fine reticular ground glass opacification. **B. Clinical course of the neonate** (ECMO = extra corporal membrane oxygenation). **C. Lung biopsy.** Lung biopsy showing the pattern of chronic pneumonitis of infancy; note increased presence of eosinophils (indicated by small block arrows, scale indicates 100 μm); for comparison a normal biopsy is given in **D.**. **E.** and **F.** show electron micrographs demonstrating plenty, albeit abnormal lamellar bodies in type II cells. Note the lack of lamellar structures and the presence of aggregates of dense material located marginally. **G.** Western blotting of a tracheobronchial aspirate (SP-B and SP-C), indicated amount of total protein of lavage added per lane and the respective standards (STD) of the patient obtained at the age of 5 weeks of life, 4.8 weeks after the administration of a single dose of exogenous surfactant. After SDS-PAGE and transfer, the membranes were probed with antibodies against SP-B and SP-C. Molecular weights (kDa) are indicated on the left side. All bands were analyzed under non-reducing conditions. SP-B was detected in large amounts (compare to standard STD of 8 ng applied to lane 2). In addition to the typical bands at 18 kDa some lower bands (monomers or degradation products), as well as higher molecular forms were observed. SP-C was detected in relatively smaller amounts making up less than 10% of the total amount (usually about 50%). Of interest was the presence of several higher molecular weight bands; this pattern is typically seen in patients with alveolar proteinosis. **H.** Schematic representation of ABCA3 protein with different sequence motifs and correct orientation. The K1388N mutation is shown as red filled hexagon. **I.** Partial amino acid alignment of ABCA3 sequences (codons 1348-1429). Alignment is showing that Lys1388 (indicated by red arrow) is extremely conserved.

Figure 2: Cellular effects of ABCA3-WT and ABCA3-K1388N stably expressed in A549 cells. A. ABCA3 mRNA levels analyzed by quantitative real time PCR ($p<0.001$ for WT/mock and K1388N/mock). **B.** Western immunoblot analysis of HA-tagged ABCA3 in total cell lysates. β-actin was used as a loading control. **C.** Ratio of upper/lower ABCA3 processing form ($p<0.5$). **D.** Cell proliferation assay of A549 cells stably transfected with WT and K1388N mutated ABCA3 protein compared to mock control. XTT tetrazolium salt was used for absolute quantification. **E.** Impact of stably transfection method on cell cytotoxicity. Therefore lactate dehydrogenase was quantified in cell supernatants. **F.** N-Glycosylation of ABCA3-HA WT and K1388N protein. The noncleaved 190 kDa ABCA3-HA protein is fully deglycosylated by PNGase F causing a shift in electrophoretic mobility to 180 kDa. Endo H digestion results in a separation of Endo H-sensitive 180 kDa ABCA3-HA protein (containing only high-mannose oligosaccharides) and Endo H-insensitive 190 kDa ABCA3-HA protein (with complex-type oligosaccharides). **G.** Co-immunostaining of HA-tagged ABCA3 with the lysosomal (lamellar body) marker CD63. **H.** Co-immunostaining of HA-tagged ABCA3 with the ER marker calnexin. (Scale: 10μm)

Figure 3: Impact of ABCA3-K1388N variant on lamellar body volume and morphogenesis. A. Left: immunofluorescence staining of HA-tagged ABCA3-WT and ABCA3-K1388N protein included in vesicles (scale: 10 μm). Vesicle volume was calculated based on diameter. Right: mean values of vesicle volumes containing either ABCA3-WT or ABCA3-K1388N protein. ***$P<0.001$. **B.** Electron microscopy of lamellar bodies showing mock control (left), ABCA3-WT (middle) and ABCA3-K1388N expressing A549 cells (right), respectively. Mock control cells contained no lamellar bodies, whereas ABCA3-WT transfected cells obtained morphological well-shaped LB with concentric membranes arranged in parallel (middle, black arrows). ABCA3-K1388N transfected A549 cells showed abnormal, fried-egg like structured lamellar bodies (right, black arrows). Scale: 0.5 μm. **C.**

Immunohistochemical staining of ABCA3 protein in lung tissues. Lung tissue of a healthy control patient expressing ABCA3 protein (left., red staining). ABCA3 expression shows strong staining intensity and typical pattern of ring-like structures located in the cytoplasm of type II pneumocytes. Right: ABCA3 protein expression in lung tissue of patient with homozygous ABCA3-K1388K protein variant. Very weak staining intensity and diffuse distribution of ABCA3 protein in type II pneumocytes can be detected. (Scale: 50 μm).

Figure 4: PC and PC 32:0 content. A. Intracellular PC and PC 32:0 content of A549 cells carrying ABCA3-K1388N variant compared to that in cells expressing ABCA3-WT protein. **P<0.01, ***P<0.001. **B.** PC and PC 32:0 content in BAL of patient with homozygous ABCA3-K1388N mutation compared to control group.

Figures

Figure 1

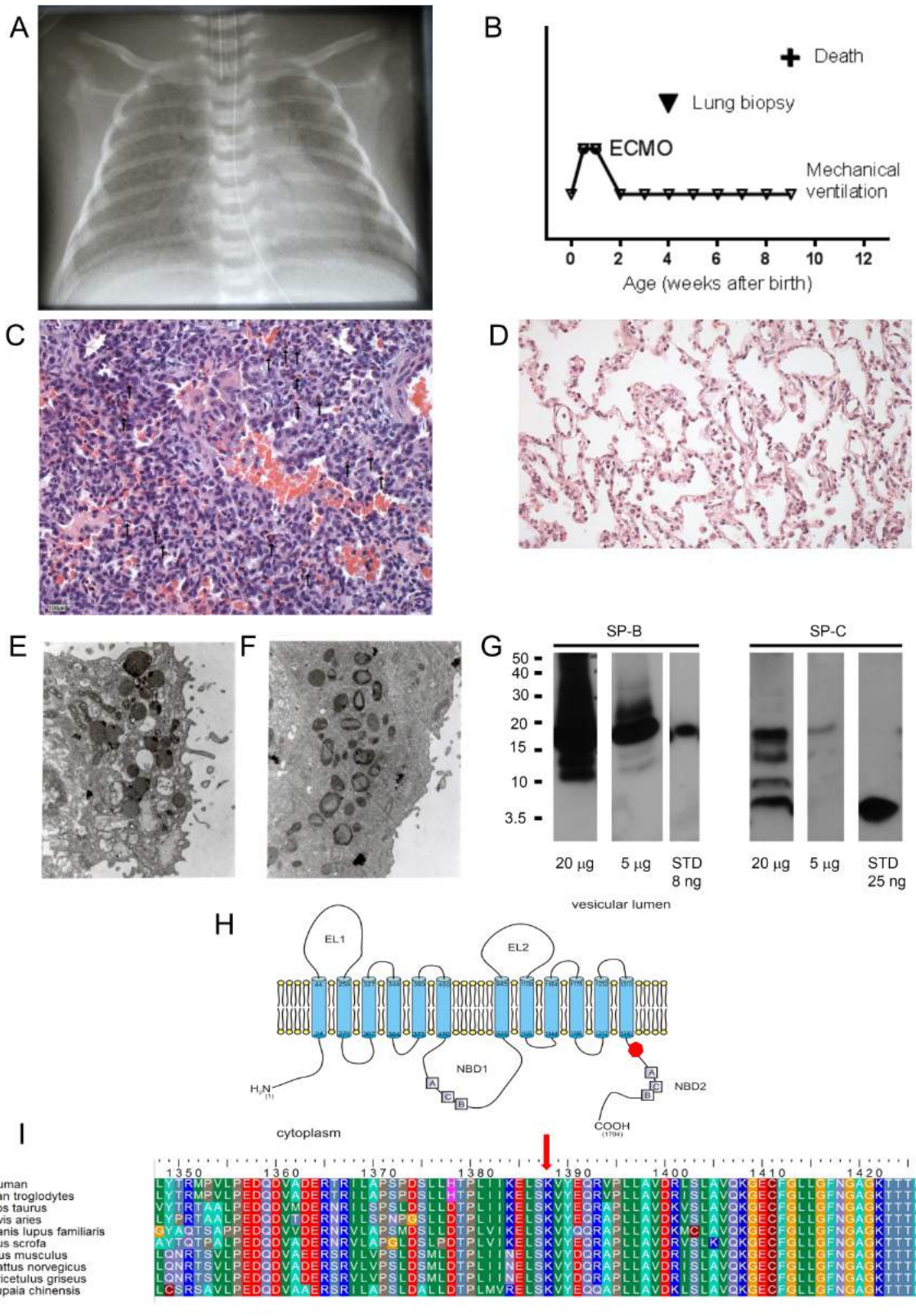

Figure 2

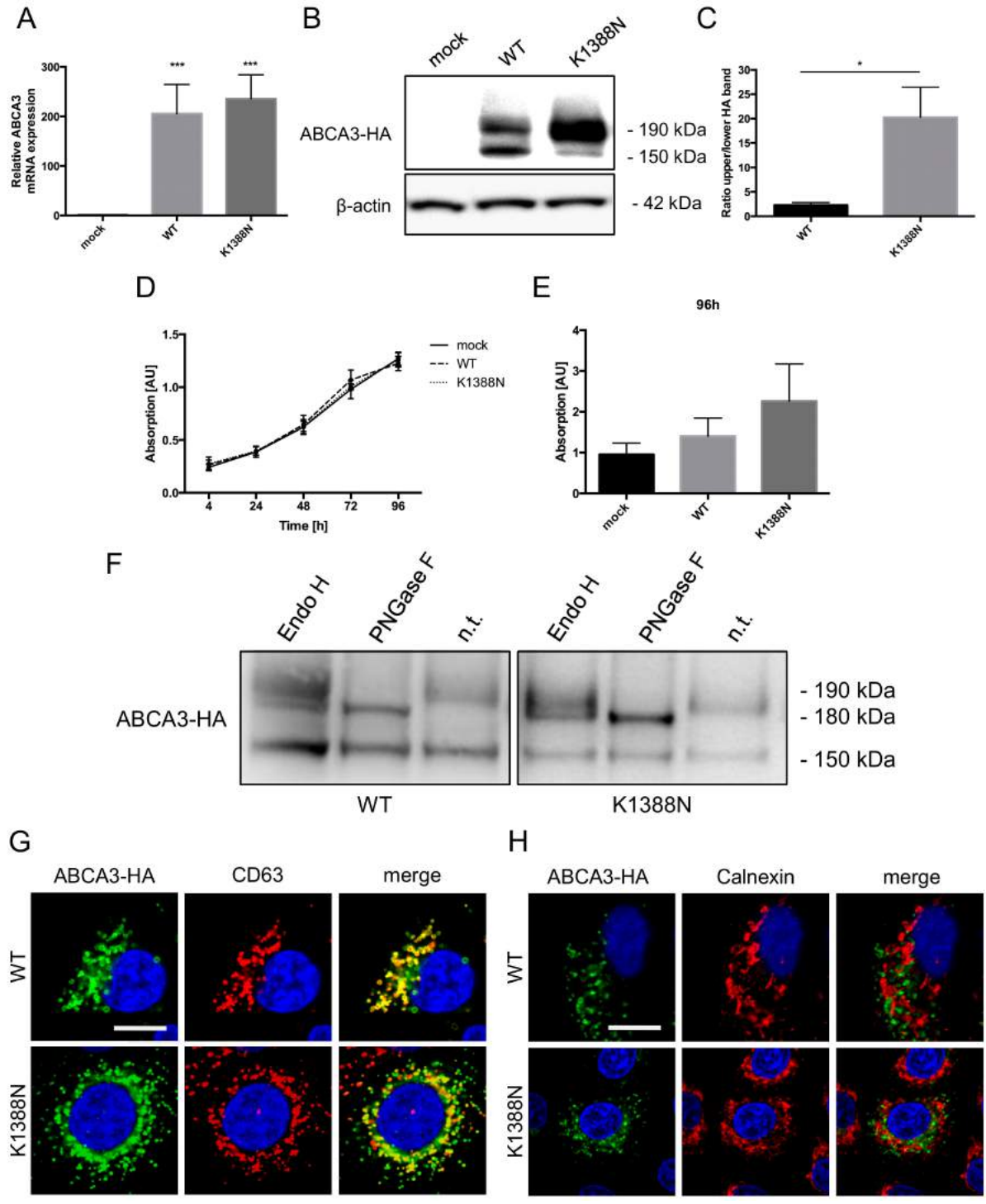
A
Relative ABCA3 mRNA expression
300
200
100
0
***
***
mock
WT
K1388N
B
mock
WT
K1388N
ABCA3-HA
- 190 kDa
- 150 kDa
β-actin
- 42 kDa
C
Ratio upper/lower HA band
30
25
20
15
10
5
0
*
WT
K1388N
D
Absorption [AU]
1.5
1.0
0.5
0.0
4
24
48
72
96
Time [h]
mock
WT
K1388N
E
96h
Absorption [AU]
4
3
2
1
0
mock
WT
K1388N
F
Endo H
PNGase F
n.t.
Endo H
PNGase F
n.t.
ABCA3-HA
- 190 kDa
- 180 kDa
- 150 kDa
WT
K1388N
G
ABCA3-HA
CD63
merge
WT
K1388N
H
ABCA3-HA
Calnexin
merge
WT
K1388N

Figure 3

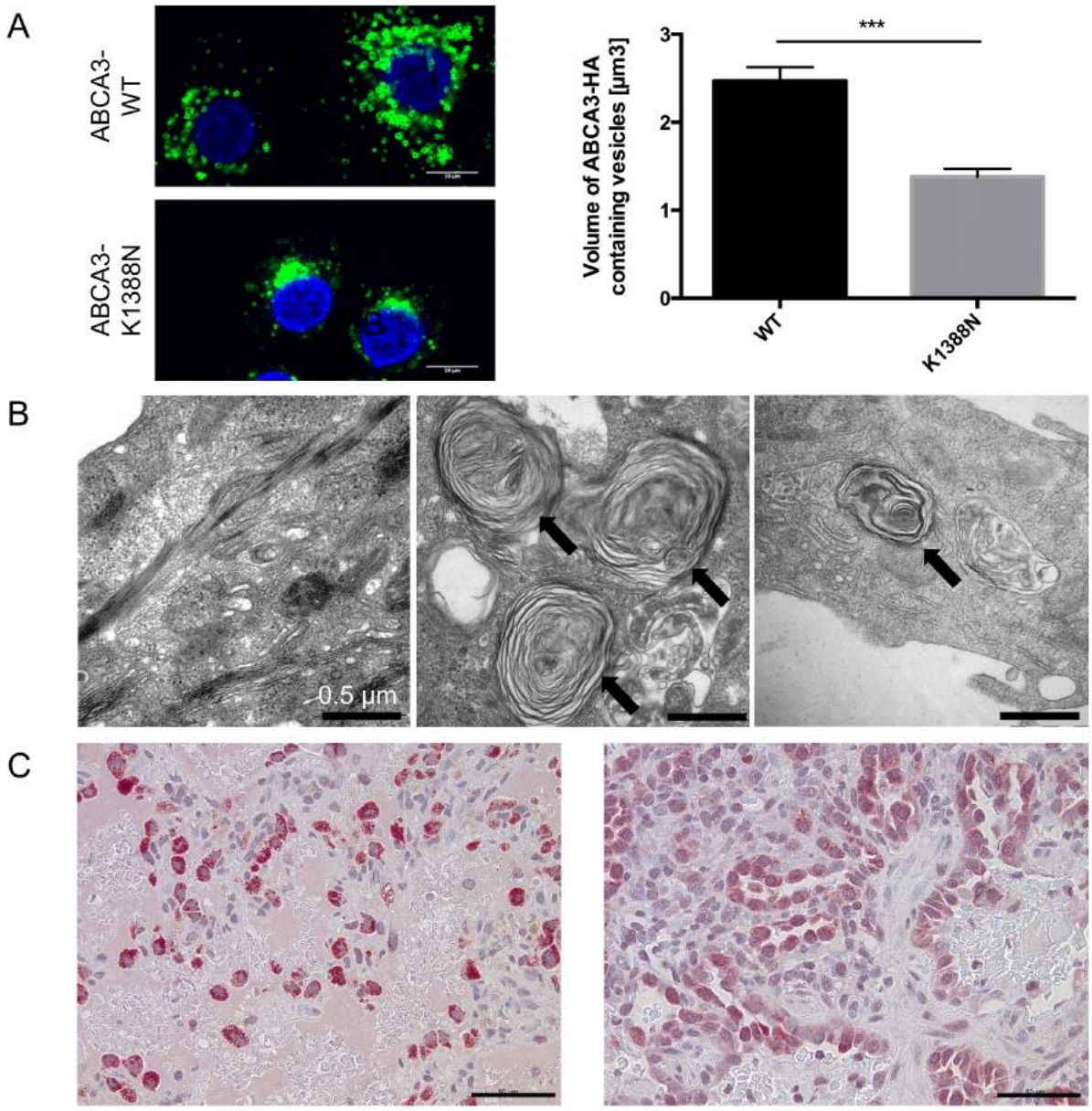
A
ABCA3-WT
ABCA3-K1388N
Volume of ABCA3-HA containing vesicles [µm3]
***
3
2
1
0
WT
K1388N
B
0.5 µm
C

Figure 4

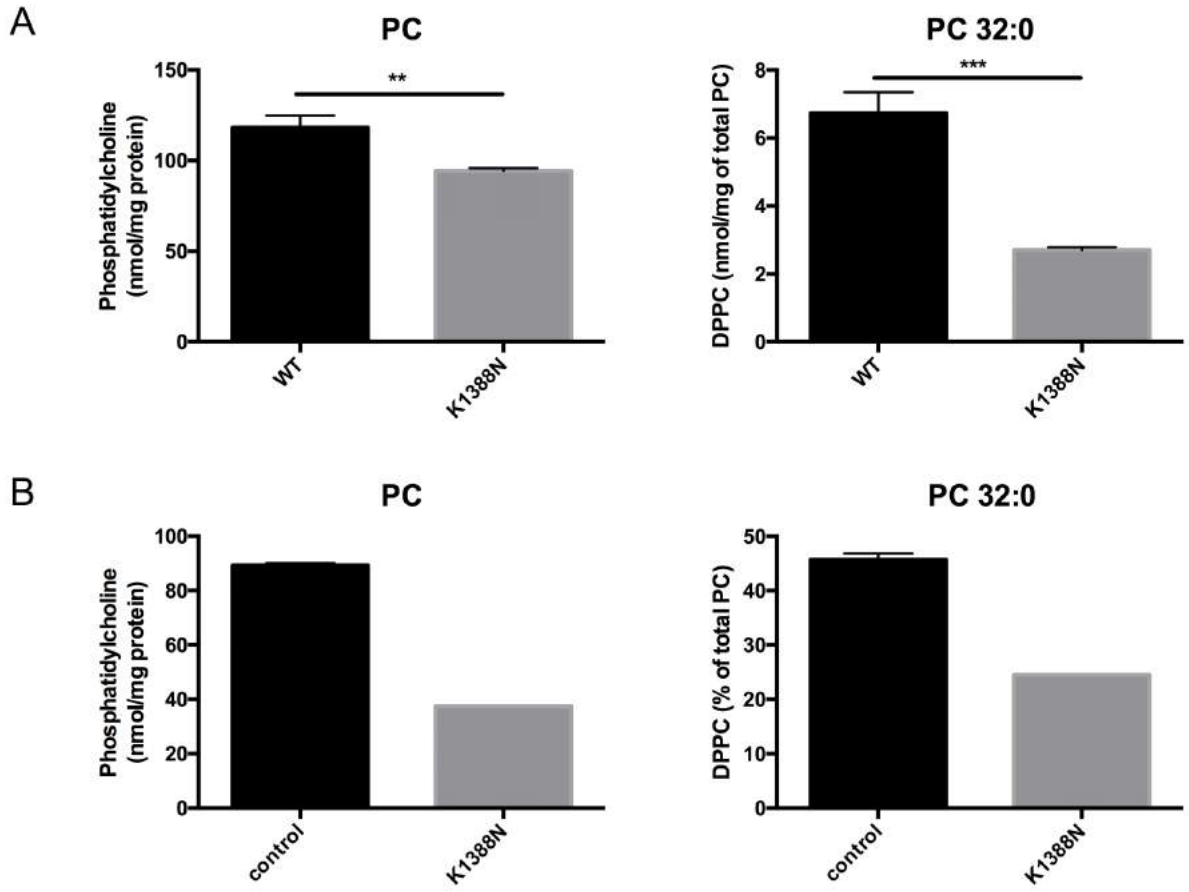
A
PC
**
Phosphatidylcholine (nmol/mg protein)
150
100
50
0
WT
K1388N
PC 32:0
***
DPPC (nmol/mg of total PC)
8
6
4
2
0
WT
K1388N
B
PC
Phosphatidylcholine (nmol/mg protein)
100
80
60
40
20
0
control
K1388N
PC 32:0
DPPC (% of total PC)
50
40
30
20
10
0
control
K1388N

Table 1: Criteria and molecular tools used to characterize the ABCA3 transporter

Criterion for classification	**Molecular tool**	**Mock transfected cells / Healthy controls**	**ABCA3-WT cells**	**Difference P-value**	**ABCA3-K1388N cells / Patient**	**Difference P-value**
Processing (Ratio 190 kDa/150 kDa form)	Western Blot	n.a.	2.26 ± 0.30	n.a.	20.30 ± 3.55	0.0316**
Intracellular protein localization	Immunofluorescence	n.a.	Co-localization with CD63	-	Co-localization with CD63	-
	Immunohistochemistry in patient tissue sections	Strong and ring-like ABCA3 staining in type II pneumocytes	n.a.	-	Weak and dispersed ABCA3 staining pattern in type II pneumocytes	-
Intracellular trafficking	N-glycosylation analysis	n.a.	Trafficking through ER and Golgi apparatus	-	Trafficking through ER and Golgi apparatus	-
Lamellar body volume	Immunofluorescence	n.a.	2.47 ± 0.16	n.a.	1.38 ± 0.10	<0.0001**
Lamellar body morphogenesis	Electron microscopy	Scarce or no lamellar bodies	Well-shaped lamellar bodies with concentric membranes	-	Abnormal fried-egg like shaped lamellar bodies	-

Table 1: Criteria and molecular tools used to characterize the ABCA3 transporter

Phosphatidylcholine content A549 cells (nmol/mg protein) (n=9)	Mass spectrometry	90.11 ± 0.97	118.25 ± 6.52	0.0061*	94.31 ± 1.57	0.1340* 0.0101+
Phosphatidylcholine content BAL (% of all analyzed lipids)		89.3 ± 0.8	n.a.	n.a.	37.5	n.a.
Dipalmitoyl-phosphatidylcholine (PC 32:0) content A549 cells (nmol/mg protein) (n=9)		4.52 ± 0.05	6.74 ± 0.61	0.0235*	2.70 ± 0.09	<0.0001* 0.0003+
Dipalmitoyl-phosphatidylcholine (PC 32:0) content BAL (% of all analyzed lipids)		45.8 ± 1.1	n.a.	n.a.	24.5	n.a.

n.a.= not available, *: P-values compared to control. **: P-values compared to ABCA3-WT. +: P-values ABCA3-K1388N compared to ABCA3-WT. Mean values (± S.E.M.) are displayed.

SUPPLEMENTAL MATERIAL

Supplemental Methods

Antibodies

The following antibodies were used: rabbit anti-HA (Sigma, Taufkirchen, Germany), rat anti-HA (Roche, Mannheim, Germany), mouse anti-CD63 (Abcam, Cambridge, United Kingdom), mouse anti-calnexin (Novus Biologicals, Cambridge, United Kingdom), chicken horse radish peroxidase (HRP)-conjugated anti-β-Actin (Santa Cruz, Heidelberg, Germany), Alexa Fluor 488 goat anti-rabbit IgG and Alexa Fluor 555 goat anti-mouse IgG (Life Technologies, Darmstadt, Germany), mouse anti-ABCA3 antibody (Seven Hills Bioreagents, Cincinnati, United States), rabbit anti-rat IgG (H+L) HRP (Southern Biotech, Eching, Germany).

In-vivo and *ex-vivo* analysis of patient materials

Mature neonate (41 week of gestation), APGAR 7 /8 after 5/ 10 min, oxygen supplementation, intubation first day of life, pulmonary hypertension (NO treatment), day 3 of life ECMO for one week, with improving oxygenation and successful decanulation, high frequency oscillatory ventilation (Fi02 0.6), treatment with surfactant with only brief improvement, slow deterioration of respiratory situation with increasing pulmonary arterial pressures, erythromycin for 7 days, lung biopsy with chronic pneumonitis of infancy pattern and tissue eosinophilia. A diagnostic BAL was taken prior to surfactant application. Methylprednisolone and hydroxychloroquine over 4 weeks without significant improvement. The respiratory situation deteriorated slowly but steadily and the patient died at age of 9 weeks. The *ABCA3* variation K1388N (c.4164G>C; AAG/AAC) was found in a patient

carrying this mutation in a homozygous state. *SFTPB* and *SFTPC* were without sequence variation.

Primers used for analysis of ABCA3, SFTPC and SFTPB. The sequence of all PCR primers is given in the 5´ to 3´ direction.

ABCA3 gene

A3-4-1	CCAAATCCCCACTCTGCGTG
A3-5-2	CAGCTGCTTCGCACATCCTG
A3-6-1	CAAAGCCCTAGAGGATTTGCC
A3-6-2	CAGACCCAAAGGAGTGACTGC
A3-7-1	CTCTCCCACTCCACCCTGTTG
A3-7-2	CTGCTATAAGGACACATGCACACG
A3-8-1	TCTCATTTGCTGTCAGTGTGTGG
A3-8-2	CTAAAACACCAAGCCTTTGGACATG
A3-9-1	CTGCTGGGACAGTCGGACTC
A3-9-2	CTGACCATCCCTGGTCACAGG
A3-10-1	CTCTTGGGAAGAACTTTGTGGTCAG
A3-10-2	GCTGACTTTCCTCCTTCCAGTCC
A3-11-1	GTGTAGATGGCAAGTGCCAGGAG
A3-11-2	CAGCTATCCAGCCCACACTCAG
A3-12-1	CATGCCAACCAAGCAGTGG
A3-12-2	CTCTCTCTGAACCAGTCCCAAGG
A3-13-1	CTGCATGGCTGTGTGCATCTAG
A3-13-2	CTATGAGGTCTCACTGCCGTGC
A3-14-1	CTAGGCTTGGTTCCTTCTGAGACG
A3-14-2	GTGCATCTCCTGCCGCTGTG
A3-15-1	CAGGGTCCTCAGAGGAAATTAGG
A3-15-2	CTCAGAACCCTGGCTCCTGC
A3-16-1	CAGCTACGTCAAGGAGAGGTTCC
A3-16-2	GCTCGTCCAGTATCAGCACCTG
A3-17-1	CCATCCTTGGAGGACTCAAGC
A3-17-2	CAGAGGCAACAGACAGGAAGTCTAG
A3-18-1	CAAGACACATTCATTCTGCTTCAGC
A3-18-2	GCAGATTCATCTGGGCTGATG
A3-19-1	GTTCAAGTGTTCTCCTGCCTCTG
A3-19-2	CTGGGCAACTAGAGTGAAACTCC
A3-20-1	CATAAGCAGATGCATGAGCAAGC
A3-20-2	CTCGCAGACTCTCCTCTGCATG
A3-21-1	GCTGGCGTCACACAGAACAG
A3-21-2	CATTCGGAACAGCCAAGAACC
A3-22-1	GTCCCTGATTAGCCATGCTCAG
A3-22-2	GCAGACACAATGCTCTATCTATGGG
A3-23-1	GTGCTTGTGCTCTCCCATAAGC
A3-23-2	CAGCTGGTTCCGGTTCTGC

A3-24-1	GTCTGAGGACCTCCAAATGCTC
A3-24-2	CATGAACTGGGCCCATTGC
A3-25-1	CTCCACACAGCACGGATAAGG
A3-25-2	CCACTCAGACGCAGAGGAGC
A3-26-1	GTCTGCCATGTCGCTCATGG
A3-26-2	GAGACCATCTGGTGCAGGAGC
A3-27-1	GATTGGGACGAGAAGCCTTG
A3-27-2	GCAAAGCAGAGCAGTCTGAGC
A3-28-1	CTGATTATCAAGGAGCTCTCCAAGG
A3-28-2	CAAGCCACAGATGCAGCAGC
A3-29-1	CACTGGCAGGAACCACAG
A3-29-2	CTCCATCCTGGAGCCACAAG
A3-30-1	CTGTTCTGCAATTGCTGGGTG
A3-30-2	GACTCTGCACCAGATGCTGATG
A3-31-1	GAGAGCCAATGCCTTCCTGTC
A3-31-2	GTGCTCAGCACTGGAGTCCTC
A3-32-1	GAGGACTCCAGTGCTGAGCAC
A3-32-2	GTGACTCCTCTGTGGAAAGAGCC
A3-33-1	CTATTGCCAGAGGACTCCCAGG
A3-33-2	GAGTGCCTGGAGAAATTCAACC

SFTPB gene

SB-1-1	GCCACAGAAATCTTGTCTCTGACTC
SB-1-2	TTACCACCTGTCCTGGCTGATG
SB-2-1	GTTGGAGGAAGCCACAAGTCC
SB-2-2	GTTAATGCCTAGCACAAAGCAGTG
SB-3-1	AGAGCTGTCTGACGTCCACATG
SB-3-2	ATCGCATCCATCCCATTCC
SB-4-1	AGCTGCATGTGCCTTGGAGTG
SB-4-2	CTCAGCTCTTCCCTGCTCTGTC
SB-5-1	TGCCCAACTACTTAACTCCTTGGC
SB-5-2	CTCCCCATGGGTGGGCACAG
SB-6-1	AGTGGTCCCTGAGCCCTTG
SB-6-2	GCTTCGGAGGTGGCTCTAGC
SB-7-1	CTAGAGCCACCTCCGAAGCC
SB-7-2	GTGTGAGTTGGGAGAGAGGTGG
SB-8-1	CTGGACTCTCTGATCCCCAGTG
SB-8-2	CAGAGGTGTTTGGTTTCTGTCCTC
SB-9-1	TCTGTGGTCCCACTGCAATG
SB-9-2	ACATCCTGTCTGCCTGTCTGTG
SB-10-1	TGATCCAGAGATGTGGAGAGGC
SB-10-2	GAGTGAGGCCTCTGAGGATCAC
SB-11-1	GTGGAGTGAGTGCTGTTCTTTCC
SB-11-2	TCTTCCTGCTTGGGGAGCAG

SFTPC gene

SC-1-1	CAGCAAGGAAGGCAGGCAC

SC-1-2	GAATGGATCTGGATAAGGAAACAGG
SC-2-1	TCCCTGTCCATCCATCGCATC
SC-2-2	GACAGTTTCCTATCGCCCATCC
SC-3-1	GAAAGAGGGAAGCGCATTTGAG
SC-3-2	CTCTAGGTTGGGCACGGGAGTC
SC-4-1	CAGATTCTAGTATGACTCCCGTGC
SC-4-2	GAGGAACAGTGCTTTACAGGTGAC
SC-5-1	CTGGTGGCTTCTGACTCTAGCAC
SC-5-2	GAGTGGGAAGTACCGGTCTGTGAG

Legends to Supplemental Figures

Supplemental Figure 1. Lipid composition and PC species content. A. Left: lipids (% of all analyzed lipid classes) in BAL of patient carrying K1388N variant compared to control group (n=11). Right: Intracellular lipid content (nmol/mg protein) of A549 cells stably expressing K1388N variant compared to A549 cells expressing ABCA3-WT protein. ****P<0.0001. Abbreviations: PC: phosphatidylcholine; SPM: sphingomyelin with dihydrosphingomyelin; PE: phosphatidylethanolamine; PE P: PE based plasmalogens; PS: phosphatidylserine; PG: phosphatidylglycerol; PI: phosphatidylinositol; LPC: lysophosphatidylcholine; Cer: ceramide. **B.** PC species content of lipids in BAL of patient carrying K1388N mutation compared to control group (left) and in A549 cells stably expressing ABCA3-K1388N compared to cells with ABCA3-WT expression (right). For better depiction ratio of lipid content relative to control group and WT respectively was calculated. A ratio below 1 indicates a decrease of the respective PC species compared to control group or WT, while a ratio above 1 indicates an increase in comparison to control group or WT. *: P-values are adjusted with Benjamini and Hochberg correction for multiple comparisons.

Supplemental Figure 2: A. Free cholesterol content and cholesteryl ester in A549 cells expressing either ABCA3-WT or ABCA3-K1388N mutated protein. *P<0.05, **P<0.001. **B.**

Lipid droplet formation in epithelial lung cells expressing ABCA3-WT and ABCA3-K1388N. Lipid droplets per cell (left) and lipid droplet volume per cell were calculated with 3D object counter software plugin in ImageJ.

Supplemental Figures

Figure 1

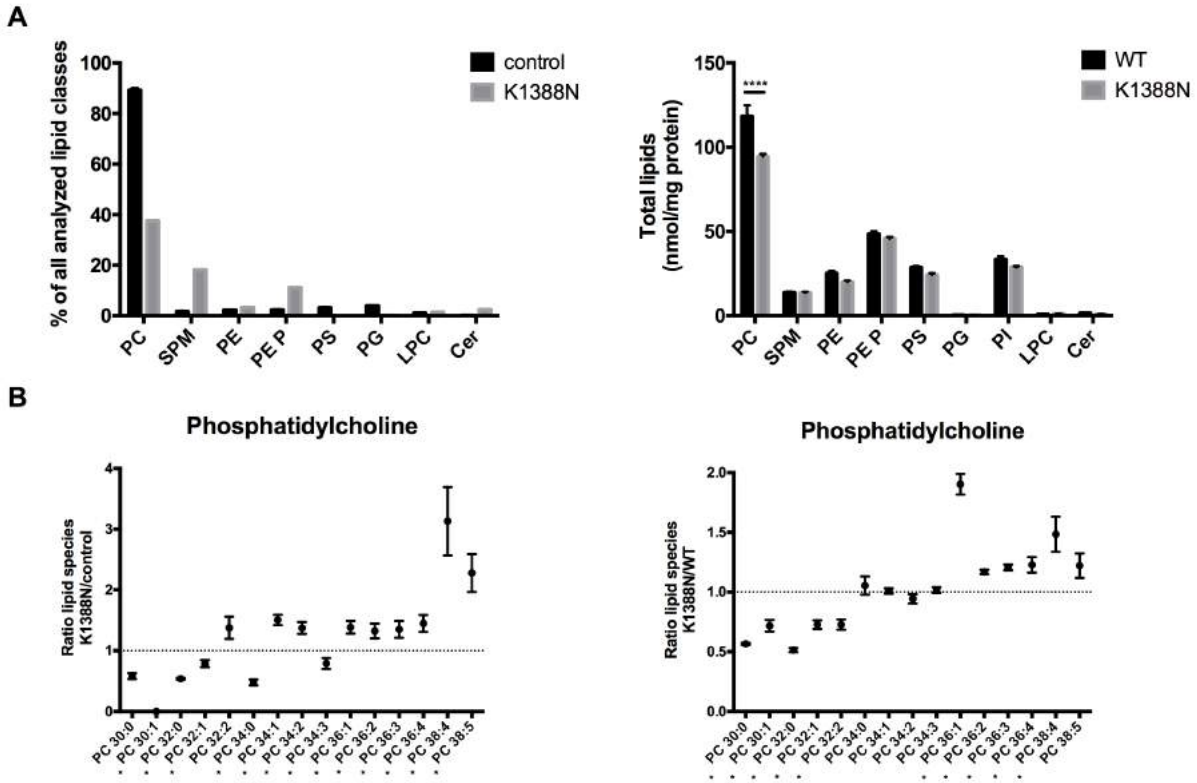

Figure 2

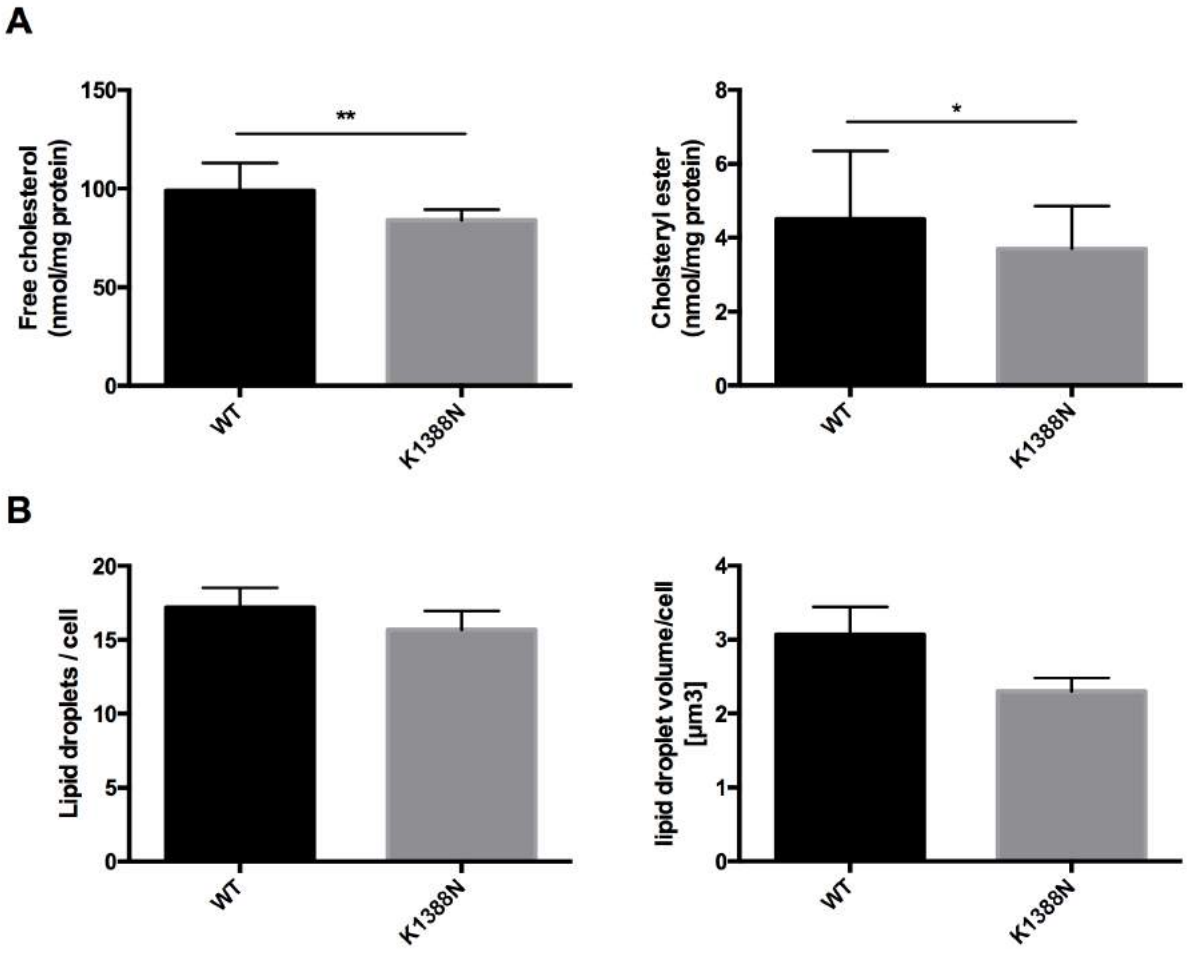
A
Free cholesterol (nmol/mg protein)
150
100
50
0
**
WT
K1388N
Cholsteryl ester (nmol/mg protein)
8
6
4
2
0
*
WT
K1388N
B
Lipid droplets / cell
20
15
10
5
0
WT
K1388N
lipid droplet volume/cell [µm3]
4
3
2
1
0
WT
K1388N

Paper 3

Hofmann N., Galetskiy D., Rauch D., **Wittmann T.**, Marquardt A., Griese M., and Zarbock R. (2015). *Analysis of the proteolytic processing of ABCA3: identification of cleavage site and involved proteases.* PloS One (accepted)

Analysis of the proteolytic processing of ABCA3: identification of cleavage site and involved proteases

Nicole Hofmann[1], Dmitry Galetskiy[2], Daniela Rauch[1], Thomas Wittmann[1], Andreas Marquardt[2], Matthias Griese[1], and Ralf Zarbock[1*]

[1] German Centre for Lung Research, Dr. von Hauner Children's Hospital, Ludwig-Maximilians University, 80337 Munich, Germany

[2] Proteomics facility, University of Konstanz, 78547 Konstanz, Germany

* Corresponding author

E-mail: Ralf.Zarbock@med.uni-muenchen.de

Phone 0049/(0)89/4400-57717

Fax 0049/(0)89/4400-57715

Abstract

Rationale

ABCA3 is a lipid transporter in the limiting membrane of lamellar bodies in alveolar type II cells. Mutations in the *ABCA3* gene cause respiratory distress syndrome in new-borns and childhood interstitial lung disease. ABCA3 is N-terminally cleaved by an as yet unknown protease, a process believed to regulate ABCA3 activity.

Methods

The exact site where ABCA3 is cleaved was localized using mass spectrometry (MS). Proteases involved in ABCA3 processing were identified using small molecule inhibitors and siRNA mediated gene knockdown. Results were verified by in vitro digestion of a synthetic peptide substrate mimicking ABCA3's cleavage region, followed by MS analysis

Results

We found that cleavage of ABCA3 occurs after Lys^{174} which is located in the proteins' first luminal loop. Inhibition of cathepsin L and, to a lesser extent, cathepsin B resulted in attenuation of ABCA3 cleavage. Both enzymes showed activity against the ABCA3 peptide *in vitro* with cathepsin L being more active.

Conclusion

We show here that, like some other proteins of the lysosomal membrane, ABCA3 is a substrate of cathepsin L. Therefore, cathepsin L may represent a potential target to therapeutically influence ABCA3 activity in ABCA3-associated lung disease.

Introduction

ABCA3 is a member of the subclass A of the large ABC transporter family which comprises transporters involved in cellular lipid transport [1]. ABCA3 is strongly expressed in the lungs where it localizes to the outer membrane of lamellar bodies (LBs) in alveolar epithelial type II cells [2,3]. It transports phospholipids and cholesterol into the LB lumen and is essential for the biogenesis of LBs [4,5]. Mutations in ABCA3 cause an often fatal severe respiratory distress syndrome in new-borns and diffuse parenchymal lung disease in children (chILD) [6,7].

To date, little is known about the cell biology of ABCA3. After folding in the ER and glycosylation in the Golgi apparatus, ABCA3 is trafficked to the endosomal compartment and finally reaches acidic, lysosome-derived multivesicular bodies, precursors of LBs [8]. The exact route ABCA3 takes remains elusive; for example, it is currently unknown whether it passes the plasma membrane. Interestingly, in immunoblots ABCA3 gives two protein bands with an apparent molecular mass of approximately 190 and 170 kDa, respectively [4,9]. We showed previously that the lower band arises by proteolytic cleavage at the N-terminus of ABCA3 [10]. In the same study, we also identified post-trans-Golgi acidic vesicles as the intracellular compartment of ABCA3 processing and provided evidence for the involvement of a cysteine protease.

Since it can be expected that cleavage of ABCA3 has an effect on the protein's function, the protease(s) involved the processing of ABCA3 represent a potential therapeutic target. Inhibition of the enzyme(s) in order to elevate the amount of ABCA3 may counteract diminished ABCA3 activity as a result of mutations or diminished expression due to disturbed

gene regulation. Therefore, the objectives of the present study were the identification of the protease(s) cleaving ABCA3 and of the precise cleavage site.

Materials and methods

Cell culture

A549 cells were obtained from DSMZ (Braunschweig, Germany). Cells were maintained in RPMI 1640 medium (Life technologies, Darmstadt, Germany) supplemented with 10 % FBS at 37°C and 5 % CO_2. Stable transfection of A549 cells with *pUB6-ABCA3-WT* vector was carried out as previously described [11]. Cleavage site mutations were introduced into *pUB6-ABCA3-WT* using the Q5 Site-Directed Mutagenesis Kit (NEB, Frankfurt/Main, Germany) according to the manufacturer's instructions. For inhibitor experiments, cells were grown to confluence, trypsinized and seeded at 200.000 cells per 6-well and grown for 48 h prior to treatment. For siRNA mediated knockdown, cells were trypsinized and cell suspension was adjusted to 200,000 cells / ml in RPMI medium with 10 % FBS. 2 ml of cell suspension was then added to a mixture of siRNA (125 pmol / well; Life technologies) and Lipofectamine 2000 (8 µl / well; Life technologies) in OptiMEM (Life technologies) dispensed in 6-well plates. Cells were harvested after incubation with siRNA for 48 h. Scrambled siRNA (Life technologies) was used as control.

Gel electrophoresis and immunoblot

After harvesting by trypsination, cells were rinsed with PBS once and subsequently lysed with radioimmunoprecipitation (RIPA) buffer (0.15 M sodium chloride, 1 % Triton-X 100, 0.5 % sodium deoxycholate, 0.1 % SDS, 5 mM EDTA and 50 mM Tris pH 8) containing complete protease inhibitor (Roche, Mannheim, Germany). The lysate was centrifuged for 30 min at 1000 x g and 4°C. The protein concentration of the post-nuclear supernatant (= whole cell lysate) was determined with Bradford assay using BSA as protein standard. 15 -

30 µg of cell lysates in 4x LDS buffer (Life technologies) were loaded onto NuPage Mini Bis-Tris or Tris-Acetate gels (Life technologies). Following gel electrophoresis, proteins were visualized using Coomassie Brilliant Blue (Sigma-Aldrich, Steinheim, Germany) or transferred to PVDF-membranes (Millipore, Billerica, USA) and immunoblotted using anti-HA-tag (Roche) and anti-β-actin HRP conjugate (Santa Cruz, Heidelberg, Germany). Chemiluminiscent signal was detected by ECL Detection Reagent (GE Healthcare, Freiburg, Germany) and analyzed by densitometry.

RNA isolation/cDNA synthesis/quantitative real time PCR

Cells grown to confluence in 6-well plates were washed once with PBS. Cells were harvested and total RNA was isolated with the High Pure RNA Isolation Kit (Roche, Mannheim, Germany) according to the manufacturer's instructions. RNA concentrations were measured with a NanoDrop spectrophotometer (Thermo Scientific, Waltham, MA, USA). 1 µg of total RNA was reversely transcribed into cDNA with the Tetro reverse transcription kit (Bioline, Luckenwalde, Germany). Quantitative real-time PCR was carried out using SensiFAST SYBR Hi-ROX Mix (Bioline) on an ABI 7900HT cycler (Applied Biosystems, Darmstadt, Germany). HPRT1 was used as housekeeper gene. For analysis of relative changes, data was analyzed according to the $\Delta\Delta C_T$ method.

In-gel digestion and peptide extraction

Gel bands visualized with Coomassie Blue were excised, destained and digested with trypsin gold mass spectrometry grade (Promega, Madisson, USA) according to the manufactures' protocol. Extracted peptides were subjected to LC-MS/MS analysis.

Liquid chromatography-tandem mass spectrometry (LC-MS/MS) and data analysis

Peptide mixtures were separated using an Eksigent nano-HPLC (Eksigent Technologies, Dublin, USA) with a reversed-phase LC column (5 μm, 100 Å pore size C18 resin in a 75 μm i.d. × 10 cm fused silica capillary; Acclaim PepMap100; Thermo Scientific, Waltham, USA). After sample injection, the column was washed for 5 min with 95% mobile phase A (0.1% formic acid) and 5% mobile phase B (0.1% formic acid in acetonitrile), and peptides were eluted using a linear gradient of 5% mobile phase B to 40% mobile phase B in 65 min, then to 80% B in an additional 5 min, at 300 nL/min. Mass spectrometric analysis was performed on an LTQ-Orbitrap Discovery mass spectrometer (Thermo Fisher Scientific, Bremen, Germany) operated in a data dependent mode in which each full MS scan (*m/z* 200-1,450) acquired in Orbitrap with resolution of R=30,000 (*m/z* 400) was followed by five MS/MS scans where the five most abundant molecular ions were dynamically selected and fragmented by collision-induced dissociation (CID) using a normalized collision energy of 35% in the LTQ ion trap. Dynamic exclusion was allowed.

Mascot database searching was performed using the Mascot Server 2.3 software (Matrix Science, London, UK); all tandem mass spectra were searched against the SwissProt and NCBInr human protein databases. Search criteria for tryptic digest mixtures included trypsin as an enzyme, one missed cleavage, methionine oxidation as variable modification and mass tolerances of 5 ppm for MS and 0.5 kDa for MS/MS. The results were filtered to a 5% maximal false discovery rate; peptide score cut-off of 15 was used. Identification of modified and non-specifically cleaved peptides was additionally performed by the Mascot error tolerant search. Presence/absence of ABCA3 sequence parts ware validated with Xcalibur software

(Thermo Finnigan, San Jose, CA, USA) using extracted MS ion chromatograms of the accurate peptide *m/z* values ±5 ppm related to corresponding peptide ions.

In vitro analysis of products from cleavage of ABCA3 with cathepsins B and L

Synthetic KYHLRFSYTRRNYMWTQTGSFFLKETEGWHTTSLFPLFPNPGPR peptide (HPLC purity 98%), comprising residues 151-194 of human ABCA3, was purchased from GenScript (Piscataway, USA). Peptide cleavages were performed with cathepsin B purified from human placenta (Sigma-Aldrich) and human recombinant cathepsin L (GeneTex, Irvine, USA) using single cathepsins or their combination. Peptide and cathepsins were mixed in 100 µL 10 mM ammonium acetate pH 4.5 to a final concentration of 20 µM for the peptide and 2 µM for either of the cathepsins. After 20 min incubation at 37°C samples were immediately analyzed by LC-MS/MS.

Statistics

Comparisons of multiple groups were done using one-way repeated measure ANOVAs with Tukey's post hoc test. Results were presented as mean + S.E.M. of a minimum of three different experiments. P-values of less than 0.05 were considered statistically significant. All tests were performed using GraphPad Prism 5.0 (GraphPad Software, La Jolla, USA).

Results

Mass spectrometric analysis reveals N-terminal cleavage region of ABCA3

Protein cleavage site or region can be quantitatively determined using intensity ratios of tryptic peptides or their fragments in cleaved and non-cleaved protein forms [12]. We separate proteins of A549 cells transfected with *pUB6-ABCA3-WT* vector by gel electrophoresis, visualized them with Coomassie Blue, and analyzed by LC-MS/MS. ABCA3 protein was identified in gel bands at 190 kDa and 170 kDa (Fig 1A). Profile analysis using highly accurate (±5 ppm) MS chromatograms for corresponding peptide ions revealed the presence of the C-terminal protein part comprising residues (175-1704) in both bands. Tryptic peptides from the N-terminal protein region (6-174) were detected only in the upper band. Parts of the ABCA3 protein sequence identified in 190 kDa and 170 kDa gel bands are presented in Fig 1B. Fig 1C illustrates the quantitative MS approach used for the determination of the cleavage region. The peptide intensity ratios (170 kDa / 190 kDa) was 1.7±0.4 within the sequence (175-1704) and ~0 for the peptides (6-13), (115-121) and (162-174) from the N-terminal region (Fig 1C). Remarkably, highly intense signals of doubly-charged ions at *m/z* 819.885 and at *m/z* 811.887 identified as peptide ^{162}NYMWTQTGSFFLK^{174} with and without oxidation at Met^{164} were detected in 190 kDa band (Fig 2). These signals are completely missing in 170 kDa band. This observation provides evidence of N-terminal ABCA3 processing within the region between residues 162 and 174. Due to the relatively high signal intensity of the peptide (162-174) we would have expected the signal (X-174, X-amino acid residue after the cleavage site of protein

processing) with significant intensity present only in N-terminally processed 170 kDa ABCA3. We have searched for signals with corresponding *m/z* values but could not find any. Therefore, from these experiments we propose ABCA cleavage after Lys^{174} or close to it. In this case, the peptide (X-174) is too small and lost during sample preparation or enrichment.

Prediction of the membrane topology of ABCA3 suggests that the cleavage site is located in the vesicular lumen

We used TOPCONS (http://topcons.net/) for consensus prediction of ABCA3 membrane topology [13]. The prediction generated by TOPCONS is a consensus from five different topology prediction algorithms. The results of all five algorithms are in agreement with an outside orientation of the identified cleavage region, i.e. the region is located in the lysosomal lumen (Fig 3).

Application of specific inhibitors suggests cathepsins L and B as ABCA3 processing enzymes

From earlier studies, we knew that ABCA3 is N-terminally cleaved by a cysteine protease and that acidification of the vesicles ABCA3 resides in is necessary for cleavage to occur [10]. Based on this knowledge, we aimed to narrow down the list of proteases possibly involved by application of highly specific inhibitors. ALLM (N-Acetyl-Leu-Leu-Met-CHO) is an inhibitor of calpains I and II and also very potently inhibits cathepsins B and L [14]. ALLM almost completely abolished proteolytic processing of ABCA3 and lead to a prominent accumulation of the 190 kDa band, while the 170 kDa band became weaker (Fig 4A). Since the identified cleavage site is located in the vesicular lumen, we reasoned that the protease(s) cleaving ABCA3 would have to be lysosomally located and active at acidic pH. The latter would exclude calpains. Since results with ALLM pointed to involvement of

cathepsin B and/or L, we applied inhibitors thought to be specific for cathepsin B and cathepsin L, respectively. Treatment of cells with the cathepsin B inhibitor L-trans-expoxysuccinyl-Ile-Pro-OH propylamide methyl ester (CA-074Me; [15]) resulted in accumulation of the 190 kDa ABCA3 band when concentrations of at least 60 μM were used; the 170 kDa band remained unchanged (Fig 4B). The weaker effect of CA-074Me on ABCA3 cleavage compared to ALLM suggests rather low activity of cathepsin B as an ABCA3 cleaving enzyme. For ALLM and CA-074Me, the inhibitor concentrations used did not impair the general cell growth or fitness (data not shown). Incubation of cells with the cathepsin L inhibitor N-(1-naphthalenylsulfonyl-L-isoleucyl-L-tryptophanal (NapSul-Ile-Trp-CHO; [16]) did not result in accumulation of the 190 kDa band (Fig 4C). Inhibitor concentrations exceeding 40 μM lead to a disappearing of both bands, indicating that cathepsin L inhibition with NapSul-Ile-Trp-CHO has a stronger effect on cell viability than on ABCA3 production and processing. Our results gathered using protease inhibitors thus suggest cathepsin L and - to lower extend - cathepsin B as ABCA3-processing enzymes, but the action of cathepsin L could not be proven clearly due to the adverse effects on cell viability by specific inhibition of cathepsin L.

siRNA mediated knockdown of cathepsins confirms involvement of cathepsins L and B

To further verify ABCA3 processing by cathepsins, we used siRNA-mediated knockdown of cathepsin genes. To do this, we applied siRNAs directed against all cysteine proteases of the cathepsin family that had been identified in lysosomes [17]. This included proteases encoded by *CTSB, CTSF, CTSH, CTSK, CTSL1, CTSL2, CTSO, and CTSS*. As a control, we also used siRNA knockdown of *CTSD* (Asp protease). Gene knockdown was monitored using quantitative PCR and was considered successful when expression was

reduced by more than 70% (data not shown). Immunoblot performed on cell lysates collected 48 h after siRNA transfection showed accumulation of the 190 kDa band as an indicator for inhibition of cleavage only in the case of *CTSL1* (Fig 5). The effect was slightly enhanced when knockdown of cathepsin L and cathepsin B was performed simultaneously, indicating a possible additive action of both proteases. When we quantified protein bands to assess the ratio of 190 kDa to 170 kDa ABCA3 bands, we found significant increase of the band ratio in the case of *CTSL1* alone and also for the combination of *CTSL1* and *CTSB* (Fig 6). Thus, siRNA knockdown confirms the involvement of cathepsins B and L in the processing of ABCA3 and points to combined action of these proteases.

MS analysis of ABCA3 peptide cleavage products demonstrates specific cleavage after Lys^{174} by cathepsin L

To verify the ABCA3 cleavage by cathepsins L and B, we performed proteolytic digestion of a peptide comprising residues 151-194 of ABCA3 with cathepsins L and B at acidic conditions (pH 4.5) and analyzed the cleavage products by LC-MS. Triply-charged ion at *m/z* 761.711 corresponding to the ABCA3 sequence (175-194) related to the cleavage after Lys^{174} was the most prominent signal appearing during incubation of the peptide with cathepsin L alone and in combination with cathepsin B. High cleavage specificity of cathepsin L for the peptide within the ABCA3 processing region is illustrated in Fig 7. Specificity and cleavage efficiency of cathepsin B was significantly lower in comparison to cathepsin L. Major cathepsin B cleavage products were the peptides (172-194) and (168-194) related to the cleavages after Phe^{171} and Gln^{167}, respectively, in almost equivalent amounts. Cleavage patterns resulting from the combination of cathepsins L and B suggest sequential action (data not shown). Our study thus reveals highly specific ABCA3 processing by cathepsin L after Lys^{174}.

Inactivation of putative cathepsin L cleavage site inhibits ABCA3 processing

Having identified cathepsin L as the major protease responsible for cleavage of ABCA3 as well as its cleavage site, we aimed to abolish cleavage by abrogating substrate recognition. Since it is known that both amino acid residues that precede the actual cleavage site are crucial for substrate recognition, we replaced Leu^{173} and Lys^{174} of ABCA3 with alanine residues. This operation resulted in prominent accumulation of the upper ABCA3 band (Fig 8), indicating inhibition of processing and confirming correct identification of the cleavage site.

Discussion

In the present study, we show that ABCA3 is proteolytically cleaved by cathepsin L and to a lower extent also by cathepsin B. We also identified the exact cleavage site of cathepsin L which is located after Lys^{174}.

We have previously shown that ABCA3 is N-terminally cleaved in LAMP3-positive vesicles which are supposed to be lysosome-related organelles [10]. We now report identification of the precise cleavage site. According to the predicted membrane topology of ABCA3 (Fig 2), this site is located in the proteins' first large extracellular loop. Therefore, this loop is oriented towards the acidic lumen of the vesicles and is accessible to proteases of the lysosomal matrix. This finding is in concordance with our previous report that ABCA3 is cleaved upon reaching LAMP3-positive vesicles and that cleavage is blocked by inhibition of vesicle acidification [10]. It can be speculated that the localization of the cleavage site in the largest lumenal loop of ABCA3 – which is similar to CLN7 – favours steric access for proteolytic enzymes in the lysosomal lumen [18]. The first lumenal loop also contains two N-linked glycosylation sites (Asn^{124} and Asn^{140}) in vicinity of the cleavage site [19]. N-linked glycosylation of these sites in ABCA3 may limit the rate of proteolysis as it does in the cases of LAMP-1, LAMP-2, and also CLN7 [18].

We had also shown earlier that cleavage is blocked by E-64, an inhibitor of cysteine proteases. Based on these results, it was clear that the protease(s) involved in the processing of ABCA3 had to be lysosomal cysteine proteases active at acidic pH. Using a combined approach consisting of specific protease inhibitors and siRNA mediated gene knockdown, we show here that cathepsin L and B are likely involved in ABCA3 processing. However, the effect seen in the case of CA-074Me required rather high inhibitor concentrations, implicating

that the specific activity of cathepsin B against ABCA3 is not very high. This assumption is corroborated by the results of *in vitro* digestion. Moreover, although CA-074 was thought to be specific for cathepsin B, it turned out that the cell permeable CA-074Me also inhibits cathepsin L to some extent [20]. Therefore, it cannot be used to reliably distinguish between cathepsin B and cathepsin L. The specific cathepsin L inhibitor NapSul-Ile-Trp-CHO prevented formation of both ABCA3 forms, a finding that is in concordance with earlier reports that NapSul-Ile-Trp-CHO causes a dose-dependent suppression of cell proliferation and cell-death in SaOS2 cells at concentrations of 40 μM [21]. It is thus possible that when treated with NapSul-Ile-Trp-CHO, A549 cells did not survive long enough to accumulate the 190 kDa ABCA3 form. Specific inhibition of cathepsin L seems to be a general problem if cancer cells are used; a strong inhibitory effect on cancer cell proliferation was reported also for other specific chemical inhibitors and neutralizing antibodies of cathepsin L [22, 23]. However, we reasoned that given the results from siRNA knockdown and *in vitro* digestion experiments, it was not necessary to test further inhibitors. Taken together, the results of small molecule inhibitors and siRNA knockdown indicate that both cathepsin L and cathepsin B are possibly involved in ABCA3 processing. However, the moderate effect of CA-074Me and the *in vitro* digestion of ABCA3 peptide indicate that the activity of cathepsin B towards ABCA3 is much lower than that of cathepsin L. It is thus questionable whether cleavage of ABCA3 by cathepsin B is physiologically relevant.

Cleavage of ABCA3 is a further example for a highly specific function of cathepsins. While they were long believed to perform unspecific bulk proteolysis, it has now become evident that cathepsins also carry out specific non-redundant *in vivo* functions [24]. It has also been discussed that expression of ubiquitous cathepsins in specialized cells – which certainly applies to alveolar epithelial type II cells – may indicate a highly specific function for a rather

nonspecific protease [25]. Indeed, cathepsin L was shown to be involved in the processing of cathepsin D in A549 cells [26]. There are a few examples of lysosomal membrane proteins as cathepsin L substrates [27]. In the case of cathepsin L, its involvement in the processing of DIRC2 and CLN7 has been demonstrated [18,28]. CLN7 was the first example of a disease-associated lysosomal membrane protein that is processed by cathepsin L [18].

Analysis of peptide fragments using mass spectrometry showed that the peptide was cleaved by cathepsin L after Lys^{174} in concordance with the cleavage site we had found for full-length ABCA3 in living cells. For cathepsins, it was found that S2 is the primary specificity-defining site [29]. The respective residue in the case of ABCA3 would be Leucine which is accepted at this position by most lysosomal cysteine proteases. Indeed, Leu^{173} and Lys^{174} seem to be important for the recognition by cathepsin L as exchanging both residues for alanine resulted in a marked inhibition of cleavage (Fig 7). The observation of *in vitro* cleavage by cathepsin L also implies that ABCA3 is a direct substrate of cathepsin L rather than of a downstream protease activated by cathepsin L.

Cathepsin L deficiency in mice is not associated with lung disease [24]. Although it cannot be concluded that the same is necessarily true in humans, no lung disease associated with mutations in the cathepsin L gene has been observed so far. Thus, it seems that cathepsin L-mediated cleavage is not critically required for functional activation of ABCA3. This would support the hypothesis that full-length ABCA3 is functionally active and that proteolytic cleavage serves to regulate ABCA3 levels rather than activating the transporter. However, it can be expected that a certain level of ABCA3 is needed for sufficient biosynthesis of lamellar bodies and secretion of surfactant into the alveolar space. Since the amount of ABCA3 depends on the rates of synthesis and degradation, it is reasonable to speculate that disturbances of the steady state may negatively affect surfactant homeostasis and ultimately

lead to disease. On the other hand, when ABCA3 degradation was inhibited by targeting cathepsin L activity, a positive effect on ABCA3 activity could be expected. Interfering with the activity of cathepsin L in alveolar epithelial type II cells may thus represent an approach to ameliorate ABCA3 function in patients suffering from lung disease due to ABCA3 haploinsufficiency [30].

Acknowledgements

We would like to thank Claudia Bräu-Heberger, Andrea Schams and Kathrin Schiffl for excellent technical assistance. This work was supported by a grant from the Deutsche Forschungsgemeinschaft to MG (GR 970/8-1). This work contains parts of the medical thesis of N. Hofmann.

References

1. Wenzel JJ, Piehler A, Kaminski WE. ABC A-subclass transporters--key regulators of molecular lipid transport. Med Klin (Munich) 2007;102: 524–530.
2. Yamano G, Funahashi H, Kawanami O, Zhao LX, Ban N, Uchida Y, et al. ABCA3 is a lamellar body membrane protein in human lung alveolar type II cells. FEBS Lett. 2001;508: 221–225.
3. Mulugeta S, Gray JM, Notarfrancesco KL, Gonzales LW, Koval M, Feinstein SI, et al. Identification of LBM180, a lamellar body limiting membrane protein of alveolar type II cells, as the ABC transporter protein ABCA3. J Biol Chem. 2002;277: 22147–22155.
4. Cheong N, Madesh M, Gonzales LW, Zhao M, Yu K, Ballard PL, et al. Functional and trafficking defects in ATP binding cassette A3 mutants associated with respiratory distress syndrome. J Biol Chem. 2006; 281: 9791–9800.
5. Matsumura Y, Sakai H, Sasaki M, Ban N, Inagaki N. ABCA3-mediated choline-phospholipids uptake into intracellular vesicles in A549 cells. FEBS Lett. 2007;581: 3139–3144.
6. Campo I, Zorzetto M, Mariani F, Kadija Z, Morbini P, Dore R, et al. A large kindred of pulmonary fibrosis associated with a novel ABCA3 gene variant. Respir Res. 2014;15: 43.
7. Wambach JA, Casey AM, Fishman MP, Wegner DJ, Wert SE, Cole FS. Genotype-phenotype correlations for infants and children with ABCA3 deficiency. Am J Respir Crit Care Med. 2014;189: 1538–1543.
8. Weaver T, Na CL, Stahlman MT. Biogenesis of lamellar bodies, lysosome-related organelles involved in storage and secretion of pulmonary surfactant. Semin Cell Dev Biol. 2002;13: 263–270.

9. Matsumura Y, Ban N, Ueda K, Inagaki N. Characterization and classification of ATP-binding cassette transporter ABCA3 mutants in fatal surfactant deficiency. J Biol Chem. 2006;281: 34503–34514.
10. Engelbrecht S, Kaltenborn E, Griese M, Kern S. The surfactant lipid transporter ABCA3 is N-terminally cleaved inside LAMP3-positive vesicles. FEBS Lett. 2010;584: 4306–4312.
11. Kaltenborn E, Kern S, Frixel S, Fragnet L, Conzelmann KK, Zarbock R, et al. Respiratory syncytial virus potentiates ABCA3 mutation-induced loss of lung epithelial cell differentiation. Hum Mol Genet. 2012;21: 2793-2806.
12. Bai B, Chen P-C, Hales CM, Wu Z, Pagala V, High AA, Levey AI, Lah JJ, Peng J. Integrated Approaches for Analyzing U1-70K Cleavage in Alzheimers Disease. J. Proteome Res., 2014;13: 4526-4534.
13. Bernsel A, Viklund H, Hennerdal A, Elofsson A. TOPCONS: consensus prediction of membrane protein topology. Nucleic Acids Res. 2009;37: W465-W468.
14. Sasaki T, Kishi M, Saito M, Tanaka T, Higuchi N, Kominami E, et al. Inhibitory effect of di- and tripeptidyl aldehydes on calpains and cathepsins. J Enzyme Inhib. 1990;3: 195–201.
15. Buttle DJ, Murata M, Knight CG, Barrett AJ. CA074 methyl ester: a proinhibitor for intracellular cathepsin B. Arch Biochem Biophys. 1992;299: 377–380.
16. Yasuma T, Oi S, Choh N, Nomura T, Furuyama N, Nishimura A. Synthesis of peptide aldehyde derivatives as selective inhibitors of human cathepsin L and their inhibitory effect on bone resorption. J Med Chem. 1998;41: 4301–4308.
17. Schröder BA, Wrocklage C, Hasilik A, Saftig P. The proteome of lysosomes. Proteomics 2010;10: 4053–4076.

18. Steenhuis P, Froemming J, Reinheckel T, Storch S. Proteolytic cleavage of the disease-related lysosomal membrane glycoprotein CLN7. Biochim Biophys Acta 2012;1822: 1617–1628.
19. Beers MF, Zhao M, Tomer Y, Russo SJ, Zhang P, Gonzales LW et al. Disruption of N-linked glycosylation promotes proteasomal degradation of the human ATP-binding cassette transporter ABCA3. Am J Physiol Lung Cell Mol Physiol. 2013;305: L970-L980.
20. Montaser N, Lalmanach G, Mach L. CA-074, but not its methyl ester CA-074Me, is a selective inhibitor of cathepsin B within living cells. Biol Chem. 2002;383: 1305–1308.
21. Zheng X, Chu F, Mirkin BL, Sudha T, Mousa SA, Rebbaa A. Role of the proteolytic hierarchy between cathepsin L, cathepsin D and caspase-3 in regulation of cellular susceptibility to apoptosis and autophagy. Biochim Biophys Acta 2008;1783: 2294–2300.
22. Joyce JA, Baruch A, Chehade K, Meyer-Morse N, Giraudo E, Tsai FY. Cathepsin cysteine proteases are effectors of invasive growth and angiogenesis during multistage tumorigenesis. Cancer Cell 2004;5: 443–453.
23. Rousselet N, Mills L, Jean D, Tellez C, Bar-Eli M, Frade R. Inhibition of tumorigenicity and metastasis of human melanoma cells by anti-cathepsin L single chain variable fragment. Cancer Res. 2004;64: 146–151.
24. Reinheckel T, Deussing J, Roth W, Peters C. Towards specific functions of lysosomal cysteine peptidases: phenotypes of mice deficient for cathepsin B or cathepsin L. Biol Chem. 2001;382: 735–741.
25. Brömme D. Papain-like cysteine proteases. Curr Protoc Protein Sci. 2001;Chapter 21: Unit 21.2.

26. Wille A, Gerber A, Heimburg A, Reisenauer A, Peters C, Saftig P, et al. Cathepsin L is involved in cathepsin D processing and regulation of apoptosis in A549 human lung epithelial cells. Biol Chem. 2004;385: 665–670.
27. Schwake M, Schröder B, Saftig P. Lysosomal membrane proteins and their central role in physiology. Traffic 2013;14: 739–748.
28. Savalas LR, Gasnier B, Damme M, Lübke T, Wrocklage C, Debacker C, et al. Disrupted in renal carcinoma 2 (DIRC2), a novel transporter of the lysosomal membrane, is proteolytically processed by cathepsin L. Biochem J. 2011;439: 113–128.
29. Bühling F, Waldburg N, Reisenauer A, Heimburg A, Golpon H, Welte T. Lysosomal cysteine proteases in the lung: role in protein processing and immunoregulation. Eur Respir J. 2004;23: 620–628.
30. Herber-Jonat S, Mittal R, Huppmann M, Hammel M, Liebisch G, Yildirim AÖ, et al. Abca3 haploinsufficiency is a risk factor for lung injury induced by hyperoxia or mechanical ventilation in a murine model. Pediatr Res. 2013;74: 384–392.

Figures

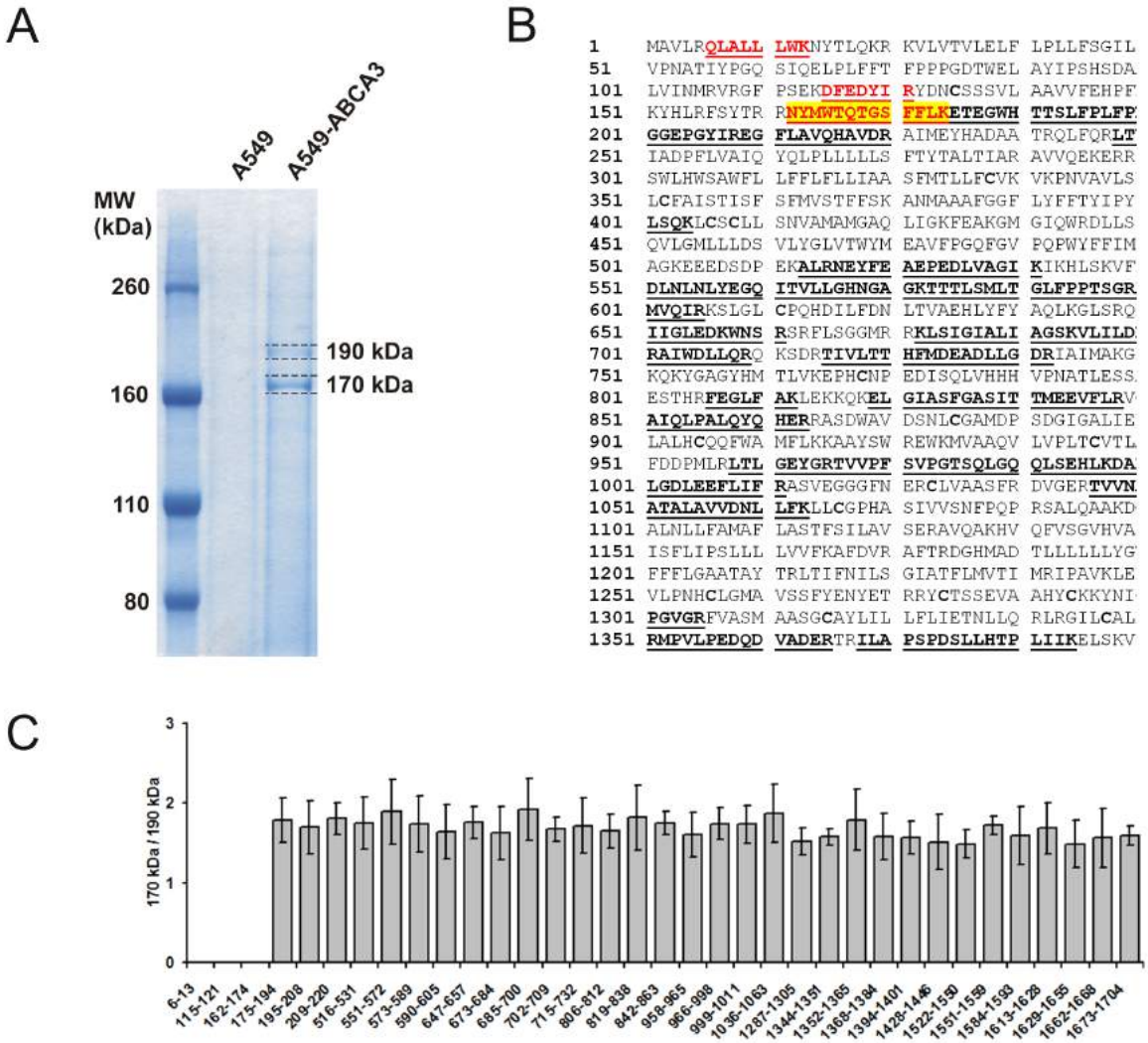

Fig 1. Analysis of ABCA3 cleavage region. A: ABCA3 containing gel bands were excised, digested with trypsin and analysed. **B:** Partial sequences of unprocessed (190 kDa) and processed (170 kDa) ABCA3 forms identified by LC-MS/MS. Identified sequence parts of ABCA3 precursor protein including HA-TAG with spacer (shown in blue) are underlined. Sequences identified only in unprocessed form and absent in processed form are shown in red. Cleavage region (162-174) is highlighted in yellow. **C:** Peptide intensity ratios from MS ion chromatograms (three measurements), leading to the predicted cleavage region

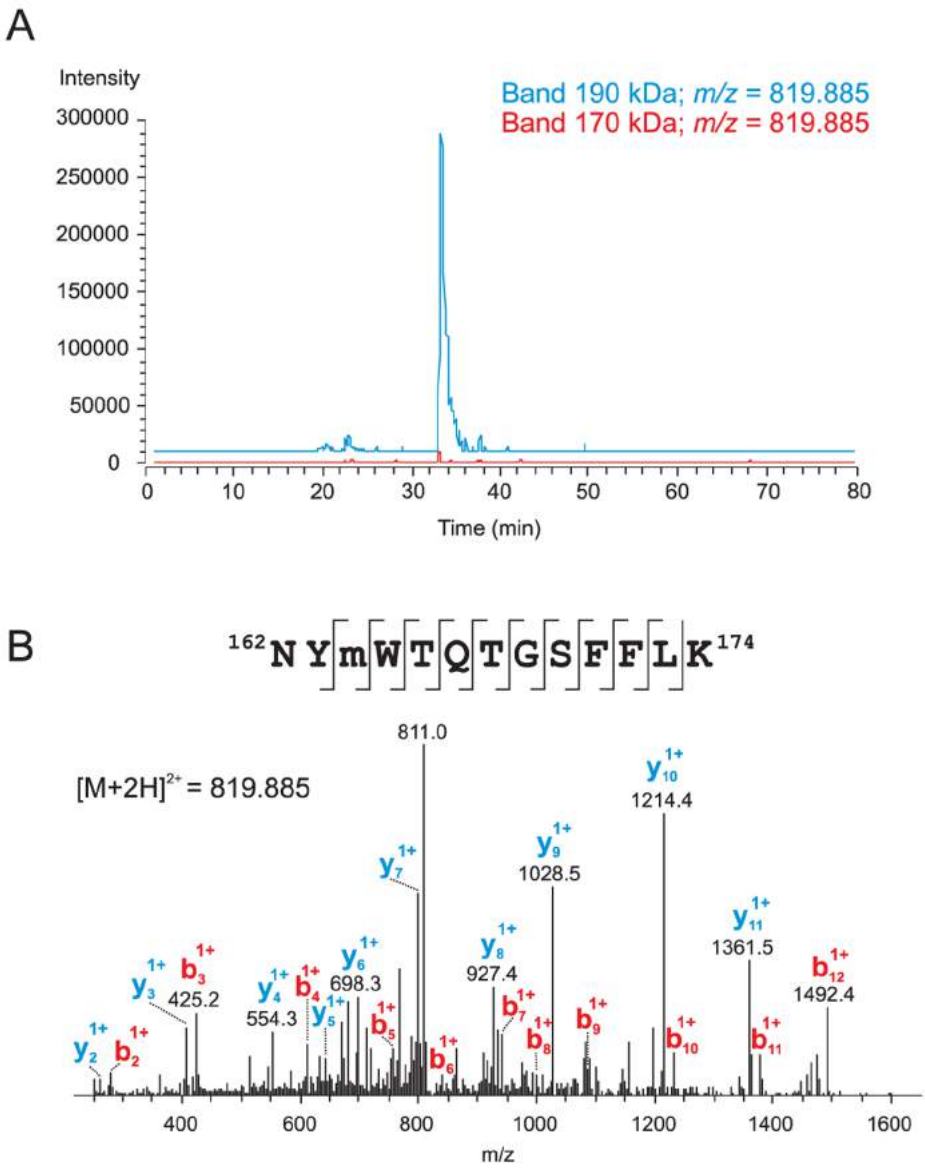

Fig 2. Partial sequence (162-174) is present in unprocessed ABCA3 and missing in processed protein form. A: Intensity profiles of an *m/z* range corresponding to the monoisotopic peak of the doubly-charged ion at *m/z* 819.885 (*m/z* window ±5 ppm) for 190 kDa and 170 kDa gel bands acquired in Orbitrap. **B**: Identification of the ABCA3 tryptic peptide comprising amino acid residues 162–174 of the precursor protein and containing methionine sulfoxide at position 164. MS/MS spectra after CID fragmentation measured in the LTQ ion trap are shown. Major *b* and *y* ions are labelled on the spectra and all fragment

ions obtained are marked on the identified sequence. The ion at *m/z* 811 corresponds to the loss of water from the parent ion.

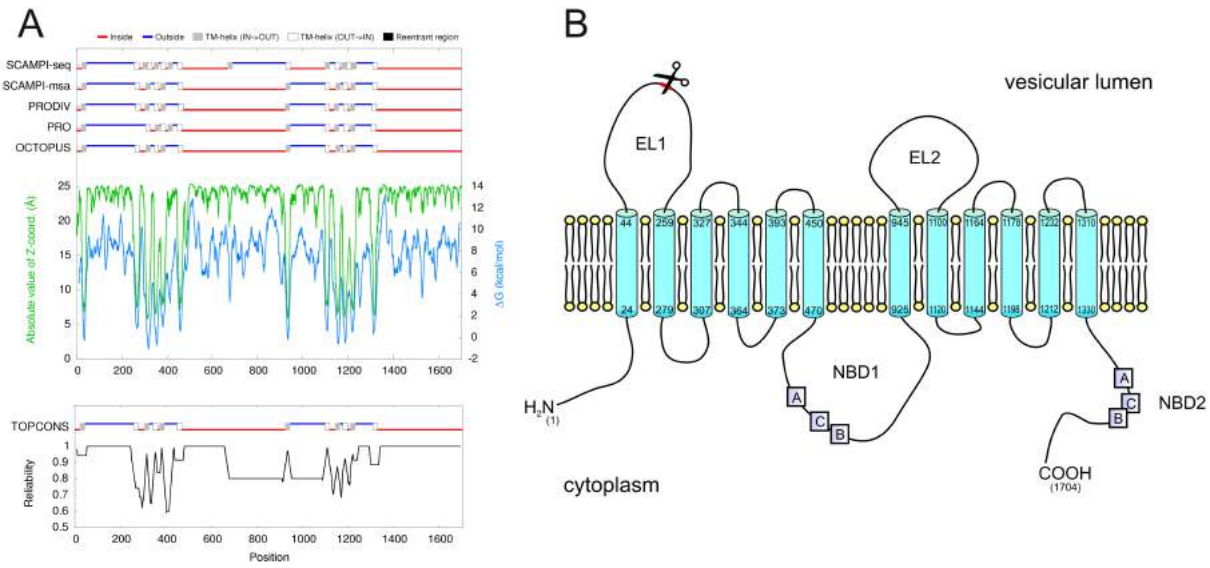

Fig 3. Predicted membrane topology of ABCA3 and localization of the identified cleavage site. A) Membrane topology of ABCA3 as predicted by different algorithms (top) and consensus prediction generated by TOPCONS (bottom) [13]. B) Model of ABCA3 in the vesicular membrane generated based on the TOPCONS prediction. Scissors indicate the identified cleavage site in the first extracellular loop (EL1).

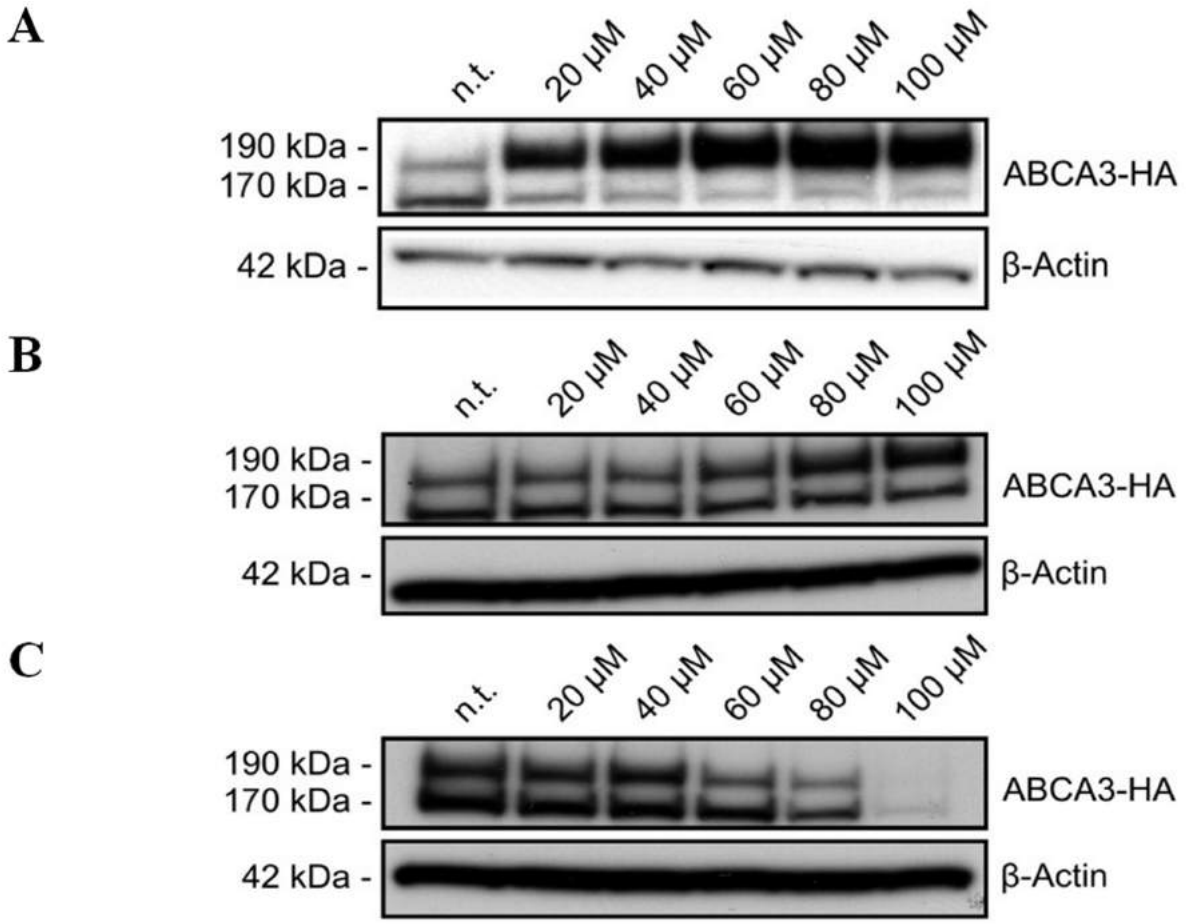

Fig 4. Effects of protease inhibitors on ABCA3 processing. Cells were treated with ALLM (N-Acetyl-Leu-Leu-Met-CHO) (A), CA-074 (L-trans-Expoxysuccinyl-Ile-Pro-OH propylamide) methyl ester (B), and N-(1-naphthalenylsulfonyl-L-isoleucyl-L-tryptophanal (C), and cleavage of ABCA3 was assessed by Western blotting.

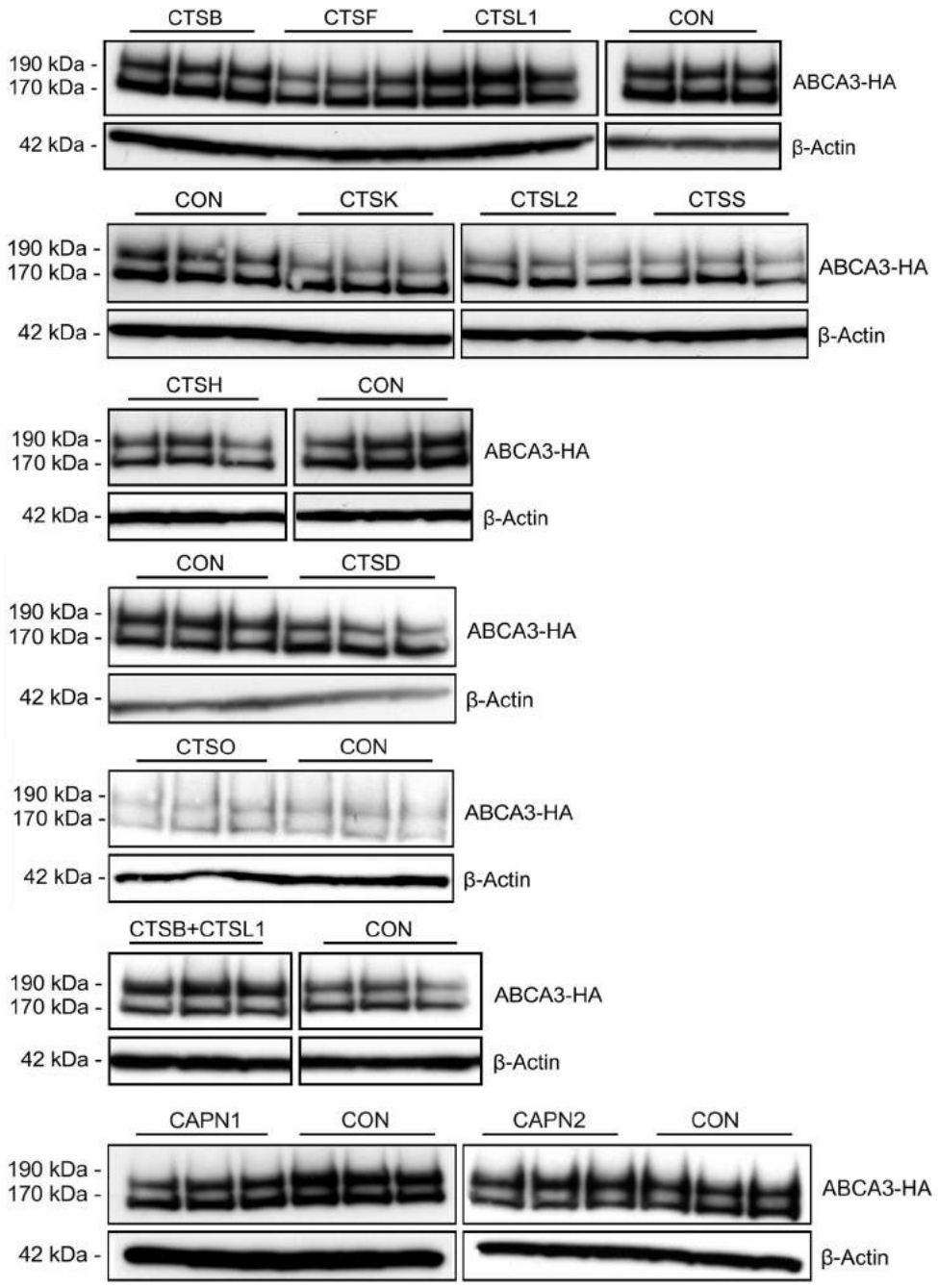

Fig 5. Effect of knockdown of single proteases on ABCA3 processing. Expression of lysosomal cathepsins was silenced using siRNA mediated knockdown and ABCA3 cleavage was assessed by Western blotting. Experiments were performed thrice, every time in triplicates. Representative Immunoblots are shown.

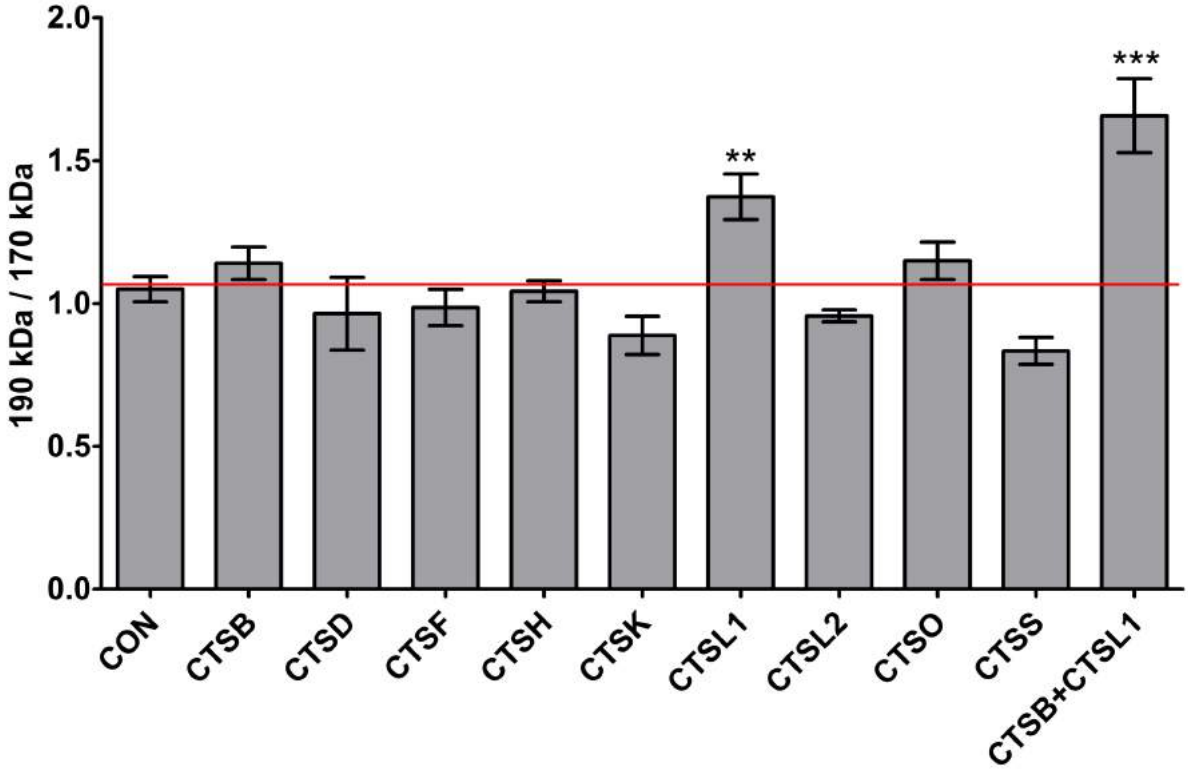

Fig 6. Quantitative analysis of the inhibition of ABCA3 processing. The ratio of 190 kDa to 170 kDa ABCA3 bands points to an inhibition of processing by knockdown of either CTSL1 alone or CTSL1 in combination with CTSB. Accumulation of the 190 kDa ABCA3 species is a result of inhibition of proteolytic cleavage due to cathepsin knockdown. ** $p < 0.01$; *** $p < 0.001$.

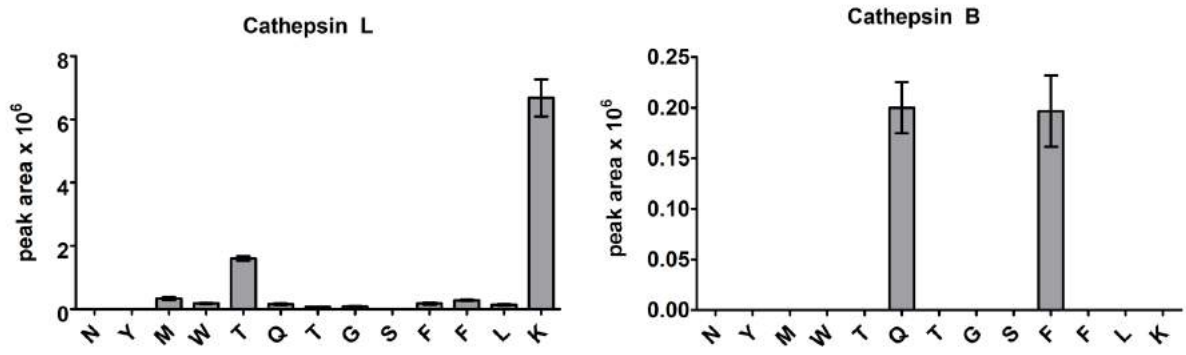

Fig 7. Cathepsin L cleaves ABCA3 peptide preferentially after Lys[174]. Shown are signal intensities of C-terminal cathepsins L and B cleavage products of ABCA3 peptide (151-194) within the sequence [162]NYMWTQTGSFFLK[174] analyzed by LC-MS/MS. Extracted MS ion chromatograms of the accurate m/z values ±5 ppm related to the corresponding peptide ions (peak areas) from three experiments were used for the diagram.

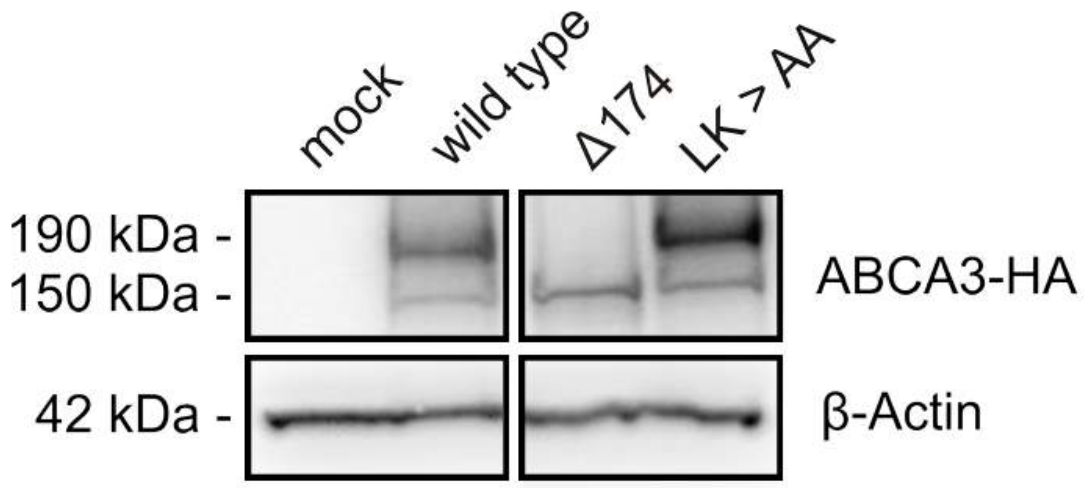

Fig 8. Mutation of potential Cathepsin cleavage sites. Amino acids forming potential cleavage sites were replaced by alanine residues using site directed mutagenesis. Lane 1: cells transfected with empty vector; lane 2: wild type ABCA3; lane 3: deletion of the first 174 amino acids of ABCA3; lane 4: 173LK174 > AA.